AN ABSTRACT OF THE DISSERTATION OF

Dale H. Burns for the degree of Doctor of Philosophy in Geology presented on May 20, 2014.

Title: Crustal Architecture and Magma Dynamics in a Large Continental Magmatic System: A Case Study of the Purico-Chascon Volcanic Complex, Northern Chile.

Abstract approved:

_____

Shanaka L. de Silva

Abstract approved:

_____

Frank J. Tepley III

The ~1 Myr history of the Purico-Chascon volcanic complex (PCVC) records significant changes in the production and storage of magmas in the crust. At ~1 Ma activity at the PCVC initiated with the eruption of a large 80-100 km^3 crystal-rich dacite ignimbrite with restricted whole rock $^{87}Sr/^{86}Sr$ isotope ratios between 0.7085-0.7090. In-situ analyses of plagioclase from the Purico ignimbrite have $^{87}Sr/^{86}Sr$=0.7087-0.7090. The dacite magma accumulated and evolved at relatively low temperatures around 800-850 °C in the upper crust at 4-8 km depth. Minor andesite and rhyolite pumice late in the sequence have similar restricted whole rock $^{87}Sr/^{86}Sr$=0.7089-0.7091. The radiogenic isotopes of this 0.98 Ma activity are consistent with all these compositions resulting from 50 to 70%

crustal assimilation by parental Central Andean “baseline” magmas at depths between 15-30 km.

The final eruptions at the PCVC occurred <0.18 Ma producing three small < 5 km^3 crystal-rich dacite lava domes with whole rock $^{87}Sr/^{86}Sr$ ratios 0.7075 to 0.7081 containing abundant basaltic-andesite enclaves with whole rock $^{87}Sr/^{86}Sr$ ratios of 0.7057- 0.7061. Plagioclase and amphibole from samples from the largest of these domes, Cerro Chascon, record two distinct magmatic environments; an upper crustal environment identical to the Purico ignimbrite and a second deeper, ~15-20 km depth, higher temperature (~922-1001 °C) environment consistent with conditions recorded in the basaltic andesite enclaves. Accordingly, plagioclase cores in the host dacite lava and enclaves have enriched in-situ $^{87}Sr/^{86}Sr$ isotopic compositions of 0.7083 to 0.7095 while plagioclase rims and microphenocrysts in the enclaves have $^{87}Sr/^{86}Sr$ isotope ratios from 0.7057 to 0.7065 and 0.7062 to 0.7064 respectively. Lavas from Cerro Chascon also contain abundant Fo_{82} olivine with spinel and basaltic melt inclusions that crystallized in a deep crustal environment (>1250 °C) consistent with a lower crustal MASH zone. The high baseline isotopic ratios observed in bulk rock and plagioclase crystals from Cerro Chascon (0.7057-0.7065) are consistent with MASH processes.

The evolution of the PCVC is a microcosm of the Andean arc in this region where, from 10 – 1 Ma, dominantly dacitic upper crustal magmatism of the Altiplano-Puna Volcanic Complex ignimbrite flare-up persisted until ~1 Ma, when smaller volume, more heterogeneous and less isotopically enriched basaltic andesite to dacite composite volcanoes signal a return to steady state arc volcanism. I suggest that the PCVC captures the transition of the Andean arc from flare-up to steady state. The temporal trend at the PCVC is consistent with a waning thermal flux. High magmatic fluxes during the flare-up would have resulted in elevated geothermal gradients and efficient crustal processing leading to a dominantly dacitic upper crust (0 to 35 km) that fed the large volume Purico ignimbrite. As magmatic flux and thermal energy wanes, crustal isotherms relax

resulting in greater thermal contrast between parental magmas, crust and remnant upper crustal dacite magma. This manifests in more heterogeneity and the survival of less isotopically enriched magmas in the upper crust. These arc scale magma dynamics are recorded even at the intra-crystalline scale.

Individual crystals from Cerro Chascon also record vital information on the crystallization and evolution of mantle-derived magmas in continental magmatic arcs. Fo_{82} olivine, olivine hosted spinel, and basaltic melt inclusions record the crystallization of olivine at >1250 °C in conditions consistent with a lower crustal (~70 km depth) MASH zone. Another significant crystallization event appears to have occurred at ~20 km depth, characterized by the crystallization of high An plagioclase (An_{72-84}) at ~1100-1050 °C followed by high-Al amphibole (~12-15 wt.% Al2O3) at ~1000-950 °C. The appearance of amphibole on the liquidus appears to have resulted from a nearly 2-fold increase in melt water content following ~45% crystallization of high An plagioclase. Following this extensive crystallization the highly crystalline mafic magma ascended into the upper crust and interacted with the remnant crystal mush from the Purico ignimbrite magma reservoir. Low An plagioclase (An_{39-55}), low Al amphibole (~6-9 wt.% Al_2O_3), sanidine, and biotite retain the chemical composition of the Purico ignimbrite magma, whereas, olivine, high An plagioclase, and high Al amphibole record the mafic recharge magma. The textures and compositions observed in Cerro Chascon are common in both continental and oceanic magmatic arcs worldwide and I propose that multiple crystallization events and upper crustal assimilation are fundamental processes intrinsic to arc magmatism.

I have also used *in situ* $^{87}Sr/^{86}Sr$ isotope ratios in plagioclase from andesite, dacite, and rhyolite pumice from the ~1 Ma Purico ignimbrite to determine the cause for compositional zoning in the Purico ignimbrite magma reservoir. Andesite pumice contains two texturally, compositionally, and isotopically distinct types of plagioclase, small (<500 µm) subhedral to euhedral crystals with high MgO (130-490 ppm) and low $^{87}Sr/^{86}r$ crystals (0.7076-0.7084) record a hot (>900 °C) andesite magma derived from an ~20 km deep magma

reservoir. In contrast, the second type of plagioclase in the andesite appear to broken fragments of larger crystals and have significantly lower MgO (90-240 ppm), higher $^{87}Sr/^{86}Sr$ (0.7096-0.7114), and appears to be derived from the lower temperature (crystallized at ~800-900 °C), upper crustal (<10 km) plutonic basement. Dacite pumice also contains two texturally and compositionally distinct types of plagioclase. However, both types have very restricted MgO (b.d.l.-200 ppm) and $^{87}Sr/^{86}Sr$ (0.7085-0.7095) ratios and appear to have grown at ~850°C. These crystals are also significantly larger (>1000 μm) than plagioclase from the andesite pumice and have clear euhedral rims. Rhyolite pumice from the Purico ignimbrite also contains distinct types of plagioclase. Both types of plagioclase are similar in size (<500 μm) and appear to be fragments of larger crystals. One type is characterized by low MgO (b.d.l.-240 ppm) and restricted $^{87}Sr/^{86}Sr$ isotope ratios (0.7088-0.7095) similar to plagioclase in the dacite pumice, and the other has significantly higher $^{87}Sr/^{86}Sr$ ratios (0.7095-0.7103) consistent with the upper crustal ignimbrite basement. The compositional variations observed in plagioclase crystals from the Purico ignimbrites are consistent with the recharge of a previously emplaced upper crustal (4-8 km depth) dacite magma reservoir by a hotter, deeper (20 km deep) andesite. During ascent, the andesite incorporated crystals from the surrounding upper crustal plutonic bodies before pooling against the residence dacite magma and crystallizing. Crystallization of the andesite resulted in the expulsion of a rhyolite interstitial melt that ascended through the dacite reservoir and pooled at the top of the reservoir. The rhyolite melt incorporated crystals from the dacite magma during ascent as well as crystals from the roof rock, which in the case of the Purico ignimbrite represents the plutonic remnants from other large silicic magmatic systems associated with the APVC. Thus, the compositional variations observed in the Purico ignimbrite results from a combination of crustal assimilation, crystallization, and melt extraction all initiated by mafic recharge.

Crustal Architecture and Magma Dynamics in a Large Continental Magmatic System: A Case Study of the Purico-Chascon Volcanic Complex, Northern Chile

by
Dale H. Burns

A DISSERTATION

submitted to

Oregon State University

in partial fulfillment of
the requirements for the
degree of

Doctor of Philosophy

Presented May 20, 2014
Commencement June 2014

Doctor of Philosophy dissertation of Dale H. Burns presented on May 20, 2014.

APPROVED:

Co-Major Professor, representing Geology

Co-Major Professor, representing Geology

Dean of the College of Earth, Ocean, and Atmospheric Sciences

---

Dean of the Graduate School

I understand that my dissertation will become part of the permanent collection of Oregon State University libraries. My signature below authorizes release of my dissertation to any reader upon request.

Dale H. Burns, Author

ACKNOWLEDGEMENTS

"Volcaners are crool" –Steven Doyle

I would first to thank my parents Stephen and Patricia Burns. Their love and support has been instrumental in my personal and academic success. It was through them that I developed the sense of wonder and inquisition that ultimately led me down the path to a Ph.D. I would also like to thank "Uncle" Mark Kelley. The work ethic that I gained from our years on and off the basketball court truly shaped my future. To Steven Doyle, the man behind the quote, you moving to California 25 years ago and the time that we have shared together have truly altered the trajectory of my life. I could not imagine my life without you in it and I truly love you, as well as Abbey, and look forward to the experiences the future holds. I would also like to thank the rest of my family along with the community of Leggett, California. The support that I have received from all of you is truly remarkable.

To the teachers that helped to develop my scholarship I am forever indebted to you all. I would like to specifically thank Meredyth Phillips, Lloyd Allen, Katie Granich (Ms. G), and Joe Willis. It was a high school geology field trip to Mt. Shasta with Ms. G during my junior year of high school that set into place the trajectory of my academic career. I would also like to thank Dr. Aaron Pietruszka, Dr. Michael Garcia, and Dr. Vic. Camp for their support and advising during my time at San Diego State University. I want to give a special thanks to the VIPER group at OSU. I would specifically like to thank my advisors Shan de Silva and Frank Tepley, my committee members Anita Grunder and Adam Kent, Matt Loewen for his countless hours in the ICP-MS lab helping develop a procedure for measure Sr isotopes, and Mark Ford and Amy Lange for great conversation and friendship during my time at OSU. I give special thanks to Stephanie Grocke, Jason Kaiser, and Casey Tierney. You have been great friends and there is no way that I could have done this without you.

I would also like to thank a few friends in Corvallis and beyond. To Dr. Clinton Epps, thank you for your friendship over the past years. You have rekindled parts of my past that had somehow slipped away during my academic voyage and for that I am very thankful. I have also greatly enjoyed the journey through the Corvallis bluegrass circuit to which I can thank you for the introduction. I would also like to give thanks to Arron Steiner. I have greatly enjoyed our years together as friends and the adventures that we find are truly unbelievable. May our future hold many more…..Hollywood Moto Bandits-style.

Last and certainly not least, I would like to thank my wonderful wife Cerise Burns. You have been by my side for nearly a decade as I have traveled through academia and I am truly lucky to have you. As we move on, away from graduate life, I look forward to a long prosperous life with you by my side. I love you.

TABLE OF CONTENTS

Page

TABLE OF CONTENTS (CONTINUED)

Page

TABLE OF CONTENTS (CONTINUED)

Page

TABLE OF CONTENTS (CONTINUED)

Page

LIST OF FIGURES

LIST OF FIGURES (CONTINUED)

LIST OF FIGURES (CONTINUED)

LIST OF TABLES

LIST OF APPENDICES

LIST OF CD-ROM APPENDICES

Crustal Architecture and Magma Dynamics in a Large Continental Magmatic System: A Case Study of the Purico-Chascon Volcanic Complex, Northern Chile

Dale H. Burns

CHAPTER 1

General Introduction

Argument

The volcanic eruptions associated with magmatic flare-ups represent some of the largest explosive volcanic eruptions found in the geologic record (e.g. ~5,000 km^3 Fish Canyon Tuff; Lipman et al., 2000). The plutonic rocks associated with these events record magma bodies characterized by thousands of cubic kilometers of intermediate magma (e.g., Smith, 1960; Lipman, 1984) and represents one of the primary ways in which new continental crust is formed (e.g. Sierra Nevada and Peninsular Range batholiths; Ducea, 2001; Silver and Chappel, 1988). After ~30 years of study, it has become clear that magmatic flare-ups are common in continental arc settings with examples including the Sierra Nevada Batholith (Ducea, 2001), Peninsular Range Batholith (Silver and Chappell, 1988), and Southern Colorado Volcanic Field (Lipman et al., 1978) in the western United States, as well as the Sierra Madre Occidental in Mexico (Ferrari et al., 2002), and the Altiplano-Puna Volcanic Complex in South America (de Silva, 1989a).

It has been proposed that the transition from typical arc magmatism to flare-up magmatism is characterized by major changes in the production, storage, and accumulation of magma in the crust (e.g. de Silva et al., 2006). Lipman et al., (1978) proposed that isotopic changes during the transition from flare-up to typical arc magmatism in the San Juan volcanic field in the western United Stated are consistent with a transition from middle to upper crustal magmatism during the flare-up to predominantly lower crustal magmatism during typical arc magmatism. This relationship has been further explored in the past 35 years and it is now generally accepted that high mantle flux during flare-ups results in the production and storage of large amounts of silicic magma in the upper crust (de Silva, 1989; de Silva and Gosnold, 2007). Although the change from largely mantle/lower crustal magmatism during typical arc magmatism to upper crustal magmatism during flare-ups has been discussed for the past 40 years no detailed study exists that shows clearly shows the transition from flare-up to steady-state magmatism. The transition between the two types of magmatism is thought to represent major changes in the architecture and magmatic processes occurring in the arc crust, yet as of now, no study that confirms these changes has been published. In addition, the composition(s) of the mantle-derived magmas that drive flare-up magmatism remains elusive. This is most certainly due to the high degrees of modification during melting and mixing in the upper crust.

In this dissertation, I investigate how the changes in the textures and compositions of ignimbrites and lavas erupted in the Purico-Chascon volcanic complex (PCVC) in northern Chile record the transition from flare-up to steady-state magmatism over ~800 Kyr. I combine bulk rock and *in situ* isotopic information with crystal chemistry and thermo-barometric modeling to investigate how the generation, accumulation, and storage magmas changes during the transition from flare-up to steady-state magmatism. I also combine crystal chemistry with thermodynamic modeling and published experimental datasets to determine the source of mafic magmas in a flare-up magmatic system

Tectono-Magmatic Context for the PCVC

The PCVC is one of the last major erupted centers associated with the Altiplano-Puna Volcanic Complex (APVC), a large silicic volcanic field located between 21 and 24°S in the Central Andes of South America. The Central Andes are a ~7000 km orogenic belt that formed through a protracted history of accretion, crustal shortening, crustal thickening, extension, and extensive magmatism starting in the Proterozoic (Coira et al., 1982). The basement of the Central Andes is made up of Arequipa-Antofalla terrains, two large blocks that are dominated by mid- to high-grade amphibolites, gneisses, and granulites accreted to the South American continent during the Grenville-Sunsás Orogeny ~1.05 Ga (Loewy et al, 2004). The region underwent extensive tectonic,

metamorphic, and magmatic modification during the Pampean (~550-500 Ma) and Famatinian (~495-400 Ma) orogenies, recording thermal perturbations and magmatism consistent with a convergent plate boundary (Coira, 1982). The APVC, including the PCVC lie predominantly on the Antofallo terrain and straddle the border between the older, Grenville-Sunsán aged terrain, and the younger Famatinian aged terrain.

The current tectonic-magmatic cycle in the Central Andes began in the early Jurassic coincident with the opening of the Southern Atlantic Ocean (Stern et al., 2004). Arc-related magmatism initiated in the Early Jurassic (~200 Ma) and has evolved as a result of variations in subduction geometry and subduction rate (Coira et al., 1982; Rogers and Hawkesworth, 1989). The most significant variations have occurred since the late Oligocene following the breakup of the Farralon plate ~30 Ma (Stern et al., 2004). In the Late Eocene to Early Oligocene, increased convergence rates and a subsequent transition from “normal” subduction to flat slab subduction resulted in extensive crustal shortening and deformation in the Central Andes. Flat slab subduction continued during much of the Oligocene resulting in a hiatus in arc volcanism. In the late Oligocene-early Miocene, the transition from flat slab back to steeper subduction resulted the re-establishment of arc magmatism, and a slab geometry similar to the current plate geometry (Coira et al., 1993; James and Sacks, 1999; Kay and Coira, 2009). The re-intiation of arc magmatism occurred to the east of the present day arc and occurred over a much broader area consistent with a flatter slab. Subsequent

steepening of the slab is thought to have continued through the Miocene eventually reaching its present dip of 25-30° (Coira et al., 1993; Allmendinger et al., 1997; Kay et al., 1999). Importantly, it has been proposed that the steepening of the slab was accompanied by delamination of the subcontinental lithosphere and the subsequent emplacement of hot buoyant mantle against the hydrated lithosphere and lower crust (Kay et al., 1999), ultimately resulting in a regional ignimbrite flare-up (de Silva, 1989).

Rogers and Hawkesworth (1989) showed that since the onset of the current magmatic cycle in the Central Andes ~200 My there have been two major compositional and isotopic trends in the CVZ. For most of the CVZ history the compositional and isotopic nature of erupted products have clear mantle affinities (Rogers and Hawkesworth, 1989). In contrast, rapid compositional and isotopic excursions starting at ~10 Ma record the initiation of crustal melting following the late Miocene delamination event. The initiation of crustal melting was also accompanied by a significant change in the magnitude and style of eruption in the CVZ. Massive intermediate ignimbrites erupted from a series of multicyclic caldera complexes from ~8 to 3 Ma (de Silva, 1989b; Salisbury et al., 2010) constructing the Altiplano-Puna Volcanic Complex (APVC), a large silicic volcanic field that erupted >13,000 km^3 of predominantly crystal-rich dacite between 21 and 24 °S (de Silva, 1989a). Multiple workers have attributed the onset of crustal melting to the delamination of the lower crust leading to ascent and subsequent melting of the mantle wedge (Kay et al., 2009). Ignimbrite activity in the region

peaked at ~4 Ma, with the last major eruptions occurring ~1 Ma. Quaternary volcanism in the CVZ has been characterized by what appears to be a transition back to normal arc activity resulting from continued steepening of the subducting slab.

There are several striking differences between the ignimbrites of the APVC and typical CVZ arc lavas and tuffs. The APVC ignimbrites are orders of magnitude larger than typical arc eruptions (individual eruptions >1,000 km^3) and are texturally, compositionally, and isotopically homogeneous typifying the "monotonous intermediate" classification of Hildreth (1981). The ignimbrites also have significantly more radiogenic isotope ratios consistent with higher degrees of crustal assimilation. de Silva et al. (2006) and de Silva and Gosnold (2007) proposed that the during the APVC increased mantle heat input resulted in significant elevation of the geothermal gradient. The elevated geotherm had two major effects on arc magmatism: 1. Significant crustal melting and magma accumulation between 30 and 15 km depth resulted in the formation of a large predominantly dacite, with minor andesite, magma reservoir at ~20 km depth (**Figure 1.2**). Once established, this melting and mixing zone trapped ascending mafic melts creating a positive melting-mixing loop and generated homogeneous hybrid magmas with high crustal affinities, and 2. The elevated geotherm changed the location of the brittle-ductile transition in the uppermost crust allowing large felsic magma reservoirs to develop between 4-8 km depth (**Figure 1.2**). Typical arc lavas have significantly lower radiogenic isotope ratios and often

preserve significant textural, compositional, and isotopic heterogeneity (e.g. Clynne et al., 1999; Tepley et al., 1999; Koleszar et al., 2012), possibly due to limited crustal assimilation during ascent and lower upper crustal geotherms resulting in a more brittle crust that is prone to failing when new magma is added.

Purico-Chascon Volcanic Complex

The PCVC is the last major eruptive center associated with the APVC. Activity at the PCVC initiated ~1 Ma with the eruption of the ~80-100 km^3 predominantly dacitic Purico ignimbrite followed by a series of small volume dacite lava domes with up to 20% basaltic-andesite inclusions. The first study on the PCVC was conducted by Hawkesworth et al., (1982). Hawkesworth et al., (1982) showed that early, pre-glacial, lava domes in the PCVC have significantly higher $^{87}Sr/^{86}Sr$ isotope ratios and trace element abundances than the later, post-glacial, Cerro Chascon and Cerro Aspero lava domes. They also convincingly argued that the variations are best explained by systematic variations in the degree of crustal melting. The first study that compared the Purico ignimbrite with the post-ignimbrite lava domes was conducted by Francis et al., (1984). Francis et al., (1984) noted that the Purico ignimbrite had significantly higher $^{87}Sr/^{86}Sr$ isotope ratios and Rb/Sr than the Cerro Chascon lavas and lavas associated with the CVZ arc and speculated that variable degrees of crustal assimilation may explain the variations. The next study on the PCVC was conducted by de Silva,

(1991) who compared pumice types from the Purico ignimbrite to determine the cause of compositional zoning in the Purico ignimbrite. Davidson et al., (1990) conducted a detailed study of the interactions between mafic inclusions and the dacite host from Cerro Chascon and determined that the Cerro Chascon dacite is a hybrid of a new pulse of mantle-derived magma and the Purico ignimbrite basement. The most recent study on the PCVC, conducted by Schmitt et al., (2001), utilized thermobarometry and melt inclusion chemistry from the pumice from the Purico ignimbrite to revise the model for compositional zoning in the Purico ignimbrite. Schmitt et al., (2001) also used bulk rock isotope ratios to evaluate the amount of crustal contamination required to explain the compositions of the Purico ignimbrite and the Cerro Chascon and Cerro Aspero lavas.

Hawkesworth et al., (1982), Francis et al., (1984), and Schmitt et al., (2001) all recognized that the Purico ignimbrite and early Purico domes have significantly more radiogenic isotope ratios than younger lava domes. Francis et al., (1984) also recognized that mafic inclusions in the young domes are broadly similar to lavas erupted along the CVZ arc in the Quaternary. The textural, compositional, and isotopic differences between the early Purico eruptions and the later lava domes served as the motivation for this study.

Directions

In Chapter 2, I combine bulk rock compositional and isotopic information with *in situ* plagioclase and amphibole data and intra-crystalline isotope ratios in plagioclase to investigate how the generation, ascent, and storage of magmas changed in PCVC in response to the thermal waning of the flare-up. Using thermobarometry and *in situ* isotopic information I construct a time-transgressive cross-section of the sub-PCVC crust between ~1 Ma and <180 Ka. I show that ~1 Ma melting in the upper crust played a significant role in the magmas that ultimately erupted at the surface, whereas by ~180 Ka upper crustal melting was a trivial process. I also discuss how the variations record changes in the CVZ geothermal gradient. In Chapter 3, I combine the plagioclase and amphibole data from Chapter 2 with olivine, spinel, clinopyroxene, K-feldspar, and olivine-hosted melt inclusion chemistry to investigate the source, ascent path, and crystallization of the mafic magma that triggered the eruption of the < 180 Ka Cerro Chascon dacite lava dome. Using thermobarometry and thermodynamic modeling I reconstruct the P-T-t pathway of the ascending mafic magma and determine the relative order of crystallization. In addition, I explain how textural-compositional relationships in crystals from Cerro Chascon record the remobilization of the residual crystal mush from the Purico ignimbrite. In Chapter 4, I present new *in situ* compositional and isotopic information for plagioclase crystals in the Purico ignimbrite to determine the cause of compositional zonation in the ignimbrite.

Further, I use experimentally calibrated plagioclase major and trace element partitioning data to identify the closed system processes occurring during the formation of the zoned Purico magma reservoir. I also combine partitioning data with published intensive parameter information from the Purico ignimbrite to investigate the magma storage conditions differed between the three pumice types.

	Hypothesis	Objectives	Data/Methods
Chapter 4	The cause of compositional zoning in the Purico ignimbrite is mafic recharge from a large regional felsic magma reservoir Over ~800 Kyr, the PCVC records the transition from flare-up to steady-state arc magmatism	Determine the evolution of multiple, distinct plagioclase populations and reconstruct the magmatic processes that led to the formation of compositionally distinct magmas in the upper crust Characterize how and where the production and storage of magmas has occurred in the crust during the evolution of the PCVC	→EMP characterization of plagioclase crystals from three compositionally distinct types of pumice in the Purico ignimbrite →EMP characterization of major and trace elements in plagioclase and amphibole crystals in the Purico ignimbrite and Cerro Chascon lavas →TIMS and LA-MC-ICP-MS characterization of plagioclase crystals from three pumice types in Purico ignimbrite →TIMS and LA-MC-ICP-MS characterization of $^{87}Sr/^{86}Sr$ isotope ratios in plagioclase from the Purico ignimbrite and Cerro Chascon lavas →Determine temperature relationship between isotopically distinct plagioclase populations using plagioclase partitioning information →Model crystallization pressures and temperatures for plagioclase and amphibole using multiple thermobarometers
Chapter 3	The Cerro Chascon lava domes represents a mixture of mantle derived magma and upper crustal ignimbrite magma	Characterize the crystalline phases in the Cerro Chascon lavas, determine from where they were derived, and identify a potential mantle-derived source	→EMP characterization of major and trace elements in plagioclase, amphibole, olivine, spinel, cpx, K-feldspar, and melt inclusions from the Cerro Chascon lavas →Integrate EMP data with plagioclase isotope data from Chapter 1 →Model crystallization pressures and temperatures for multiple phases, and determine crystallization sequence

References

Allmendinger, R.W., Jordan, T.E., Kay, S.M., & Isacks, B. (1997). The Evolution Of The Altiplano-Puna Plateau Of The Central Andes. *Annual Review of Earth and Planetary Science 25*, 139-174.

Clynne, M. (1999). A complex magma mixing origin for rocks erupted in 1915, Lassen Peak, California. *Journal of Petrology* 40, 104-132.

Coira, B., Davidson, J., Mpodozis, C., & Ramos, V. (1982). Tectonic and magmatic evolution of the Andes of northern Argentina and Chile. *Earth-Science Reviews* 18, 303-332.

Coira, B., Mahlburg-Kay, S., & Viramonte, J. (1993). Upper Cenozoic magmatic evolution of the Argentine Puna: a model for changing subduction geometry. *International Geological Review* 35, 677-720.

Davidson, J., de Silva, S., Holden, P., & Halliday, A. (1990). Small-Scale Disequilibrium in a Magmatic Inclusion its More Silicic Host. *Journal of Geophysical Research* 95, 17661-17675.

de Silva, S. (1989a). Altiplano-Puna volcanic complex of the central Andes. *Geology* 17, 1102.

de Silva, S. (1989b). Geochronology and stratigraphy of the ignimbrites from the 21°30'S to 23°30'S portion of the central Andes of northern Chile. *Journal of Volcanology and Geothermal Research* 37, 93-131.

de Silva, S. & Gosnold, W. (2007). Episodic construction of batholiths: Insights from the spatiotemporal development of an ignimbrite flare-up. *Journal of Volcanology and Geothermal Research* 167, 320–335.

de Silva, S., Zandt, G., Trumbull, R., Viramonte, J., Salas, G., & Jimẽnez, N. (2006). Large ignimbrite eruptions and volcano-tectonic depressions in the Central Andes: a thermomechanical perspective. *Geological Society, London, Special Publications* 269, 47-63.

Ducea. M. (2001). The California arc: Thick granitic batholiths, eclogitic residues, lithospheric-scale thrusting, and magmatic flare-ups. *GSA Today* 11, 4-10.

Ferrari, L., López-Martínez, M., & Rosas-Elguera, J (2002). Ignimbrite flare-up and deformation in the southern Sierra Madre Occidental, western Mexico: Implications for the late subduction history of the Farallon plate. *Tectonics* 21, 1-24.

Francis, P., McDonough, W., Hammill, M., O'Callaghan, L., & Thorpe, R. (1984). The Cerro Purico Shield Complex, North Chile. *Andean Magmatism*, 106-123.

Hawkesworth, C., Hammill, M., Gledhill, A., van Calsteren, P., & Rogers, G. (1982). Isotope and trace element evidence for late-stage intra-crustal melting in the High Andes. *Earth and Planetary Science Letters* 58, 240-254.

Hildreth, W. (1981). Gradientsin Silicic Magma Chambers Implications for Lithospheric Magmatism. J*ournal Of Geophysical Research* 86,10153-10192.

James, D.E. & Sacks, I. (1999). Cenozoic Formation of the Central Andes: A Geophysical Perspective. *Society of Economic Geologists* 7, 1-25.

Kay, S.M. & Coira, B.L. (2009). Shallowing and steepening subduction zones,

continental lithospheric loss, magmatism, and crustal flow under the Central Andean Altiplano-Puna Plateau. *Geological Society of America Memoirs* 204, 229-259.

Koleszar, A.M., Kent, A.J.R., Wallace, P.J., & Scott, W.E. (2012). Controls on long-term low explosivity at andesitic arc volcanoes: Insights from Mount Hood, Oregon. *Journal of Volcanology and Geothermal Research* 219-220, 1-14.

Lipman, P., Doe, B., Hedge, C., & Steven, T. (1978). Petrologic evolution of the San Juan volcanic field, southwestern Colorado: Pb and Sr isotope evidence. *Geological Society of America Bulletin* 89, 58-92.

Loewy, S.L., Connelly, J.N., & Dalziel I.W.D. (2004). An orphaned basement block: The Arequipa-Antofalla Basement of the central Andean margin of South America. *Geological Society of America Bulletin* 116, 171.

Rogers, G. & Hawkesworth, C. (1989). A geochemical traverse across the North Chilean Andes: evidence for crust generation from the mantle wedge. *Earth and Planetary Science Letters* 91, 271-285.

Salisbury, M.J., Jicha, B.R., de Silva, S.L., Singer, B.S., Jimẽnez, N.C., & Ort, M.H. (2011) 40Ar/39Ar chronostratigraphy of Altiplano-Puna volcanic complex ignimbrites reveals the development of a major magmatic province. *Geological Society of America Bulletin* 123, 821-840.

Schmitt, A., de Silva, S., Trumbull, R., & Emmermann, R. (2001). Magma evolution in the Purico ignimbrite complex, northern Chile: evidence for zoning of a dacitic magma by injection of rhyolitic melts following mafic recharge. *Contributions to Mineralogy and Petrology* 140, 680-700.

Silver, L.T. & Chappell, B.W. (1988). The Peninsular Ranges batholith: An insight into the evolution of the Cordilleran batholiths of southwestern North America. *Transactions of the Royal Society of Edinburgh: Earth Sciences* 79, 105-121.

Stern, C.R. (2004). Active Andean volcanism: its geologic and tectonic setting. *Revista Geológica de Chile* 31, 161-206.

Tepley, F.J.T., Davidson, J.P., & Clynne, M.A. (1999). Magmatic Interactions as Recorded in Plagioclase Phenocrysts of Chaos Crags, Lassen Volcanic Center, California. *Journal of Petrology* 40, 787-806.

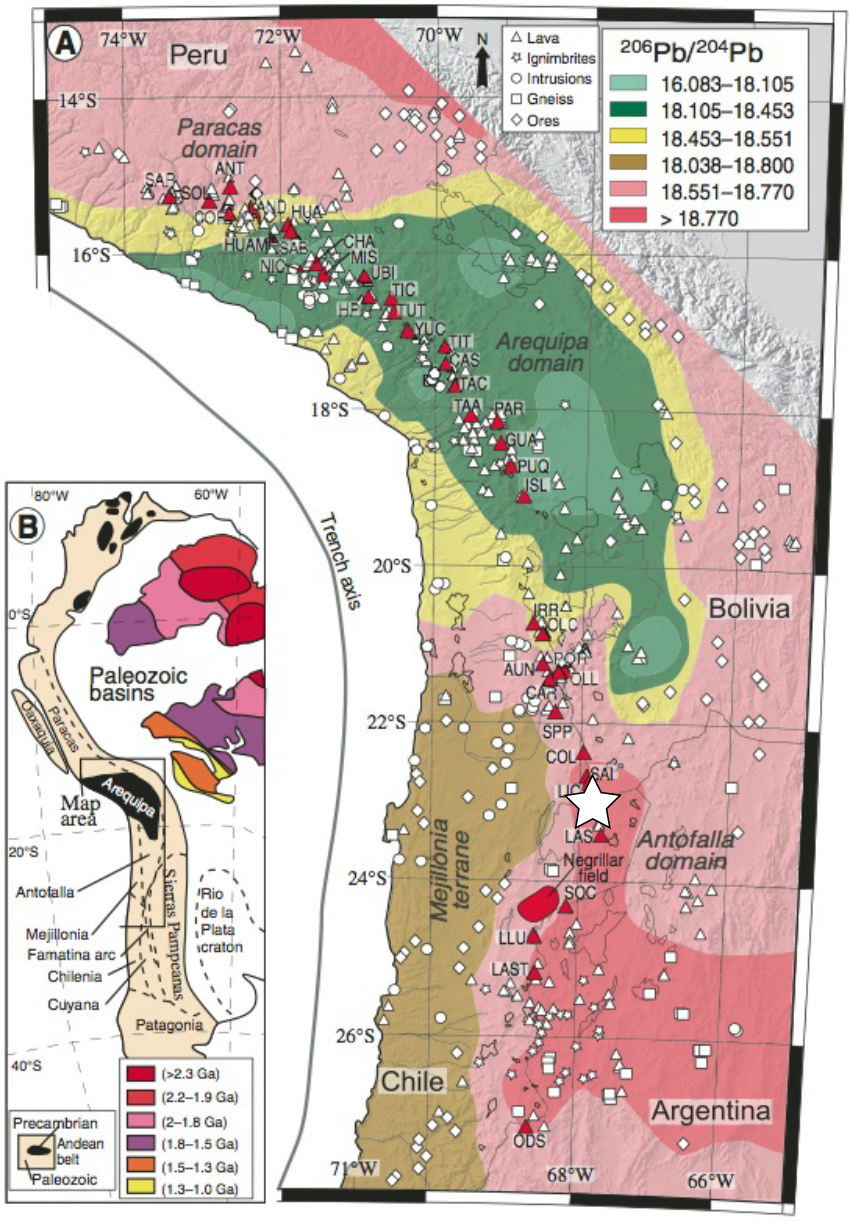

Figure 1.1. Map shows the basement rocks of the central Andes as defined by the Pb isotope ratios of lavas and ignimbrites erupted on the surface. The star represents the location of the Purico-Chascon Volcanic Complex (PCVC), the focus of this dissertation. Note that the PCVC is on the Antofalla domain. Map is modified from Mamani et al., (2010).

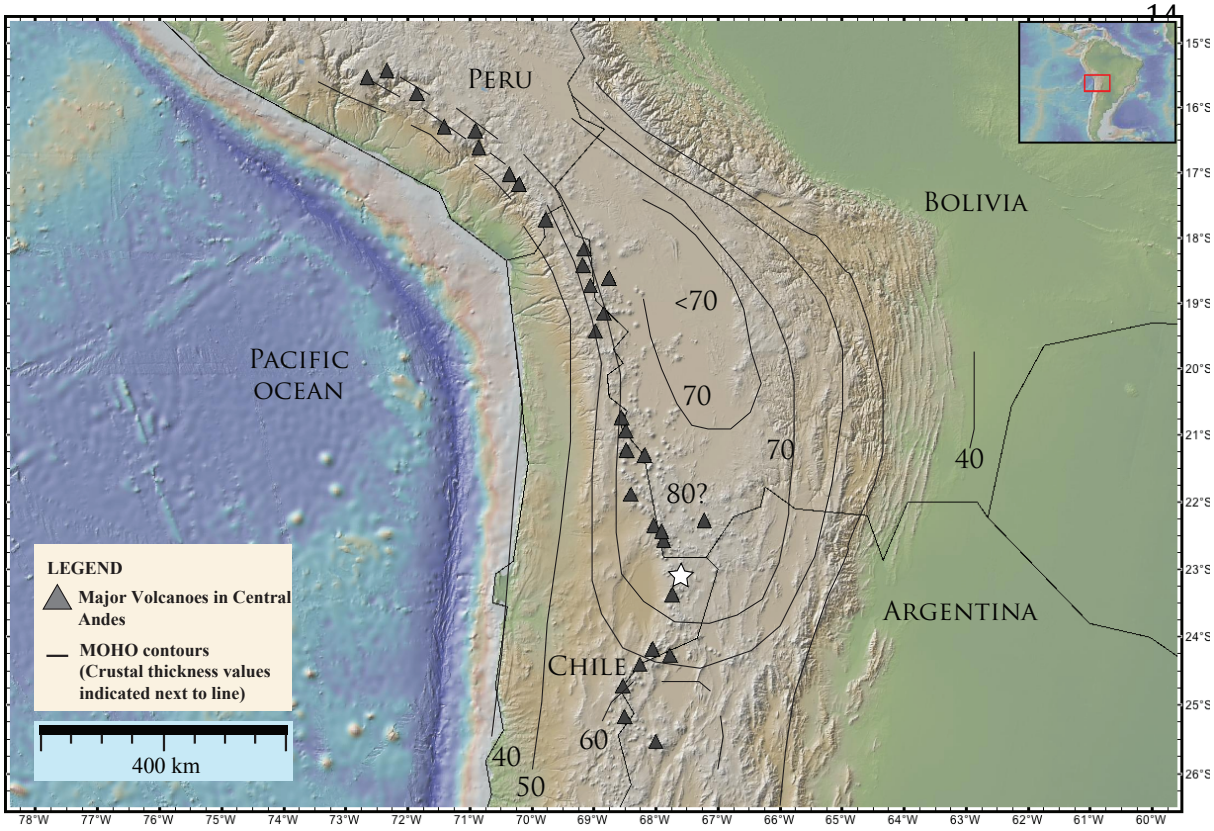

Figure 1.2. Map shows the seismically modeled crustal thickness of the central Andes. The white star shows the location of the PCVC. Map modified from Allmendinger et al., (1997).

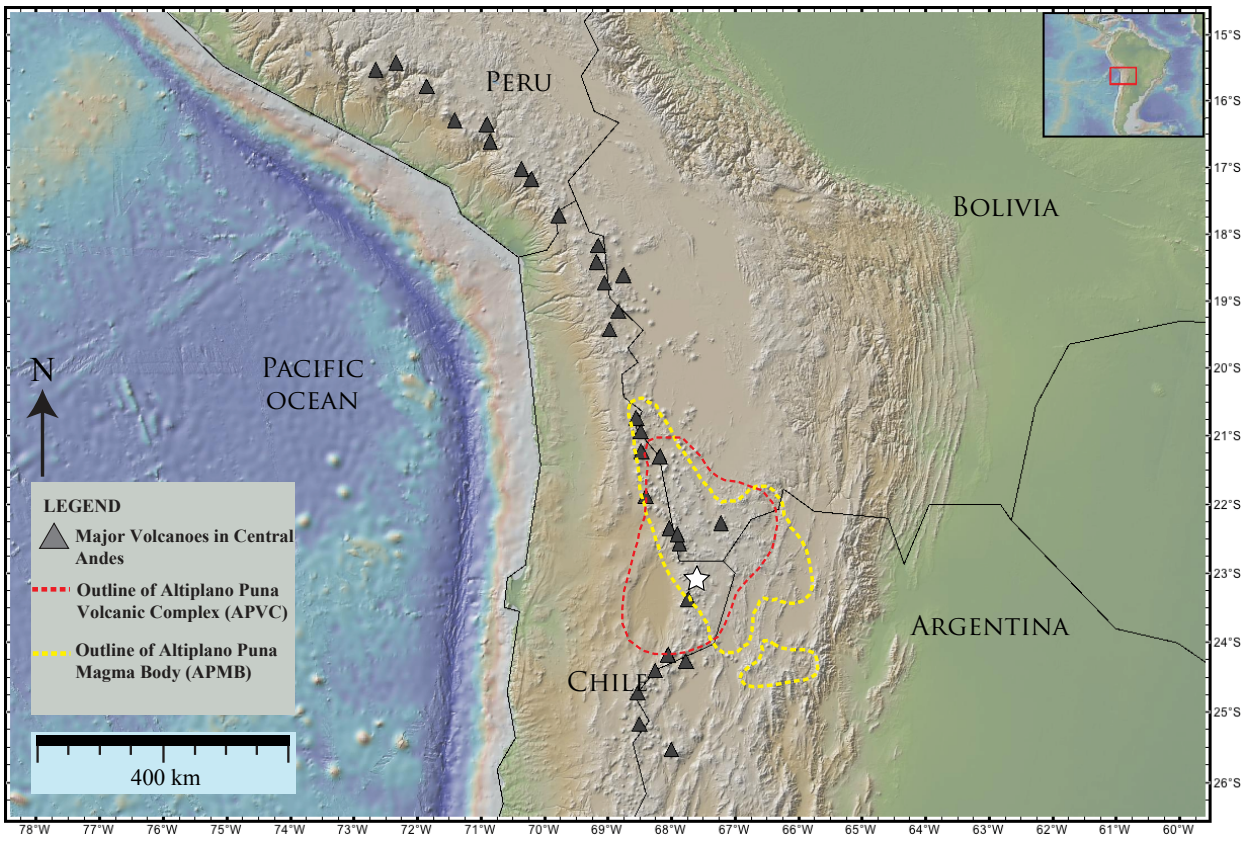

Figure 1.3. Map shows the extent of the Altiplano-Puna Volcanic Complex (APVC) ignimbrites (red dashed line), and the seismically imaged Altiplano-Puna Magma Body (APMB). The white star represents the PCVC. Map modified from de Silva et al., (2006).

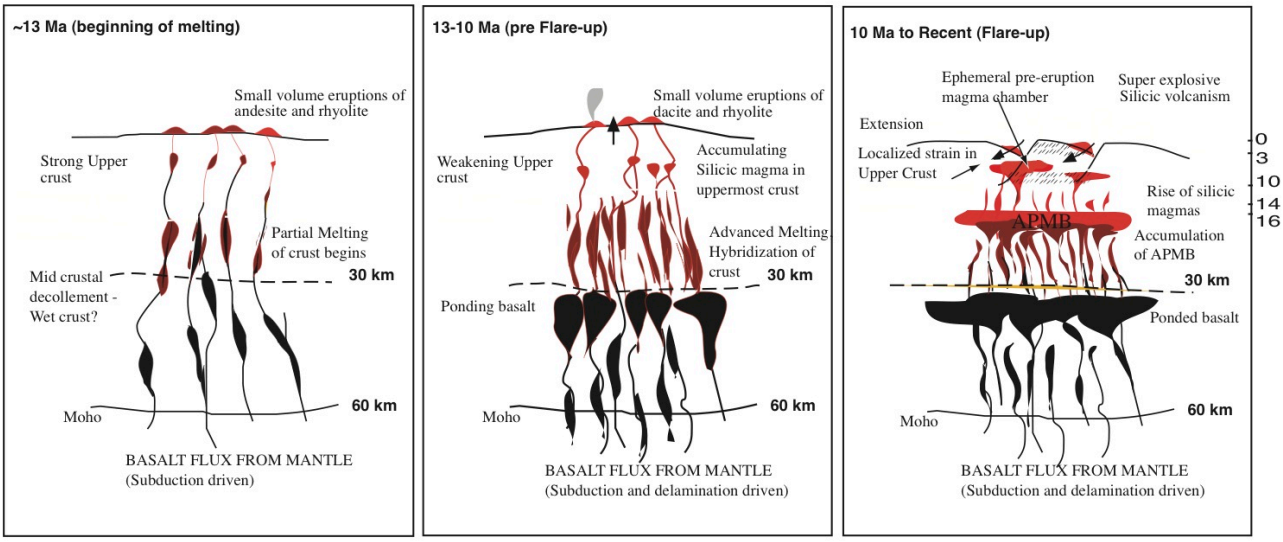

Figure 1.4. Schematic crustal sections of the CVZ crust during the transition from steady-state arc magmatism (far left) to flare-up magmatism. During the transition the thermal maturation of the crust between ~30 and 15 km deep results in the production and storage of crustal melts in the ~20 km deep APMB. Note that during the flare-up deep primitive magmas are filtered from and do not reach the upper crust.

CHAPTER 2

Recording the transition from flare-up to steady-state arc magmatism at the Purico-Chascon volcanic complex, northern Chile

Dale H. Burns

Shanaka L. de Silva

Frank Tepley III

Axel K. Schmitt

Matthew W. Loewen

In review:

Earth and Planetary Science Letters

2.1. Abstract

The ~1 Myr history of the Purico-Chascon volcanic complex (PCVC) records significant changes in upper crustal magmatic conditions with time. At ~1 Ma activity at the PCVC initiated with the eruption of a large 80-100 km^3 crystal-rich dacite ignimbrite with restricted whole rock $^{87}Sr/^{86}Sr$ isotope ratios between 0.7085-0.7090. In-situ analyses of plagioclase from the Purico ignimbrite have $^{87}Sr/^{86}Sr$=0.7087-0.7090. The dacite magma accumulated and evolved at relatively low temperatures around 800-850 °C in the upper crust at 4-8 km depth. Minor andesite and rhyolite pumice late in the sequence have similar restricted whole rock $^{87}Sr/^{86}Sr$=0.7089-0.7091. The radiogenic isotopes of this 0.98 Ma activity are consistent with all these compositions resulting from 50 to 70% crustal assimilation by parental Central Andean “baseline” magmas at depths between 15-30 km.

The final eruptions at the PCVC occurred <0.18 Ma producing three small < 5 km^3 crystal-rich dacite lava domes with whole rock $^{87}Sr/^{86}Sr$ ratios 0.7075 to 0.7081 containing abundant basaltic-andesite enclaves with whole rock $^{87}Sr/^{86}Sr$ ratios of 0.7057- 0.7061. Plagioclase and amphibole from samples from the largest of these domes, Cerro Chascon, record two distinct magmatic environments; an upper crustal environment identical to the Purico ignimbrite and a second deeper, ~15-20 km depth, higher temperature (~922-1001 °C) environment consistent with conditions recorded in the basaltic andesite enclaves. Accordingly, plagioclase cores in the host dacite lava and enclaves have

enriched in-situ $^{87}Sr/^{86}Sr$ isotopic compositions of 0.7083 to 0.7095 while plagioclase rims and microphenocrysts in the enclaves have $^{87}Sr/^{86}Sr$ isotope ratios from 0.7057 to 0.7065 and 0.7062 to 0.7064 respectively.

These temporally linked characteristics attest to broad homogeneity in large-volume dacitic upper-crustal magmas ~1 Ma, and more compositional heterogeneity in smaller volume dacite to basaltic andesite magmas during the last stages of the Purico magmatic system when less-enriched isotopic compositions appear. The evolution of Purico is a microcosm of the Andean arc in this region where, from 10 – 1 Ma, dominantly dacitic upper crustal magmatism of the Altiplano-Puna Volcanic Complex ignimbrite flare-up persisted until ~1 Ma, when smaller volume, more heterogeneous and less isotopically enriched basaltic andesite to dacite composite volcanoes signal a return to steady state arc volcanism.

We suggest that the PCVC captures the transition of the Andean arc from flare-up to steady state. The temporal trend at the PCVC is consistent with a waning thermal flux. High magmatic fluxes during the flare-up would have resulted in elevated geothermal gradients and efficient crustal processing leading to a dominantly dacitic upper crust (0 to 35 km) that fed the large volume Purico ignimbrite. As magmatic flux and thermal energy wanes, crustal isotherms relax resulting in greater thermal contrast between parental magmas, crust and remnant upper crustal dacite magma. This manifests in more heterogeneity and

the survival of less isotopically enriched magmas in the upper crust. These arc scale magma dynamics are recorded even at the intra-crystalline scale.

2.2. Introduction

The development of continental magmatic arcs is recognized as exhibiting cyclic behavior. Much of the lifetime of an arc is characterized by the steady low-volume volcanism that builds composite cones and minor centers. This steady state is periodically punctuated by short-lived high intensity flare-ups, or high-flux events, during which cordilleran batholiths and their eruptive equivalents, ignimbrites form (Lipman et al., 1972; Noble, 1972; Coney, 1978; Hildreth, 1981; de Silva, 1989; Ducea, 2001). DeCelles et al. (2009) characterize these flare-ups as "*10-15 Ma periods where magma production rates in the mantle wedge are 3-4 times greater than steady-state arc magma production rates*". Such transient excursions of elevated mantle to crust flux are most likely triggered by major changes in the subducting slab - mantle wedge – upper plate architecture (e.g. delamination, slab-rupture; Ferrari, 2002; DeCelles et al., 2009). This sets up a series of feedbacks that leads to elevated geotherms and prodigious "upper plate" or "crustal" magmatism that is characteristic of flare ups and quite distinct from "normal" or steady-state magmatism in its enriched isotopic character (e.g. Lipman, 1978; Johnson, 1991; Ducea and Barton 2007; DeCelles et al., 2009). The space-time-volume character of flare-up episodes defines a broad pulse-like pattern that is product of the topology of the mantle flux and it's modulation by the

crustal column. A waxing, catastrophic, and waning pattern of volcanism is produced (de Silva and Gosnold, 2007; Bachmann et al., 2007; Lipman, 2007) and is thought to reflect the thermal state (maturity) of the upper crust (de Silva et al., 2006; Grunder et al., 2006) - a concept that has been a foundation of our understanding of large silicic magmatic systems for decades (e.g Lipman, 1972; Coney, 1978).

Volcanic activity during flare-up events is dominated by the eruption of tens-of-thousands of cubic kilometers of ignimbrites (hence the term ignimbrite flare-up) and the formation of multiple spatially and temporally related caldera complexes (Elston, 1984; Best et al., 1991; de Silva et al, 2006; Lipman et al., 2007). The plutonic systems associated with flare-up magmatism are batholith-scale magma bodies (Lipman et al., 1972; Silver and Chappell, 1988; Ducea, 2001), which have been shown to be a critical component in the formation of new continental crust (e.g. Johnson, 1991; Ducea, 2001).

Conversely, steady state magmatism that constructs arc composite volcanoes is thought to be characterized by low mantle power input, low magmatic fluxes, and normal geothermal gradients. This manifests as small volume largely effusive eruptions with only occasional explosive caldera forming events. Eruption volumes and eruptive and magmatic fluxes are typically orders of magnitude lower than during flare ups (de Silva and Gosnold, 2007) and the chemical character of the eruptive products is typically less evolved and less enriched in crustal components. Thus, flare-ups are typically distinguishable from

steady-state magmatism in both the volcanic and plutonic record by their large volumes, textural and compositional homogeneity, and high crustal affinities (e.g. Lipman, 1978; de Silva, 1989; Best and Christiansen, 1992). However, while the general characteristics and signatures of flare-up and steady-state magmatism are well characterized and understood independently, there are few studies that address the transition from flare-up to steady-state magmatism as a stage in magmatic evolution.

Capturing this transition is tricky and has typically been addressed at the regional scale. Lipman (1978) contrasts the Oligocene intermediate composition magmatism with significant crustal involvement that we now recognize as a "flare-up" with later Miocene-Pliocene bimodal volcanism of more mantle affinity in the San Juan Volcanic Field of southwestern Colorado (now known as the Southern Rocky Mountain Volcanic Field). This switch is thought to have happened ~25 Ma and reflects a waning thermal environment where crustal geotherms returned to normal steady state. Johnson (1991) suggested that the transition reflected "basaltification" of the lower crust, but implicit in his models are the change in high to low flux and attendant changes in the geotherm. Ducea and Barton, (2007) emphasize the correlation between ε_{Nd} (and $^{87}Sr/^{86}Sr$) and magmatic flux in these arcs—episodes of high-flux magmatism coincide with negative ε_{Nd} excursions while "normal" arc flux correlates with the opposite characteristics.

Resolution of this transition at a finer scale has been challenging, but we describe here the volcanic and magmatic record of the ~1 Myr duration Purico-Chascon Volcanic Complex (PCVC) of the Central Andes. In the subduction-related Central Andes, the transition from steady state to flare-up and back in the Neogene is recorded physically and chemically in the evolution of the arc. Steady state magmatism is characterized by predominantly mafic to andesitic volcanism that has less evolved $^{87}Sr/^{86}Sr$ ratios <0.708, while the flare-up is dominantly dacitic with crustal isotopic compositions with $^{87}Sr/^{86}Sr$ ratios > 0.708. These differing characteristics are thought to be a reflection of variable degrees of crustal melting in response to changing thermal fluxes (de Silva et al., 2006; de Silva and Gosnold, 2007). The transition from flare-up to steady state happens some time after 1 Ma and is captured by the PCVC. We couple whole rock chemical characteristics, mineral phase equilibria, and *in situ* mineral compositional and isotopic data to show that the transition from flare-up to steady-state arc magmatism in the Altiplano-Puna Volcanic Complex (APVC) is recorded at all scales. With these data we develop a time transgressive view of the upper crustal magma dynamics beneath PCVC and find that the transition from flare-up to steady state at the PCVC scale mimics the transition at the arc scale as a whole.

2.3. Geologic Background

The Central Volcanic Zone (CVZ) is a ~1600 km segment of continental arc (14-28° S) located in the Andean cordillera of South America. Arc magmatism has occurred continuously in the region since ~200 Ma (e.g., Rogers and Hawkesworth 1989; Wörner, 1992) with magmatism migrating eastwards and then back westwards to its current position in response to changes in the dip of the subducting slab (Allmendinger et al., 1997). The westward migration, linked to steepening of the slab, started ~25 Ma coincident with the inception of crustal shortening that continued until at least 10 Ma resulting in crustal thicknesses in excess of 70km beneath the PCVC . Shortening was succeeded by a regional magmatic flare-up that generated significant volumes of silicic magma with strongly enriched crustal character. The most intense and most recent expression of this is the APVC between 21 and 24°S (**Figure 2.1**A; de Silva, 1989). Here, from 10-1 Ma, inferred magmatic fluxes increased by over an order of magnitude relative to steady state CVZ volcanism (de Silva and Gosnold, 2007) resulting in the eruption of >13,000 km^3 of compositionally homogeneous crystal-rich dacite magma. Activity during the flare-up occurred in distinct pulses at ~8, 6, and 4 Ma (de Silva and Gosnold, 2007; Salisbury et al., 2010). Activity has waned since 4 Ma and the last major ignimbrite eruption occurred ~0.7 Ma. Subsequent eruptions in and around the APVC have been less voluminous and primarily effusive, manifested by lava dominated composite volcanoes, numerous post-glacial dacitic lava domes and the appearance of volumetrically significant

andesite (Hawkesworth et al., 1982; de Silva et al., 1994; Watts et al., 1999; Grunder et al., 2006; Sparks, et al., 2008; Michelfelder et al., 2014; Godoy et al., 2014).

The most complete record of this transition is the PCVC, the youngest major volcanic center associated with the APVC (**Figure 2.1**). The complex is comprised of the ~1 Ma Purico ignimbrite shield (0.98 ± 0.03 Ma; Salisbury et al., 2010), the result of the eruption of ~100 km^3 crystal-rich, predominantly high-K dacite (rare andesite and rhyolite pumice are limited to one stratigraphic unit). The Purico ignimbrite is physically, texturally, compositionally, and isotopically similar to other large ignimbrites associated with the APVC (**Figure 2.3, 2.4**). The ignimbrite is capped by a summit complex of younger dacite lava domes (<10 km^3), the youngest being the ~0.18 Ma Cerro Chascon and Cerro Aspero domes (**Figure 2.1B, 2.2**; Hawkesworth et al., 1982; Francis et al., 1984; de Silva, 1991; Schmitt et al., 2001).

In contrast to the Purico ignimbrite, the younger (<0.18 Ma) lava domes (Cerro Aspero and Cerro Chascon) are significantly less voluminous (<10 km^3) and are texturally, compositionally, and isotopically heterogeneous (**Figure 2.2, 2.3, 2.4**). The domes are comprised of crystal-rich, high-K dacite lava (**Figure 2.3**) with abundant (up to 20 vol.%) under-cooled basaltic-andesite inclusions (Hawkesworth et al., 1982; Francis et al., 1984; Davidson et al., 1990). The basaltic-andesite inclusions have some of the least enriched bulk $^{87}Sr/^{86}Sr$ isotopic ratios found in the APVC and are indistinguishable from nearby steady-

state arc volcanoes and minor mafic centers (**Figure 2.4**; de Silva et al., 1993; Feeley and Davidson, 1994; Davidson and de Silva, 1992), The whole rock isotopic composition of the crystal-rich dacite of the Chascon dome falls on a linear trend between the Purico ignimbrite and basaltic-andesite lavas (Schmitt et al., 2001; **Figure 2.4**).

2.4. Petrography

Dacite pumice from the Purico ignimbrite (**Figure 2.2A, D**) is coarse-grained and crystal rich (~50 % crystals) consisting of, in decreasing abundance, plagioclase, amphibole, quartz, biotite, and rare orthopyroxene, oxides, and accessory zircon, apatite, and sphene in a groundmass of fresh, moderately to highly indurated, highly vesicular (65 vol.%) rhyolite glass (74 wt.% SiO_2). Phenocrysts are generally large (>1 mm), range from euhedral to subhedral, and are highly fractured. Disequilibrium textures are rare and restricted to resorbed zones in the interior of plagioclase crystals (<5% of plagioclase crystals).

Dacite lavas from Cerro Chascon (**Figure 2.2B, E**) are course-grained and crystal-rich (~65 % crystals), containing, in decreasing abundance, plagioclase, amphibole, quartz, clinopyroxene, biotite, k-feldspar, orthopyroxene, olivine, oxides, and accessory zircon, apatite, and sphene in a finely crystalline, moderately vesicular (24 vol.%) groundmass consisting of amphibole micro-phenocrysts in high-silica rhyolite glass (76 wt.% SiO_2). Phenocrysts are typically large (>1 mm) and range from euhedral to anhedral. K-feldspar oikocrysts are up

to ~4 cm containing plagioclase, amphibole, biotite, and quartz. Disequilibrium textures are common and include resorbed quartz with clinopyroxene mantles, dusty sieved plagioclase, and olivine with amphibole rims.

Basaltic-andesite inclusions from Cerro Chascon (**Figure 2.2C, F**) are fine-grained and porphyritic (~65 % crystals) consisting of, in decreasing abundance, amphibole, clinopyroxene, olivine, plagioclase, oxides, and rare quartz and biotite in a finely crystalline, moderately vesicular (27 vol.%) groundmass comprised of plagioclase and amphibole micro-phenocrysts in rhyolite glass (75 wt.% SiO_2). Phenocrysts are typically large (>1 mm) subhedral to anhedral, and out of equilibrium with the groundmass glass. Disequilibrium textures are prevalent including resorbed quartz with clinopyroxene mantles, dusty sieved plagioclase, and olivine with amphibole rims. Microphenocrysts are typically small (<0.5 mm) and appear to be in equilibrium with the groundmass glass.

Two striking petrographic features of rocks from the PCVC are the physical and textural similarity between individual phenocrysts from all three units and the general trend of increasing in textural maturity between the Purico ignimbrite and Cerro Chascon dacite. Phenocrysts from the Cerro Chascon dacite have similar textures and sizes as crystals from the Purico ignimbrite. However, plagioclase crystals in the Purico ignimbrite occur exclusively as individual crystals sitting in groundmass glass, whereas, plagioclase in the Cerro Chascon dacite often occur in clumps of two or more crystals annealed to one another. The Cerro Chascon dacite also contains K-feldspar oikocrysts that contain the same phenocrysts

found in the Purico ignimbrite. The lack of perthitic textures in the K-feldspar indicates the magma in which the crystals were hosted never cooled below ~600 ° C (Bowen and Tuttle, 1950). We interpret these characteristics to indicate that during the development of the Cerro Chascon magmatic system, remnants of the Purico ignimbrite magma reservoir existed as a near-solidus (>600 °C) crystal mush.

2.5. Analytical Methods

In situ major and trace element abundances were measured via electron microprobe (EMP) using a Cameca SX100 electron microprobe at Oregon State University (OSU) with five wavelength dispersive spectrometers, including two high-sensitivity large diffraction crystals for trace element analyses. Detailed run conditions, calibration procedures, and analytical errors are presented in the supplementary materials. *In situ* isotopic analyses where conducted using two methods. Selected crystals were sampled using a NuWave computer-automated micro-drill at OSU (see Charlier et al., 2006), and sampled aliquots where sent to New Mexico State University (NMSU) where elemental Sr was separated using cation-exchange chromatography. $^{87}Sr/^{86}Sr$ was then measured using thermal ionization mass spectrometry (TIMS) at NMSU. *In situ* isotopic analyses were also measured using a NuPlasma MC-ICP-MS and Photon Machines G2 Excimer laser system in the W.M. Keck Collaboratory for Mass Spectrometry at

OSU. Detailed comparison of the two methods along with analytical methods for LA-ICP-MS analyses are discussed in supplementary materials.

2.6. Crystal Chemistry

2.6.1. Plagioclase Chemistry

Plagioclase crystals from the Purico ignimbrite typically have relatively low anorthite (An_{40-55}) and MgO contents (<200 ppm; **Figure 2.5A, F; Table 2.1**) and high, restricted $^{87}Sr/^{86}Sr$ isotope ratios (0.7087-0.7090; **Figure 2.5G**). The rare crystals with resorbed surfaces have cores that define a much broader range in An (An_{39-85}; **Figure 2.5B, F**). However, these crystals show no significant core to rim differences in MgO content or $^{87}Sr/^{86}Sr$ isotope ratios (**Figure 2.5F**).

Plagioclase phenocrysts from the Chascon dacite (**Figure 2.5C**) have low anorthite (~80% of analyses between An_{40-55}; **Figure 2.5F**) and MgO contents (<200 ppm) similar to the Purico ignimbrite. Isotopically, phenocryst interiors have slightly more variable $^{87}Sr/^{86}Sr$ ratios, but they overlap with the ignimbrite (0.7083-0.7095; **Figure 2.5G**). In contrast to the plagioclase in the ignimbrite, these crystals show significant rim-ward increases in An and MgO (An_{65-80} and 500-800 ppm MgO, respectively) and decreases in $^{87}Sr/^{86}Sr$ (0.7065-0.7072; **Figure 2.5F, G; Table 2.1**).

Mafic inclusions from Cerro Chascon contain two distinct types of plagioclase (**Figure 2.5D, E**). Phenocrysts with dusty sieved textures have clear cores with low An and MgO contents (An_{39-55} and <200 ppm, respectively) and

high $^{87}Sr/^{86}Sr$ ratios (0.7085-0.7091; **Figure 2.5D, F, G; Table 2.1**). Dusty sieved zones and clear growth rims surrounding the sieved zone have significantly higher An and MgO contents (An_{65-85} and 400-800 ppm MgO) with lower $^{87}Sr/^{86}Sr$ ratios (0.7057-0.7065). Plagioclase micro-phenocrysts (**Figure 2.5E**) in the inclusions have high An and MgO contents (An_{64-84} and 500-800 ppm MgO; **Figure 2.5F**) and low, restricted $^{87}Sr/^{86}Sr$ ratios (0.7062-0.7064; **Figure 2.5G**) similar to the outermost rims of the larger crystals.

2.6.2. Amphibole Chemistry

Amphibole crystals in the PCVC can be divided into two distinct groups based on their size and major element compositions (**Figure 2.6A, B, C**). Large (typically >1 mm) low-Al amphiboles found in both the Purico ignimbrite and the Cerro Chascon lava dome (**Figure 2.6A, C**) have relatively low Al_2O_3 with high SiO_2. Site-specific cation abundances calculated using the methods outlined by Tepley et al., (2013) are presented in Figure 2.6D-F and show that low-Al amphiboles have relatively low ^{IV}Al, ^{C}Ti, and Mg# [Mg/(Mg+Fe2+)] and high ^{T}Si. Following the classification scheme of Leake et al., (1997) the amphiboles are tschermakites (**Figure 2.6D**). There are no systematic compositional differences between cores and rims in these crystals. Rims range from ~ +1 to -1 wt.% Al_2O_3 relative to crystal cores and many amphiboles have cores and rims that are indistinguishable. Similarly, SiO_2, ^{IV}Al, ^{C}Ti, and Mg# do not vary systematically between cores and rims.

Cerro Chascon lavas contain a second population of high-Al amphibole (**Figure 2.6B, C**) not found in the Purico ignimbrite (most prevalent in mafic inclusions). This population is dominated by micro-phenocrysts (<0.5 mm) with significantly higher Al_2O_3, and lower SiO_2 than the low-Al magnesiohornblendes. These high-Al amphiboles also have significantly higher ^{IV}Al, ^{C}Ti, and Mg#, and lower ^{T}Si (**Figure 2.6D-F**) and are classified as tschermakites (Leake et al., 1997; Figure6D-F). Similar to the magnesiohornblendes, these crystals show no systematic core to rim variations in major elements or cation abundances.

An important observation is that the two amphibole populations form distinct groups in major element space separated by ~3 wt. Al_2O_3 (**Figure 2.6C**). In addition, significant differences in site-specific cation abundances are consistent with amphibole populations that grew at distinct pressures and temperatures (e.g., Helz, 1982; Hammarstrom and Zen, 1986; Holland and Blundy, 1994; Anderson and Smith, 1995; Ridolfi et al., 2010). In the following section, we investigate the relationships between amphibole compositions and crystallization pressures and temperatures for the Purico ignimbrite and Cerro Chascon lavas and show how the crystallization conditions change over the history of the PCVC.

2.7. P-T conditions

Magmatic temperatures were determined using the amphibole thermobarometer of Ridolfi et al., (2010) and the plagioclase-amphibole

thermometer of Holland and Blundy (1994) and are presented in Figure 2.7. Low-Al magnesiohornblendes from the Purico ignimbrite and Cerro Chascon lavas yield temperatures between 788 and 865 ± 25 °C (Ridolfi et al., 2010), similar to temperatures reported by Abbot (2009) for the Purico ignimbrite (766-845 °C) and Schmitt et al., (2001) for the Purico ignimbrite and Cerro Chascon dacite (795-800 and 830 °C, respectively). In contrast, high-Al tschermakites from Cerro Chascon modeled using the amphibole thermobarometer of Ridolfi et al., (2010) yield significantly higher temperatures (928- 1001 ± 25 °C). To verify the temperatures calculated using the model of Ridolfi et al., (2010) magmatic temperatures were also calculated using the edenite-richterite exchange thermometer of Holland and Blundy, (1994) for touching plagioclase-amphibole micro-phenocryst pairs (**Figure 2.7**). Temperatures calculated using this method (925-973 ± 40 °C) are indistinguishable from temperature estimates calculated using the Ridolfi et al., (2010) model when uncertainties are factored in.

Amphibole crystallization pressures were determined using the amphibole thermobarometer of Ridolfi et al. (2010) and the Al-in-amphibole barometer of Anderson and Smith (1995) (**Figure 2.7**). Low-Al magnesiohornblendes from the Purico ignimbrite and Cerro Chascon crystallized between 85 and 205 ± 15 MPa (Ridolfi et al., 2010), similar to pressures reported by Abbot (2009) and Schmitt et al., (2001) for the Purico ignimbrite using the Al-in-amphibole barometer of Anderson and Smith (1995; 70-200 MPa and 150-160 MPa, respectively). These pressures are also similar to pressures reported from other large ignimbrites in

the APVC (~100-200 MPa; Folkes et al., 2011; Abbot, 2009). In contrast, high-Al tschermakites from the Cerro Chascon lavas yield significantly higher pressures (396-580 MPa), with 80% of crystals between 396 and 550 MPa. Al-in-amphibole pressures were not calculated for the high-Al tschermakites as their crystallization temperatures far exceeded the temperatures at which the Anderson and Smith (1995) barometer is calibrated.

2.8. The story in the crystals: magma dynamics at the Purico-Chascon Volcanic Complex

Plagioclase crystals from the Purico ignimbrite have high, relatively restricted $^{87}Sr/^{86}Sr$ isotope ratios (0.7087-0.7090), while amphiboles are low-Al magnesiohornblendes that record crystallization in cool (~800-850° C) upper crustal (4-8 km depth) conditions. Crystals from Cerro Chascon domes record two distinct magmatic environments. High $^{87}Sr/^{86}Sr$ plagioclase crystals and low-Al amphiboles in both the dacite and basaltic-andesite inclusions are texturally, compositionally, and isotopically identical to crystals from the Purico ignimbrite and grew in a similar low temperature (~800-850 °C), upper-crustal (4-8 km depth) environment. In contrast, low $^{87}Sr/^{86}Sr$ plagioclase micro-phenocrysts from the basaltic andesite inclusions with significantly lower $^{87}Sr/^{86}Sr$ isotope ratios and high-Al tschermakitic amphibole equilibrated between 20 and 15 km. Based on these data we construct a time-transgressive cross section of the magma dynamics beneath the Purico-Chascon volcanic system to show how magma

generation, accumulation, and storage changed over the 800 kyr history of the PCVC (**Figure 2.9**).

Comparison of the Purico ignimbrite shield and the Cerro Chascon lava dome reveals two very distinct upper crustal magmatic plumbing systems (Figure 9). During the eruption of 1 Ma Purico ignimbrite, thermobaromety indicates the presence of a large, relatively cool (~800-850 °C), 4-8 km deep upper crustal magma reservoir. The reservoir was predominantly dacite and had high, relatively restricted isotope ratios reflecting high degrees of crustal contamination (de Silva, 1991; Schmitt et al., 2001). Schmitt et al., (2001) combined bulk rock radiogenic isotope and trace element data and determined that the crustal contamination occurred in the mid-crust (between 30 and 15 km depth) in response to the ponding of ascending arc-derived basalts. Approximately 50 to 70% assimilation of crust, represented by basement compositions analyzed by Lucassen et al. (2001), is required to explain the isotopic composition of the Purico ignimbrite (Schmitt et al. 2001). Although andesite is rare in the Purico ignimbrite, temperature and pressure estimates for the andesite pumice record magma storage in a higher temperature (965 °C) mid-crustal (~20-17 km depth) magma reservoir (Schmitt et al., 2001), consistent with a regional low gravity anomaly thought to represent the Altiplano-Puna magma body (APMB; Chmielowski, 1999; de Silva et al., 2006). Andesite pumice within the Purico ignimbrites have isotopic ratios identical to the dominant dacite pumice and indicate that the baseline isotopic signature of the APMB was between 0.7085

and 0.7090 during the formation of the Purico magma body (de Silva, 1991; Schmitt et al., 2001). So, while andesite and dacite magmas were clearly being supplied from a deeper APMB source, the magmas had enriched isotopic compositions >0.708, and appear to have crystallization exclusively in a cool, shallow crustal reservoir between 4-8 km deep.

Approximately 800 Kyr later, during the eruption of the Cerro Chascon lava dome, there is evidence for a major change in the magmatic dynamics below Purico. Two compositionally and isotopically distinct magmas crystallized in two distinct magma reservoirs (**Figure 2.9**). The upper crustal reservoir is compositionally and isotopically indistinguishable from the Purico ignimbrite magma reservoir. The deeper APMB is represented by basaltic-andesite inclusions, plagioclase micro-phenocrysts and high-Al amphiboles, and lower $^{87}Sr/^{86}Sr$ isotope ratios (0.7057-0.7065) that are clearly distinguishable from the upper crustal reservoir (0.7085-0.7091). Davidson et al., (1990) proposed that these basaltic-andesite inclusions represent a recharge magma that reheated and mixed with the Purico ignimbrite basement, exchanged crystals and material, and creating the hybrid Cerro Chascon dacite. However, our observations of the increase in textural coarseness of the Chascon dacite compared to the Purico ignimbrite pumice and the presence K-feldspar oikocrysts within the Cerro Chascon dacite suggest that during the time of the recharge event, the Purico magma reservoir existed as a near-solidus crystalline mush in the upper crust. We also add that the recharging basaltic andesite crystallized extensively at

APMB depths, which is supported by macroscopic and microscopic textures, plagioclase micro-phenocrysts, high-Al amphibole, and less enriched $^{87}Sr/^{86}Sr$ isotope ratios in both basaltic andesite inclusions and plagioclase micro-phenocrysts. Importantly, in the ~800 ky between the eruptions of the Purico ignimbrite and the Cerro Chascon lava dome the baseline isotopic composition of magmas supplied into the shallow (4-8 km) Purico magma reservoir from the APVC decreased dramatically. These changes in the upper crustal magmatic architecture during the evolution of the PCVC can be examined in the context of evolutionary and thermal state of the CVZ arc from 1 Ma to present.

2.9. Recording the transition from flare-up to steady-state arc magmatism in the Purico-Chascon Volcanic Complex

2.9.1 The Purico Ignimbrite represents the flare-up

Previous work clearly established the 10 to 1 Ma APVC flare-up was characterized by dacitic magmas with a strong "crustal" affinity (de Silva, 1989; Coira et al., 1993; Ort et al., 1996; Lindsay et al., 2001; de Silva et al., 2006). These have significantly higher $^{87}Sr/^{86}Sr$ isotope ratios than typical steady state CVZ lavas (**Figure 2.8A**; compiled from Mamani et al., 2010). Bulk pumice from the 1 Ma Purico ignimbrite is isotopically indistinguishable from other APVC ignimbrites (**Figure 2.8A, B**; de Silva, 1991; Schmitt et al., 2001). Here we have shown that individual plagioclase crystals from the Purico ignimbrite are also isotopically identical to bulk rock isotopic measurements from the ignimbrite

pumice; the elevated isotopic signal of the APVC flare-up is thus recorded at the crystal scale (**Figure 2.8C**).

In addition to the elevated radiogenic isotope ratios, the isotopic homogeneity of the pumice and crystals from the Purico ignimbrite are evidence that these are flare-up magmas. Folkes et al. (2013) proposed that compositional and isotopic homogeneity in ignimbrites from the Cerro Galan caldera in NW Argentina are generated in a lower-crustal (>35 km) processing center similar to the MASH (melting, assimilation, storage, and homogenization) zone as proposed by Hildreth and Moorbath (1988). Multiple workers (e.g. de Silva, 1989; Lindsay et al., 2001; Schmitt et al., 2001) argue that during the APVC flare-up, extensive crustal assimilation and fractional crystallization between 35 and 15 km depth led to the generation of large amounts of isotopically enriched (0.7080-0.7132); Schmitt et al., 2001; **Figure 2.9A**) intermediate magma and the formation of the APMB at >17 km depth (Chmielowski, 1999; de Silva et al., 2006). Once established, APMB would have buffered the composition(s) of magmas by trapping ascending mafic magmas to offset extensive fractionation (Glazner and Ussler, 1988). Del Potro et al., (2013) suggest that the APMB maybe vertically zoned with dacitic magmas overlying dominant andesite. Thus the APMB represents an accumulation zone of dacite and andesite where extensive differentiation may occur through mixing, crystallization, and assimilation. From here dacite and andesite ascend and accumulate in the upper crust to form the upper crustal APVC magma reservoirs. Once the magmas

reach the upper crust, convective stirring (e.g. Sparks et al., 1984) and diffusive equilibration (Blake and Koyaguchi, 1991) may have further homogenized magmas. U-series isotope studies focused on individual crystals within these large silicic magma reservoirs indicate the magmas remain above solidus temperatures from 10^5-10^6 years (Reid et al., 1997; Vasquez and Reid, 1997; Schmitt et al., 2003; Folkes et al., 2011) increasing the likelihood that the aforementioned processes would eliminate compositional heterogeneities. It has also been shown that large silicic magma reservoirs tend to have higher aspect ratios than smaller, compositionally similar reservoirs (de Silva, 1991; de Silva and Wolff, 1995) and that homogeneity can be caused by the selective sampling of distinct magmatic horizons during the evacuation of the magma reservoir (Smith et al., 1979; de Silva, 1991; de Silva and Wolff, 1995).

2.9.2. Cerro Chascon as signaling the return to steady state magmatism

The small volume, effusive, bimodal character of Cerro Chascon is in marked contrast to the flare-up ignimbrites. The dacite lava of Cerro Chascon is consistent with it representing remnant magma from the flare-up. The most likely state was that of a near-solidus crystal mush. However, the basaltic-andesite inclusions are the most mafic compositions recorded in the APVC and similar to mafic inclusions found in other arc settings (e.g. Eichelberger, 1980; Clynne, 1999; Tepley et al., 1999; Murphy et al., 2000; Coombs et al., 2003; Browne et al., 2006). Isotopically, the mafic inclusions have the lowest $^{87}Sr/^{86}Sr$ isotope ratios in

the APVC (**Figure 2.4, Figure 2.8A, B**) and are identical to the range of isotope ratios observed in recent CVZ arc lavas (Mamani et al., 2010) and small back-arc centers on the Bolivian Altiplano. Davidson et al. (1990) proposed that the Cerro Chascon dacite is more variable in composition because it represents a mixture of the basaltic-andesite magma and the Purico ignimbrite magma. At the crystal-scale, plagioclase crystals from the basaltic-andesite inclusions span the entire isotopic range of observed at the PCVC (**Figure 2.5G, 2.8A, B**). Crystal cores record elevated $^{87}Sr/^{86}Sr$ ratios associated with the flare-up, and rims record much lower $^{87}Sr/^{86}Sr$ ratios characteristic of steady-state CVZ arc (**Figure 2.8A, C**). The most non-radiogenic Sr isotopic signatures from the Central Andes are ~0.705, referred to as "baseline" composition by Davidson et al., (1991). These these have been attributed to both enriched mantle compositions (e.g. Rogers and Hawkesworth, 1989; Kay et al., 2010) and lower crustal assimilation of MASH (Davidson et al, 1991). We do not try to distinguish between these models, but note that the low $^{87}Sr/^{86}Sr$ ratios of Cerro Chascon and CVZ arc volcanoes attest to significantly less crustal processing of magmas from the APVC ignimbrites, and basaltic-andesite inclusions and plagioclase micro-phenocrysts from Cerro Chascon record very little isotopic modification in the in the crust. We interpret this as signaling that conditions in the crust were not conducive to producing significant "crustal" magmas ~200 ka, thus recording the isotopic character of the enriched upper mantle or lower crust.

The preservation of textural and chemical heterogeneities in the Cerro Chascon system provides insight into the changes occurring in the PCVC during the transition away from an ignimbrite flare up. In contrast to the Purico ignimbrite, which signals upper crustal processes, Cerro Chascon lavas and enclaves record the textural, compositional, and isotopic signature of two distinct magmas from two distinct storage environments; a waning upper crustal system and a lower crust or mantle signal. This bimodality indicates that the magmas did not thoroughly mix prior to eruption, a common feature of arc-related rocks (e.g. e.g. Davidson and Tepley, 1997; Tepley et al., 1999, 2013; Kent et al., 2010; Koleszar at el., 2012). Instead, injection of the mafic magma into the near-solidus remnant Purico magma reservoir likely triggered an eruption (e.g., Anderson, 1976; Sparks et al., 1977; Blake, 1981, 1984; Eichelberger et al., 1986; Pallister, 1992; Watts et al., 1999; Murphy et al., 2000; de Silva et al., 2008; Tepley et al., 2013) interrupting the mixing processes before the magmas could homogenize. Note that by ~200 ka, the buffering feedbacks operating deeper in crust, the APMB, during the flare-up were no longer a factor. In contrast to enriched dacites and andesites being delivered to the upper crust during the flare-up, more “primitive” basaltic-andesites were able to ascend into the upper crust with only limited modification at ~20 km, and heterogeneities were maintained the individual lavas.

2.10. Recording the waning of a flare-up

The concept of increased mantle heat flux and elevated geothermal gradients is central to our understanding of magmatic flare-ups (Lipman et al., 1972; Coney, 1978; de Silva, 1989; Best and Christiansen, 1992). The thermal history of a flare up can be characterized in distinct waxing, peak, and then waning stages. The time-volume signal of large silicic volcanic fields is posited to record this evolution during the development and death of a large regional magma reservoir. In the case of the APVC, this regional magma reservoir is the APMB (de Silva and Gosnold, 2007; Salisbury et al., 2010). de Silva and Gosnold (2007) created a 2-D, conductive heat flow model to evaluate the response of the CVZ crustal geothermal gradients to the emplacement of a large sill in the mid-crust (17-19 km) and found that (1) after 1 Ma the local geothermal gradient (within ~2 km of the heat source) would elevate to above the wet solidus of the average CVZ crust, and (2) after 10 Ma the geothermal gradient would elevate to where the brittle-ductile transition extends into the upper crust. The high degrees of upper crustal assimilation needed to explain the compositional and isotopic character of the Purico ignimbrite are consistent with the relationship between the upper crustal temperatures and the estimated wet solidus of the regional basement. During the formation of Purico magmatic system, the crust would have been thermally primed following ~10 Ma of high mantle heat input, including an apparent focusing of flare-up magmatism ~ 25 km E of the PCVC at the Guacha and La Pacana caldera systems. The inferred elevated flux of mafic magmas would have had sufficient thermal energy to induce significant assimilation and

melting in the thermally matured upper crust. Elevated geotherms and associated temperature-dependant effects, such as elevation of the brittle-ductile transition in the uppermost crust would have permitted the accumulation of larger magma bodies like that which fed the Purico ignimbrite (de Silva and Gosnold, 2007; Gregg et al., 2012).

In contrast, the lack of evidence for significant modification of lower crustal or mantle derived mafic magmas from Cerro Chascon indicate that the APMB buffering feedbacks were no longer in operation. The geothermal gradient had relaxed by ~200 ka (**Figure 2.9B**) and a higher temperature contrast between low-flux mafic magma and the crust meant that ascending mafic magmas were emplaced into the shallow crust without being trapped, filtered and processed. The textural, compositional, and isotopic heterogeneity of the Cerro Chascon lavas are also consistent with a decreased geothermal gradient, increased thermal contrast, and relaxation of the brittle-ductile transition from flare-up time. Rather than accommodating large volumes of magma, magmatic addition under brittle upper crustal conditions would be more likely to trigger an eruption (Gregg et al., 2012, 2013), interrupting the mixing process and preserving the two distinct magmas.

2.11. Conclusions

The PCVC records the transition from flare-up to steady-state arc magmatism over an ~800 ky period at a variety of scales. At ~1 Ma, the Purico

ignimbrite shield records restricted and enriched whole rock and *in situ* plagioclase $^{87}Sr/^{86}Sr$ isotope ratios >0.708. *In situ* $^{87}Sr/^{86}Sr$ isotope ratios and amphibole thermobarometry indicate that significant magma generation was occurring in the mid-crust during this time, but magmas supplied to the shallow crust (4-8 km) were compositionally and isotopically homogeneous. Approximately 800 ky later, two distinct magmatic environments, one representing the near solidus residual crystal mush from the Purico ignimbrite magma, and a second deeper, higher temperature, and isotopically "primitive" magma are recorded in the Cerro Chascon dacite, basaltic-andesite enclaves, and plagioclase and amphibole phenocrysts. The character of the Purico ignimbrite is consistent with flare-up magmatism where an elevated mantle flux results in high geothermal gradients and extensive crustal processing of parental magmas in a thermally primed upper crust. Cerro Chascon records the waning of the flare-up and return to steady state conditions. As the heat source for the flare-up decreases, thermal gradients in the crust relax resulting in less crustal processing of deep crustal or mantle-derived magmas. As these magmas penetrate they may stage briefly at ~20 km and differentiate. They then rising into the upper crust to interact with and rejuvenate remnant (flare-up related) crystal-mush. The PCVC records significant reorganization of magma dynamics and crustal architecture in an ~800 kyr period when the Andean arc transitions from flare-up to steady state. The imprint of these processes recorded at all scales

from arc to crystals implies that the crystal-scale studies, particularly *in situ* isotopes, has significant potential for unraveling large (arc-scale) scale processes.

2.12. References

Abbot M. (M.S. Thesis) Development of continental magmatic systems: insights from amphibole chemistry of the Altiplano-Puna Volcanic Complex, central Andes. Oregon State University, Corvallis, OR, USA (2009).

Allmendinger, R. W., Jordan, T. E., Kay, S. M. & Isacks, B. The evolution of the Altiplano-Puna plateau of the Central Andes. *Annual Review of Earth and Planetary Sciences* **25,** 139–174 (1997).

Anderson, A. Magma mixing: petrological process and volcanological tool. *Journal of Volcanology and Geothermal Research* **1,** 3–33 (1976).

Anderson, J. L. & Smith, D. R. The effects of temperature and fo_2 on the Al-in-hornblende barometer. *American Mineralogist* **80**, 549-559 (1995).

Bachmann, O., Miller, C.F. & de Silva, S.L. The volcanic-plutonic connection as a stage for understanding crustal magmatism. *Journal of Volcanology and Geothermal Research* **167,** 1–23 (2007).

Barquero-Molina, M. (M.S. Thesis) $^{40}Ar/^{39}Ar$ Chronology and Paleomagnetism of Ignimbrites and Lavas from the Central Volcanic Zone, Northern Chile, and $^{40}Ar/^{39}Ar$ Chronology of Silicic Ignimbrites from Honduras and Nicaragua. University of Wisconsin, Madison, WI, USA (2003).

Best, M. G. & Christiansen, E. H. Limited extension during peak Tertiary volcanism, Great Basin of Nevada and Utah. *Journal of Geophysical Research* **96,** 13,509–13,528 (1991).

Blake, S. Volcanism and the dynamics of open magma chambers. *Nature* **289**, 783-785 (1981).

Blake, S. Volatile oversaturation during the evolution of silicic magma chambers as an eruption trigger. *Journal of Geophysical Research* **89,** 8237–8244 (1984).

Blake, S. & Koyaguchi, T. Insights on the magma mixing model for volcanic rocks. *in* Didier J. & Barbarin, B., eds, Enclaves and Granite Petrology. Elsevier Science, New York, NY, USA, 403–413 (1991).

Browne, B. L., Eichelberger, J.C., Patino, L.C., Vogel, T.A., Dehn, J., Uto, K. & Hoshizumi, H. Generation of Porphyritic and Equigranular Mafic Enclaves During Magma Recharge Events at Unzen Volcano, Japan. *Journal of Petrology* **47,** 301–328 (2006).

Charlier, B.L.A., Ginibre, C., Morgan, D., Nowell, G.M., Pearson, D.G., Davidson, J.P. & Ottley, C.J. Methods for the microsampling and high-precision analysis of strontium and rubidium isotopes at single crystal scale for petrological and geochronological applications. *Chemical Geology* **232,** 114–133 (2006).

Chmielowski, J., Zandt, G. & Haberland, C. The Central Andean Altiplano-Puna magma body. *Geophysical Research Letters* **26,** 783–786 (1999).

Coira, B., Mahlburg-Kay, S. & Viramonte, J. Upper Cenozoic magmatic evolution of the Argentine Puna: a model for changing subduction geometry. *International Geological Review* **35**, 677–720 (1993)

Coney, P.J., 1978, Mesozoic-Cenozoic Cordilleram plate tectonics. *in* Smith, R.B. & Eaton, G.P., eds, Cenozoic tectonics and regional geophysics of the western Cordillera. *Geological Society of America Memoir* 152, 33-50 (1978).

Coombs, M.L., Eichelberger, J.C. & Rutherford, M.J. Experimental and textural constraints on mafic enclave formation in volcanic rocks. *Journal of Volcanology and Geothermal Research* **119,** 125–144 (2003).

Davidson, J.P., de Silva, S.L., Holden, P. & Halliday, A.N. Small-Scale Disequilibrium in a Magmatic Inclusion its More Silicic Host. *Journal of Geophysical Research* **95,** 17661–17675 (1990).

Davidson, J.P., Harmon, R.S. & Worner, G. The source of central Andean magmas; Some considerations. *Geological Society of America Special Paper* **265,** 233–245 (1991).

Davidson, J.P. & de Silva, S.L. Volcanic rocks from the Bolivian Altiplano: Insights into crustal structure, contamination, and magma genesis in the central Andes. *Geology* **20,** 1127-1130 (1992).

Davidson, J.P. & Tepley, F.J. Recharge in volcanic systems: evidence from isotope profiles of phenocrysts. *Science* **275,** 826-829 (1997).

DeCelles, P. G., Ducea, M. N., Kapp, P. & Zandt, G. Cyclicity in Cordilleran orogenic systems. *Nature Geoscience* **2,** 251–257 (2009).

de Silva, S.L. Altiplano-Puna volcanic complex of the central Andes. *Geology* **17,** 1102-1106 (1989a).

de Silva, S.L. Geochronology and stratigraphy of the ignimbrites from the 21 °30's to 23 °30's portion of the central Andes of northern Chile. *Journal of Volcanology and Geothermal Research* **37,** 93–131 (1989b).

de Silva, S.L. Styles of zoning in central Andean ignimbrites; Insights into magma chamber processes. *Geological Society of America Special Paper* **265,** 217–232 (1991).

de Silva, S.L. & Francis, P.W. Volcanoes of the Central Andes, Springer-Verlag, Berlin (1991).

de Silva, S.L., Self, S., Francis, P.W., Drake, R.E. & Ramirez, C. Effusive silicic volcanism in the Central Andes: The Chao dacite and other young lavas of the Altiplano-Puna Volcanic Complex. *Journal of Geophysical Research* **99,** 17805–17825 (1994).

de Silva, S.L. & Wolff, J.A. Zoned magma chambers: the influence of magma chamber geometry on sidewall convective fractionation. *Journal of Volcanology and Geothermal Research* **65,** 111–118 (1995).

de Silva, S.L., Zandt, G., Trumbull, R., Viramonte, J. G. & Jimenez, G. S. N. Large ignimbrite eruptions and volcano-tectonic depressions in the Central

Andes: a thermomechanical perspective. *Geological Society of London Special Publication* **269**, 1–17 (2006).

de Silva, S.L. & Gosnold, W.D. Episodic construction of batholiths: Insights from the spatiotemporal development of an ignimbrite flare-up. *Journal of Volcanology and Geothermal Research* **167,** 320–335 (2007).

de Silva, S.L., Salas, G. & Schubring, S. Triggering explosive eruptions—The case for silicic magma recharge at Huaynaputina, southern Peru. *Geology* **36,** 387-390 (2008).

del Potro, R., Díez, M., Blundy, J., Camacho, A. G. & Gottsmann, J. Diapiric ascent of silicic magma beneath the Bolivian Altiplano. *Geophysical Research Letters* **40,** 2044–2048 (2013).

Ducea, M.N. The California arc: Thick granitic batholiths, eclogitic residues, lithospheric-scale thrusting, and magmatic flare-ups. *GSA Today* **11,** 4–10 (2001).

Ducea, M.N. & Barton, M.D. Igniting flare-up events in Cordilleran arcs. *Geology* **35,** 1047-1050 (2007).

Eichelberger, J.C. Vesiculation of mafic magma during replenishment of silicic magma reservoirs. *Nature* **288,** 446–450 (1980).

Eichelberger, J.C., Carrigan, C.R. & Westrich, H.R. Non-explosive silicic volcanism. *Nature* **323,** 598-602 (1986).

Elston, W. E. Mid-Tertiary ash flow tuff cauldrons, southwestern New Mexico. *Journal of Geophysical Research* **89,** 8733–8750 (1984).

Feeley, T.C. & Davidson, J.P. Petrology of Calc-Alkaline Lavas at Volcan Ollague and the Origin of Compositional Diversity at Central Andean Stratovolcanoes. *Journal of Petrology* **35**, 1295-1340 (1994)

Ferrari, L., López-Martínez, M., Rosas-Elguera, J. Ignimbrite flare-up and deformation in the southern Sierra Madre Occidental, western Mexico: Implications for the late subduction history of the Farallon plate. *Tectonics* **21,** 1-24 (2002).

Folkes, C.B., de Silva, S.L., Wright, H.M. & Cas, R.A.S. Geochemical homogeneity of a long-lived, large silicic system; evidence from the Cerro Galán caldera, NW Argentina. *Bulletin of Volcanology* **73**, 1455-1486 (2011).

Francis, P.W., McDonough, W.F., Hammill, M., O'Callaghan, L. J. O. & Thorpe, R.S. The Cerro Purico Shield Complex, North Chile. *in* Harmon, R.S., Barreiro, B.A., eds, Andean magmatism; chemical and isotopic constraints. Birkhauser, Switzerand, 106-123 (1984).

Glazner, A. F. & Ussler, W. Trapping of magma at midcrustal density discontinuities. *Geophysical Research Letters* **15,** 673–675 (1988).

Godoy, B., Wörner, G., Kojima, S., Aguilera, F., Simon, K. & Hartmann, G. Low-pressure evolution of arc magmas in thickened crust: The San Pedro-Linzor volcanic chain, Central Andes, Northern Chile. *Journal of South American Earth Sciences* **52**, 24-42 (2014)

Gregg, P.M., de Silva, S.L., Grosfils, E.B. & Parmigiani, J.P. Catastrophic caldera-forming eruptions: Thermomechanics and implications for eruption triggering and maximum caldera dimensions on Earth. *Journal of Volcanology and Geothermal Research* **241-242**, 1-12 (2012).

Grunder, A.L., Klemetti, E.W., Feeley, T.C. & McKee, C.M. Eleven million years of arc volcanism at the Aucanquilcha Volcanic Cluster, northern Chilean Andes: implications for the life span and emplacement of plutons. *Transactions of the Royal Society of Edinburgh: Earth Sciences* **97**, 415-436 (2006).

Hammarstrom, J.M. & Zen, E. Aluminum in hornblende: An empirical igneous geobarometer. *American Mineralogist* **71**, 1297-1313 (1986).

Hawkesworth, C.J., Hammill, M., Gledhill, A.R., van Calsteren, P. & Rogers, G. Isotope and trace element evidence for late-stage intra-crustal melting in the High Andes. *Earth and Planetary Science Letters* **58,** 240–254 (1982).

Hildreth, W. Gradients in Silicic Magma Chambers: Implications for Lithospheric Magmatism. *Journal of Geophysical Research* **86,** 10153–10192 (1981).

Hildreth, W. & Moorbath, S. Crustal contributions to arc magmatism in the Andes of central Chile. *Contributions to Mineralogy and Petrology* **98,** 455–489 (1988).

Holland, J.D. & Blundy, T.J.B. Calcic amphibole equilibria and a new amphibole±plagioclase geothermometers, *Contributions to Mineralogy and Petrology* **104**, 208-224 (1994).

Isacks B.L. 1988. Uplift of the central Andean plateau and bending of the Bolivian orocline. *Journal of Geophysical Research* **93**, 3211–3231 (1988),

Jacobsen, S. B., Quick, J. E. & Wasserburg, G. J. A Nd and Sr isotopic study of the Trinity peridotite; implications for mantle evolution. *Earth and Planetary Science Letters* **68,** 361–378 (1984).

Johnson, C.M. Large-scale crust formation and lithospheric modification beneath middle to late Cenozoic calderas and volcanic fields, western North America. *Journal of Geophysical Research* **96**, 13485-13507 (1991).

Kay, S. M., Coira, B. L., Caffe, P. J. & Chen, C-H. Regional chemical diversity, crustal and mantle sources and evolution of central Andean Puna plateau ignimbrites. *Journal of Volcanology and Geothermal Research* **198,** 81–111 (2010).

Kent, A. J. R., Darr, C., Koleszar, A. M., Salisbury, M. J. & Cooper, K. M. Preferential eruption of andesitic magmas through recharge filtering. *Nature Geoscience* **3,** 1–6 (2010).

Koleszar, A. M., Kent, A. J. R., Wallace, P. J. & Scott, W. E. Controls on long-term low explosivity at andesitic arc volcanoes: Insights from Mount Hood, Oregon. *Journal of Volcanology and Geothermal Research* **219-220,** 1–14 (2012).

Martin, V.M., Davidson, J.P., Morgan, D. & Jerram, D.A. Using the Sr isotope compositions of feldspars and glass to distinguish magma system components and dynamics. *Geology* **38**, 539-542 (2010).

Michelfelder, G.S., Feeley, T.C., Wilder, A.D. & Klemetti, E.W. Modification of the Continental Crust by Subduction Zone Magmatism and *Vice-Versa*: Across-Strike Geochemical Variations of Silicic Lavas from Individual Eruptive Centers in the Andean Central Volcanic Zone. *Geosciences* **3**, 633-667 (2013).

Murphy, M.D., Sparks, R.S.J., Barclay, J., Carroll, M.R. & Brewer, T.S. Remobilization of Andesite Magma by Intrusion of Mafic Magma at the Soufriere Hills Volcano, Montserrat, West Indies. *Journal of Petrology* **41,** 21–42 (2000).

Lindsay, J.M., Schmitt, A.K., Trumbull, R.B., de Silva, S.L., Siebel, W. & Emmermann, R. Magmatic evolution of the La Pacana calderan system, central Andes, Chile: Compositional variation of two cogenetic, large-volume felsic ignimbrites. *Journal of Petrology* **42,** 459–486 (2001).

Lipman, P.W., Prostka, H.J. & Christiansen, R.L. Cenozoic volcanism and plate-tectonic evolution of the western United States. I. Early and Middle Cenozoic. *Philosophical Transactions of the Royal Society of London A* **271,** 217-248 (1972).

Lipman, P.W., Doe, B. R., Hedge, C. E. & Steven, T. A. Petrologic evolution of the San Juan volcanic field, southwestern Colorado: Pb and Sr isotope evidence. *Geological Society of America Bulletin* **89,** 59-82 (1978).

Lipman, P.W. Incremental assembly and prolonged consolidation of Cordilleran magma chambers: Evidence from the Southern Rocky Mountain volcanic field. *Geosphere* **3,** 42-70 (2007).

Lucassen, F., Becchio, R., Harmon, R., Kasemann, S., Franz, G., Trumbull, R., Wilke, H-G., Romer, R.L., & Dulski, P. *et al.* Composition and density model of the continental crust at an active continental margin—the Central Andes between 21° and 27 °S. *Tectonophysics* **341,** 195–223 (2001).

Mamani, M., Worner, G. & Sempere, T. Geochemical variations in igneous rocks of the Central Andean orocline (13 °S to °18 S): Tracing crustal thickening and magma generation through time and space. *Geological Society of America Bulletin* **122,** 162–182 (2010).

Ort, M. H., Coira, B. L. & Mazzoni, M. M. Generation of a crust-mantle magma mixture: magma sources and contamination at Cerro Panizos, central Andes. *Contributions to Mineralogy and Petrology* **123,** 308–322 (1996).

Reid, M., Coath, C., Mark Harrison, T. & McKeegan, K. Prolonged residence times for the youngest rhyolites associated with Long Valley Caldera: ^{230}Th--^{238}U ion microprobe dating of young zircons. *Earth and Planetary Science Letters* **150,** 27–39 (1997).

Ridolfi, F., Renzulli, A. & Puerini, M. Stability and chemical equilibrium of amphibole in calc-alkaline magmas: an overview, new thermobarometric formulations and application to subduction-related volcanoes. *Contributions to Mineralogy and Petrology* **160,** 45–66 (2010).

Rogers, G. & Hawkesworth, C.J. A geochemical traverse across the North Chilean Andes: evidence for crust generation from the mantle wedge. *Earth and Planetary Science Letters* **91**, 271-285 (1989).

Salisbury, M. J., Jicha, B.R., de Silva, S.L., Singer, B.S., Jiménez, N.C. & Ort, M.H. $^{40}Ar/^{39}Ar$ chronostratigraphy of Altiplano-Puna volcanic complex ignimbrites reveals the development of a major magmatic province. *Geological Society of America Bulletin* **123,** 821–840 (2011).

Schmitt, A., de Silva, S., Trumbull, R. & Emmermann, R. Magma evolution in the Purico ignimbrite complex, northern Chile: evidence for zoning of a dacitic magma by injection of rhyolitic melts following mafic recharge. *Contributions to Mineralogy and Petrology* **140,** 680–700 (2001).

Silver, L.T. & Chappell, B. The Peninsular Ranges batholith: An insight into the evolution of the Cordilleran batholiths of southwestern North America: *Transactions of the Royal Society of Edinburgh: Earth Sciences* **79**, 105–121 (1988).

Smith, R. L. Ash-flow magmatism. *Geological Society of America Special Paper* **180,** 1–23 (1979).

Sparks, R.S.J. & Sigurdsson, H. Magma mixing: a mechanism for triggering acid explosive eruptions. *Nature* **267,** 315–318 (1977).

Sparks, R.S.J. & Marshall, L.A. Thermal and mechanical constraints on mixing between mafic and silicic magmas. *Journal of Volcanology and Geothermal Research* **29,** 99–124 (1986).

Sparks, R.S.J., Huppert, H.E., & Turner, J.S. The fluid dynamics of evolving magma chambers. *Philosophical Transactions of the Royal Society of London A* **310,** 511–534 (1984).

Sparks, R.S.J., Folkes, C.B., Humphreys M.C.S., Barfod, D.N., Clavero, J., Sunagua, M.C., McNutt, S.R. & Pritchard, M.E. Uturuncu Volcano, Bolivia: Volcanic unrest due to mid-crustal magma intrusion. *American Journal of Science* **308**, 727-769 (2008).

Tepley, F. J., Davidson, J. P. & Clynne, M. A. Magmatic Interactions as Recorded in Plagioclase Phenocrysts of Chaos Crags, Lassen Volcanic Center, California. *Journal of Petrology* **40,** 787–806 (1999).

Tepley, F. J., de Silva, S.L. & Salas, G. Magma Dynamics and Petrological Evolution Leading to the VEI 5 2000 BP Eruption of El Misti Volcano, Southern Peru. *Journal of Petrology* **54,** 2033–2065 (2013).

Vazquez, J. A. & Reid, M. R. Time scales of magma storage and differentiation of voluminous high-silica rhyolites at Yellowstone caldera, Wyoming. *Contributions to Mineralogy and Petrology* **144,** 274–285 (2002).

Watts, R.B., de Silva, S.L., Jimenez de Rios, G. & Croudace, I. Effusive eruption of viscous silicic magma triggered and driven by recharge: a case study of the Cerro Chascon-Runtu Jarita Dome Complex in Southwest Bolivia. *Bulletin of Volcanology* **60,** 241–264 (1999).

Wörner, G., Moorbath, S. & Harmon, R.S. Andean Cenozoic Volcanic Centers Reflect Basement Isotopic Domains. *Geology* **20,** 1103–1106 (199

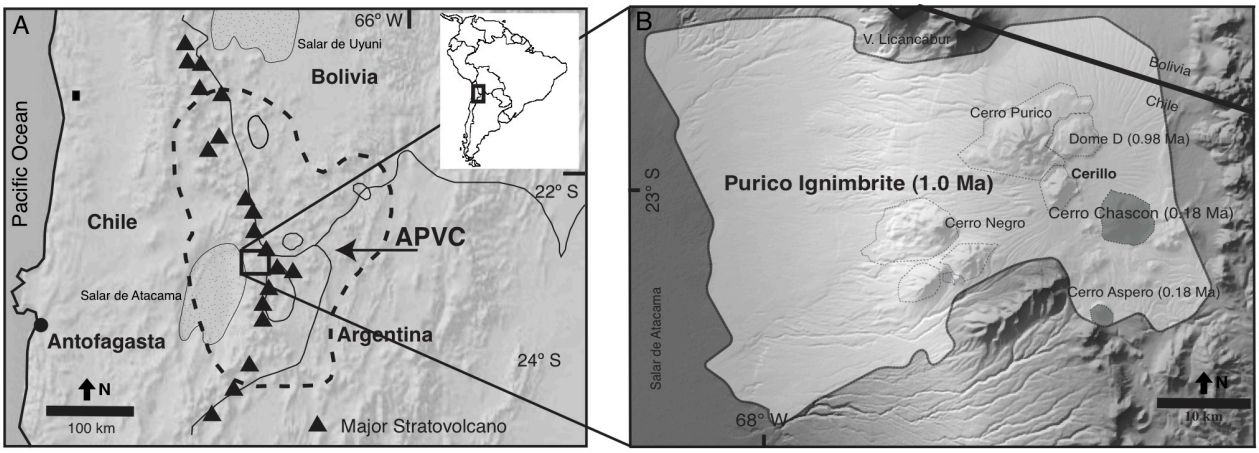

Figure 2.1. (A) Map shows the location of the Purico-Chascon Volcanic Complex in northern Chile. The dashed line field shows the extent of the Altiplano-Puna Volcanic Complex (APVC; de Silva, 1989). The circular fields represent the locations of 10-1 Ma APVC caldera complexes (Salisbury et al., 2011), the stippled fields represent salars, and the black triangles show the location of stratovolcanoes along the CVZ arc. (B) Map shows the distribution and ages of the Purico ignimbrite and associated lava domes. The white field represents the 1.0 Ma Purico ignimbrite, and the dark grey fields the 0.18 Ma Cerro Aspero and Cerro Chascon lava domes. Map modified from Francis et al., (1984) and Schmitt et al., (2001).

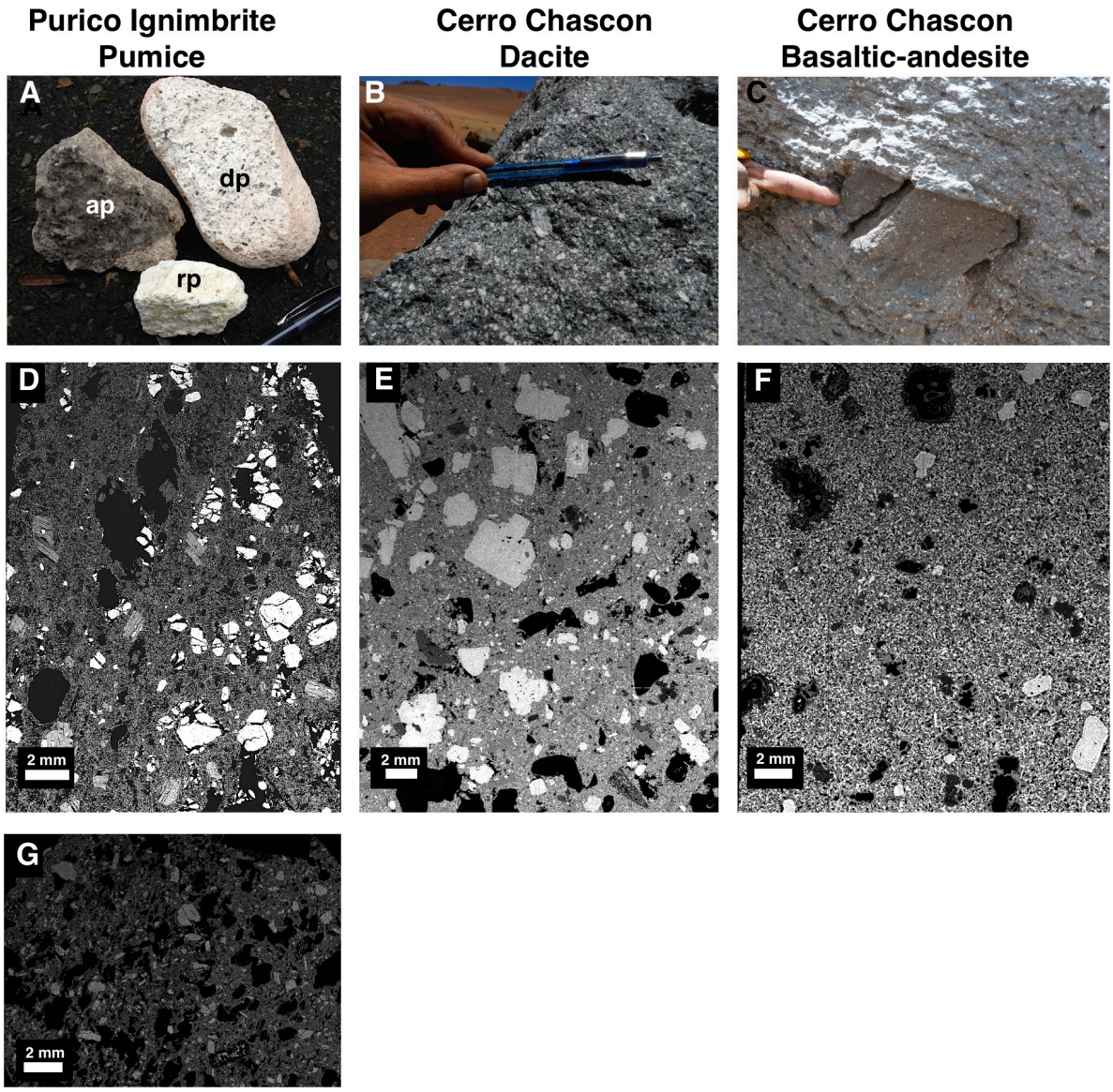

Figure 2.2. (A-C) Field photographs show the textures of Purico ignimbrite pumice (rp: rhyolite pumice; dp: dacite pumice; ap: andesite pumice) and the Cerro Chascon dacite and basaltic-andesite lavas. Note the large K-feldspar oikocryst beneath the pen in section B. (D-G) Al X-ray maps show the groundmass textures and crystal contents of pumice from the Purico ignimbrite (D: dacite pumice; G: andesite pumice) and lavas from the Cerro Chascon lava dome (E: dacite lava; F: basaltic-andesite lava).

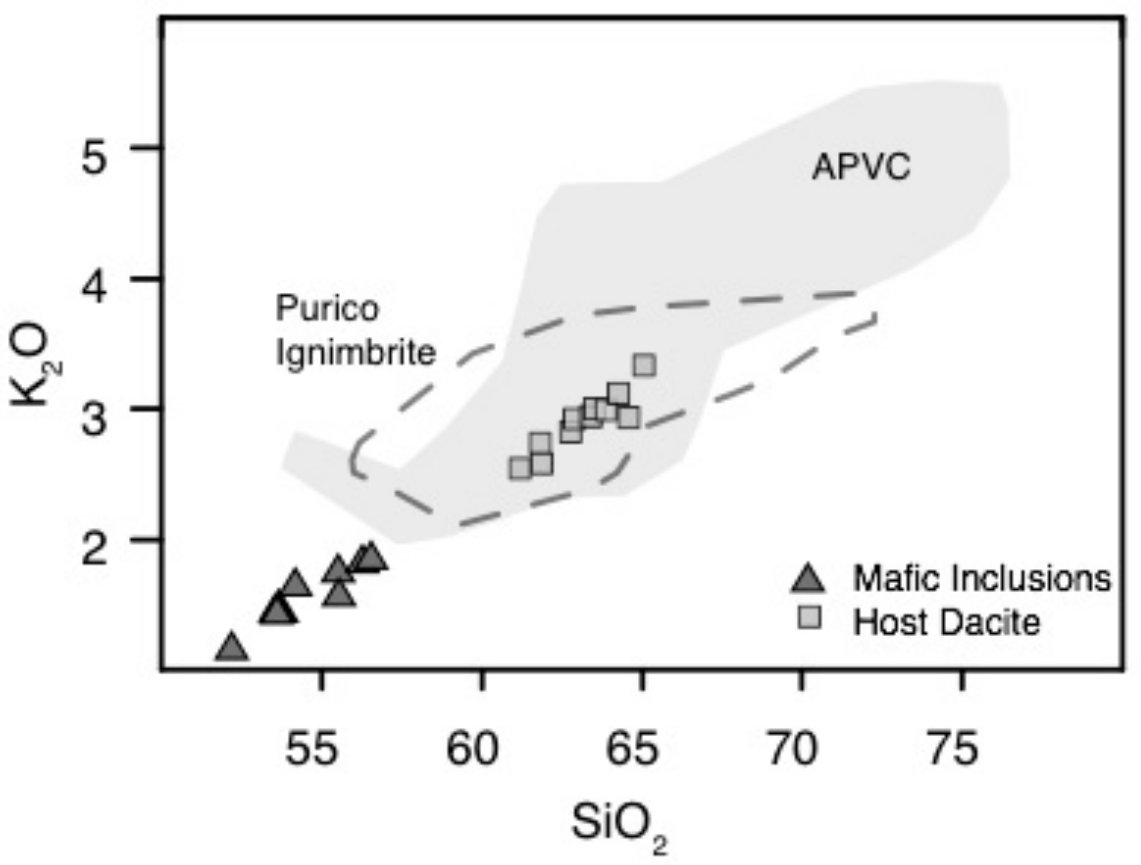

Figure 2.3. SiO_2 vs. K_2O compares crystal-rich host and mafic inclusions from Cerro Chascon with pumice from the Purico ignimbrite. The composition of the crystal-rich host is dacite, whereas, the mafic inclusions are basaltic-andesite. The Purico ignimbrite is dominated by dacite, but does contain volumetrically minor andesite and rhyolite pumice. Note the large compositional gap between the inclusions and host from Cerro Chascon. Data sources include Hawkesworth et al., (1982), Schmitt et al., (2001), de Silva (1991), and de Silva et al., (2006).

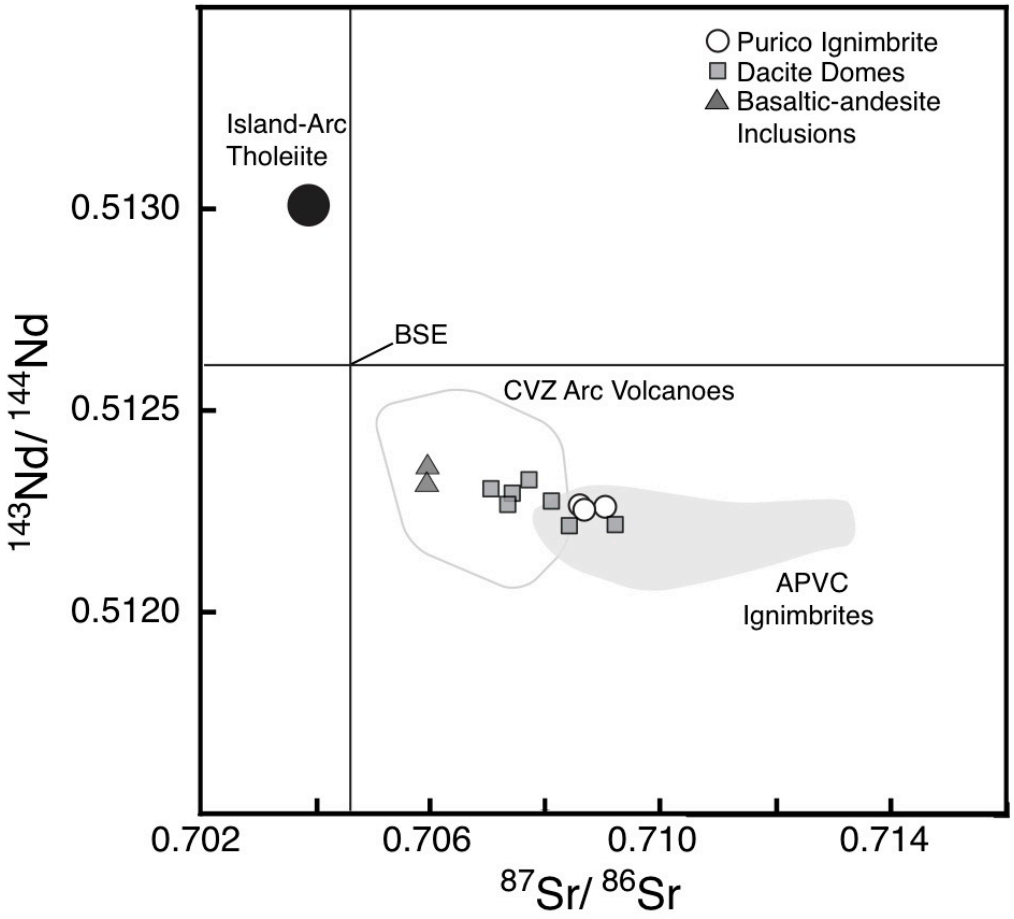

Figure 2.4. Bulk rock $^{87}Sr/^{86}Sr$ vs. $^{143}Nd/^{144}Nd$ from the Purico ignimbrite and Cerro Chascon lavas with 1Ma to recent (steady- state) lavas and tuffs from the CVZ (white field) and ignimbrites of the W. APVC (grey field) for reference. Island-arc tholeiites and bulk silicate Earth (BSE) compositions are also included. The basaltic-andesite lavas have significantly lower Sr and higher Nd isotope ratios than the dacite host and Purico ignimbrite pumice and are broadly similar to steady-state CVZ arc lavas. The Purico ignimbrite pumices have isotope ratios similar to other ignimbrites erupted during in the APVC. Note that the Cerro Chascon basaltic-andesite and CVZ lavas are more radiogenic than island-arc tholeiites. Data sources include Schmitt et al., (2001), Hawkesworth et al., (1982), de Silva et al., (2006), Lindsay et al., (2001), Jacobsen and Wasserburg (1984), and Zindler and Hart, (1986).

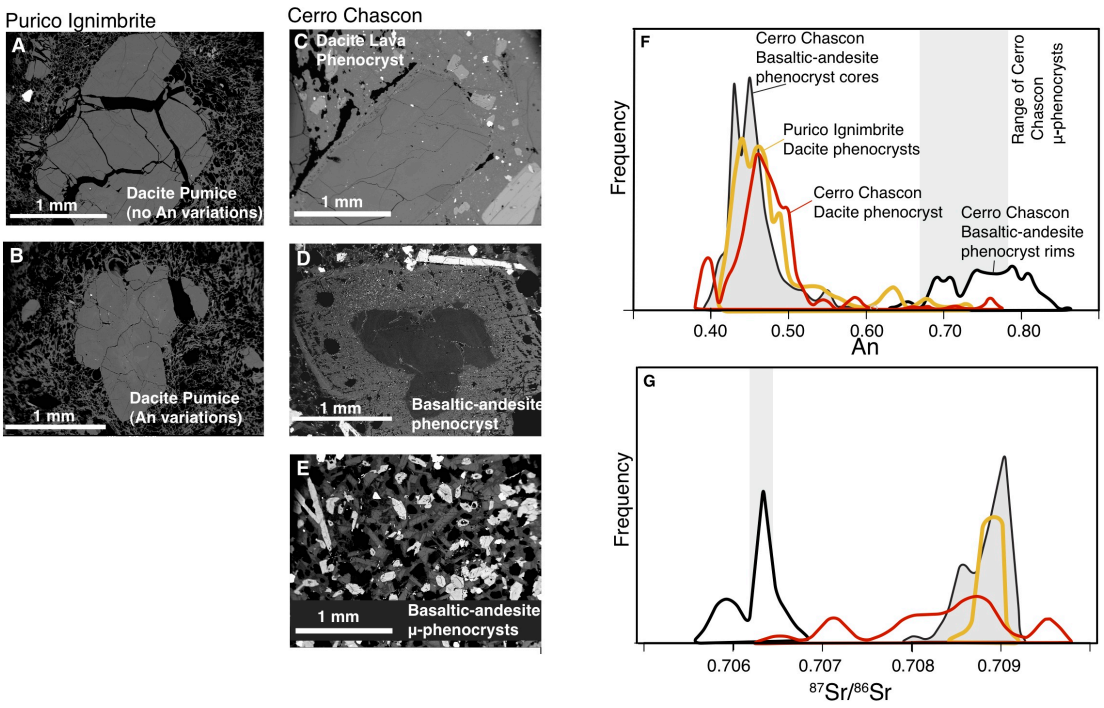

Figure 2.5. (A-E) Back-scattered electron images show the characteristic plagioclase populations from the Purico ignimbrite dacite pumice and Cerro Chascon dacite and basaltic-andesite lavas. Note the similarity in plagioclase phenocryst sizes in all three eruptive units. Also note the clear disequilibrium textures in phenocrysts from the basaltic-andesite lava (D). (F) Histogram shows the relative frequency of anorthite contents in plagioclase crystals from the units discussed above. Grey box represents the composition(s) of plagioclase micro-phenocrysts. Cores of phenocrysts from all three units have overlapping low anorthite contents, whereas, phenocryst rims and microphenocrysts from the basaltic-andesite have significantly higher anorthite contents. (G) Histogram shows the relative frequency of $^{87}Sr/^{86}Sr$ isotope ratios units described above. Grey box represents the composition(s) of plagioclase micro-phenocrysts in the basaltic-andesite inclusions. Plagioclase phenocryst cores from all three units have overlapping high $^{87}Sr/^{86}Sr$ ratios. Phenocryst rims and microphenocrysts from the basaltic-andesite lava have significantly lower $^{87}Sr/^{86}Sr$ ratios. Phenocrysts from the Cerro Chascon dacite lava are highly variable covering nearly the entire isotopic range observed in plagioclase from the PCVC.

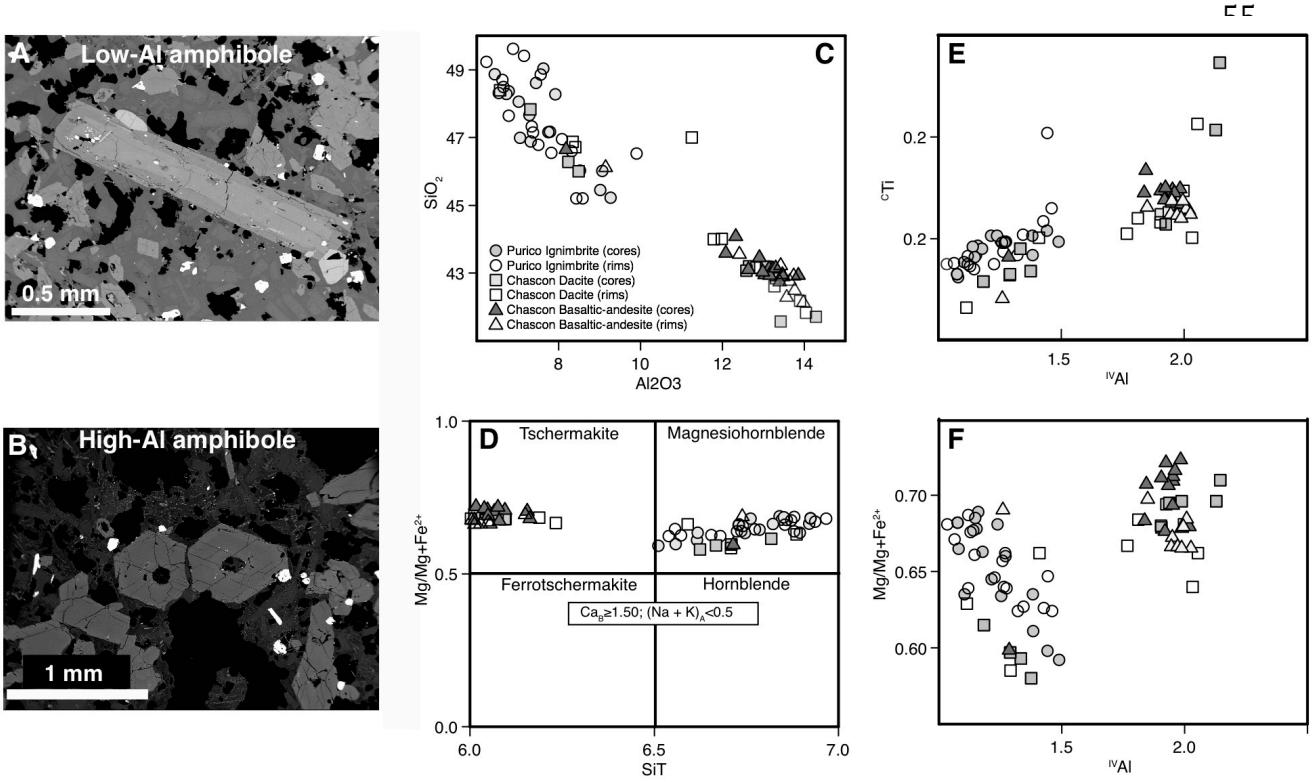

Figure 2.6. (A, B) Back-scattered electron images of representative low-Al and high-Al amphibole crystals in the Purico ignimbrite and Cerro Chascon lava dome. (C) Al_2O_3 vs. SiO_2 diagram compares high and low Al amphiboles from the Purico ignimbrite and Cerro Chascon lavas. Note the similarity between low-Al amphibole in the Purico ignimbrite pumice and Cerro Chascon lavas. Also, note the compositional gap between high- and low-Al amphiboles (~9-12 wt.% Al_2O_3). (D) Amphibole classification diagram following Leake et al., (1997) shows Si per formula unit vs. Mg# [Mg/(Mg+Fe^{2+}]. Low-Al amphibole in the Purico ignimbrite and Cerro Chascon lavas are magnesiohornblendes. High-Al amphiboles in the Cerro Chascon lavas are tschermakites. (E, F) Diagrams show tetrahedral coordinated Al vs Mg# and Ti in the c-lattice site. Note the large compositional gaps between the two groups indicating the two amphibole types grew in distinct pressure-temperature environments.

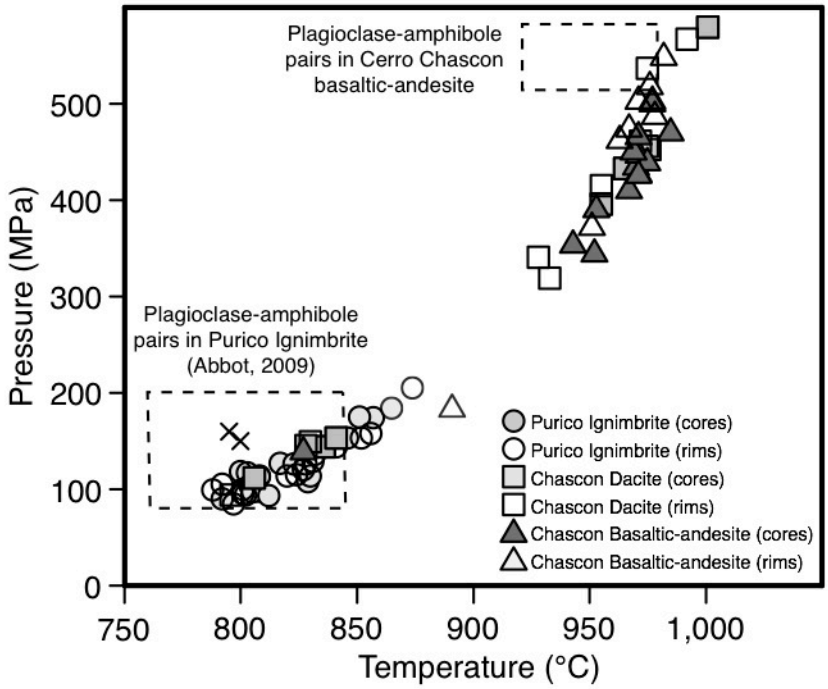

Figure 2.7. Magmatic temperatures and pressures calculated for the Purico ignimbrite and Cerro Chascon lavas. Data points represent pressures and temperatures calculated using the thermobarometer of Ridolfi et al., (2010). Individual points represent averages of multiple analyses within the core or rim region of individual crystals (see supplementary data). The white dashed boxes represent plagioclase-amphibole temperatures modeled for the Purico ignimbrite dacite pumice and Cerro Chascon basaltic-andesite using the plagioclase-amphibole thermometer of Holland and Blundy (1994). Magmatic pressures for plagioclase-amphibole pairs in the Purico ignimbrite were calculated using the Al-in-amphibole barometer of Anderson and Smith (1995). Plagioclase-amphibole temperatures from the Cerro Chascon basaltic-andesite were modeled using touching high-Al amphibole and plagioclase microphenocrysts pairs. Magmatic pressures were not calculated for these crystals as they crystallized at temperatures that exceed the calibration temperatures of Anderson and Smith (1995). Pressures were instead estimated (5.0-5.7 MPa) using regional seismic data (Chmielowski et al., 1999) and pressures obtained using the thermobarometer of Ridolfi et al. (2010). Temperatures from amphibole and plagioclase-ampibole pairs from both the Purico ignimbrite and Cerro Chascon basaltic-andesite overlap when uncertainties associated with both models are considered (±25 and ±50 °C, respectively) and clearly define two distinct pressure-temperature environments. The X symbols represent magmatic temperatures and pressures for the Purico dacite pumice determined by Schmitt et al., (2001). Data sources include Abbot (2009) and Schmitt et al., (2001).

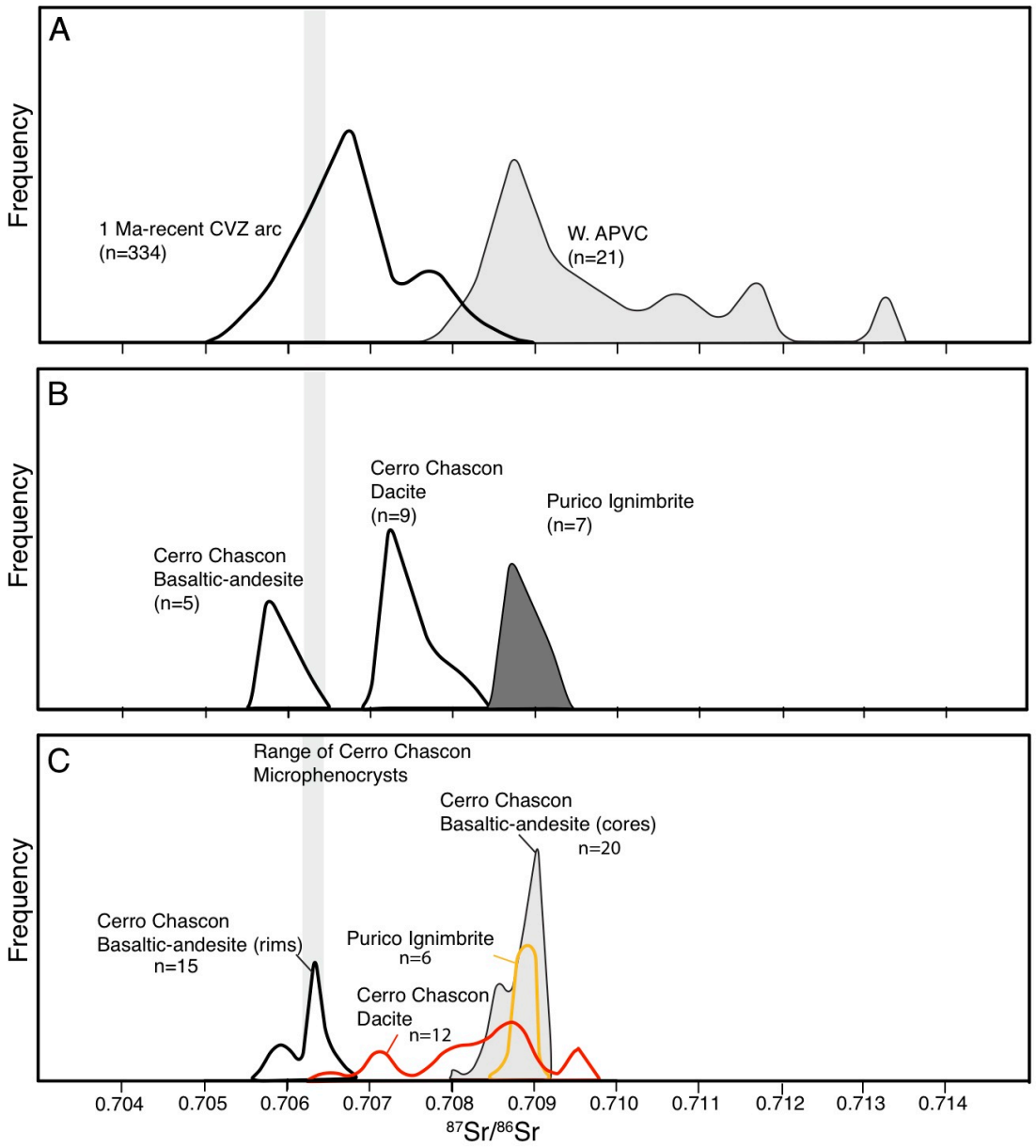

Figure 2.8. Relative frequency plots compare the $^{87}Sr/^{86}Sr$ isotopic compositions of plagioclase crystals from the Purico ignimbrite and Cerro Chascon lavas (C) with bulk rock $^{87}Sr/^{86}Sr$ ratios from the Purico ignimbrite, Cerro Chascon lavas, 10-1 Ma ignimbrites from the W. APVC, and 1 Ma to recent stratovolcanoes along the CVZ arc (medium grey). High $^{87}Sr/^{86}Sr$ ratios observed in plagioclase phenocrysts from the PCVC are identical to the bulk rock $^{87}Sr/^{86}Sr$ of the Purico ignimbrite, and the other large ignimbrites associated with the ignimbrite flare-up. Low $^{87}Sr/^{86}Sr$ rims on plagioclase phenocrysts and plagioclase microphenocrysts from the Cerro Chascon basaltic-andesite lava are similar to the bulk rock $^{87}Sr/^{86}Sr$ ratios of the Cerro Chascon basaltic-andesite, and overlap with the $^{87}Sr/^{86}Sr$ composition of recent stratovolcanoes and small volcanic centers erupted along the CVZ arc. Data sources include Mamani et al., (2010), de Silva et al., (2006), Schmitt et al., (2001), Lindsay et al., (2001), de Silva, (1991), and Hawkesworth et al., (1982). Data from Mamani et al.,(2010) was filtered prior to use.

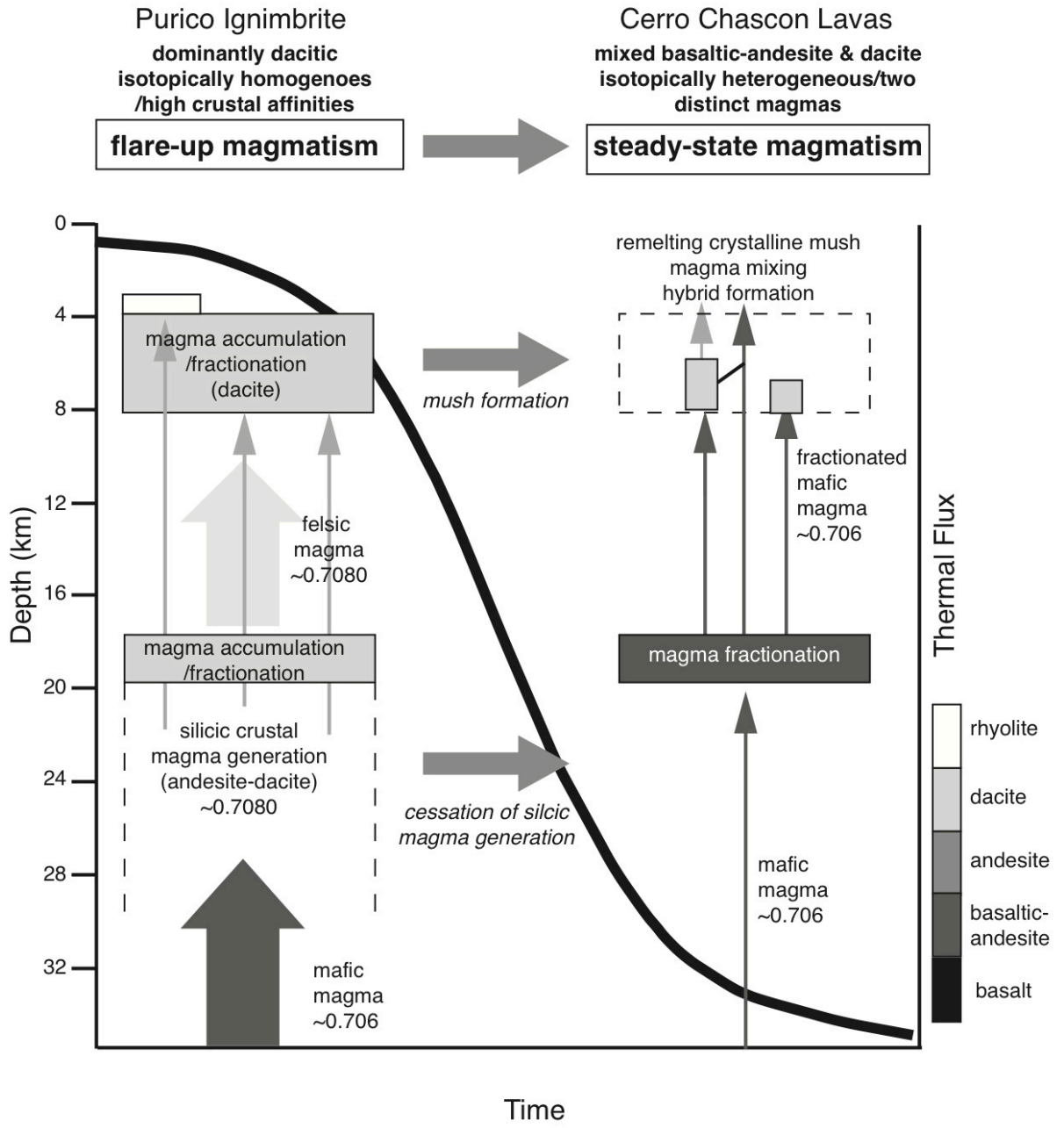

Figure 2.9. Schematic cross section shows how the generation, transportation, and storage of magmas changed throughout the history of the PCVC, and how those changes reflected changes in the regional geothermal gradient. Vertical arrows in the foreground show the composition (see composition legend in lower right) and ascent path of magmas during the evolution of the PCVC, with arrow width representing relative volume of magma. Colored boxes show the locations of magma accumulation and compositions of accumulating magmas. Text denotes the processes occurring in the crust, and the Sr isotopic composition of ascending magmas at different crustal levels. Horizontal arrows show how processes at a specific level in the crust change throughout the evolution of the PCVC. The black curve in the background illustrates how thermal flux decreased throughout the evolution of the PCVC. Note that during the eruption of the Purico ignimbrite, thermal flux was high and significant mid-crustal melting controlled the composition of magmas erupting on the surface. In contrast, during the ascent of the Cerro Chascon magmas, the thermal flux was low and mafic magmas ascended from depth into the upper crust with no significant mid-crustal interactions.

Table 2.1: Summary of plagioclase textures and compositions

Unit	Purico Ignimbrite	Cerro Chascon				
Rock Type	Dacite Pumice	Dacite Lava		Basaltic-andesite Lava		
	Phenocrysts	Phenocrysts		Phenocrysts		µPhenocrysts
Size (µm)	500-1500	500-1500		500-1500		<500
Shape	subhedral	euhedral/subhedral		subhedral/anhedral		subhedral
Texture	Cores & Rims clear	Cores clear	Rims clear/sieved	Cores clear	Rims sieved	Cores & Rims clear
An	40-55	40-55	65-80	39-55	65-85	64-84
MgO (ppm)	<200	<200	500-800	<200	400-800	500-800
$^{87}Sr/^{86}Sr$	0.7087-0.7090	0.7083-0.7095	0.7065-0.7072	0.7085-0.7091	0.7057-0.7065	0.7062-0.7064

CHAPTER 3

Understanding the sources, dynamics, and evolution of magmas in a continental arc magmatic system: A case study of the Cerro Chascon lava dome, northern Chile

Dale H. Burns

Frank Tepley III

Shanaka L. de Silva

Zachary Carter

Mathew L. Loewen[1]

In preparation for submission to:

Journal of Petrology

3.1 ABSTRACT

The ~180 Ka Cerro Chascon in northern Chile is a ~6 km^3 dacite lava dome that contains abundant (up to 20 vol.%) variably quenched basaltic-andesite mafic inclusions. Textural, chemical, and isotopic variations in individual crystals from the mafic inclusions and the dacite record the interactions between magmas derived from the lower crust and a large upper crustal magma reservoir. Fo_{82-81} olivine with abundant spinel inclusions and high-Mg basalt melt inclusions are consistent with the lower crustal mantle source. Thermobarometric calculations indicate the olivine crystallized >20 km deep at temperatures in excess of 1,250 °C. Upon ascent into the mid-crust (~20-15 km deep) the magma appears to have stalled and crystallized significant high-An (An_{72-84}) plagioclase followed by high-Al (~12-15 wt. % Al_2O_3) amphibole and possibly magnetite. *In situ* isotopic analyses of the plagioclase microphenocrysts indicate that at the time the crystals grew, the magma had experienced no significant isotopic modification after leaving the lower crust. Eventually the magma continued to ascend into the upper crust where it ponded against the residual crystal mush from the Purico ignimbrite. Partial melting of the crystal mush and eventual overturn led to the formation a hybrid dacite along with the significant transfer of crystalline material into the underlying mafic magma. Ultimately, interactions were interrupted by the eruption of the dacite lava dome. The results of this study are significant as they provide means for identifying distinct magmatic processes occurring in the crust and understanding how individual processes ultimately

control what erupts on the surface. In addition, true mafic magmas in the Central Andes are extremely rare, and very little is known about the source of mantle-derived magmas in the region.

3.2 INTRODUCTION

Continental magmatic arcs are dynamic environments were rising mantle-derived magmas ascend through, stall, and interact with the continental crust (e.g. Davidson et al., 2005). Owing to these crustal interactions, the source of magmas in continental magmatic systems can often be difficult, if not impossible, to determine. In addition, de-convolving the specific magmatic processes that control the composition of magmas reaching the surface can be problematic as arc-related rocks often have multiple distinct processes overprinted on one another. At the bulk rock scale, magmas commonly define a broad range of textures and compositions that record variable degrees of mixing and homogenization between distinct magmas (Sparks and Marshal, 1986; Frost and Mahood, 1987; Blake and Koyaguchi, 1990). These processes are commonly overprinted by single or sometimes multiple crystallization events (e.g., Davidson et al., 2005), making individual processes difficult to identify.

At the crystal scale, mixed magmas can record critical information about the distinct magmas lost during the mixing process (e.g., Eichelberger, 1978; Davidson et al., 1990). Disequilibrium textures are common in phenocrysts providing evidence of disequilibrium between crystals and their host magmas

(Eichelberger, 1978). Major and trace elements can vary significantly between distinct populations of crystals and between crystal cores and rims recording a myriad of magmatic processes including crystal fractionation, magma mixing, magma recharge, assimilation, and other open system processes (e.g., Davidson and Tepley, 1997; Ruprecht and Wörner, 2007; de Silva et al., 2008). Distinguishing between these processes using major elements can be problematic as major elements are sensitive to all of the processes described above. In the past 25 years, the development of new techniques to analyze radiogenic isotope ratios in individual crystalline phases has greatly enhanced our ability to constrain these processes (e.g., Davidson and Tepley, 1997; Davidson et al., 2007; Ramos and Tepley, 2008). *In situ* isotope ratios allow for open vs. closed system processes to be distinguished from one another, and can provide critical information about the source of previously mixed magmas prior to mixing/homogenization.

In addition to magmatic processes and magma sources, the partitioning of specific cations between distinct crystalline and crystalline/liquid phases, as well as between specific crystal-lattice sites in individual crystals have been shown to be dependent on the intensive parameters (i.e. T, P, H_2O, fO_2) of the crystallizing magma (e.g., Roeder and Emslie, 1970; Helz, 1982; Hammarstrom and Zen, 1986; Blundy and Holland, 1990; Andersen et al., 1993; Beattie, 1993; Holland and Blundy, 1994; Anderson and Smith, 1995; Ghiorso and Sack, 1995; Putirka, 2007, 2008; Ridolfi et al., 2010). Thus, by measuring the elemental compositions

of distinct crystalline and glass phases within an igneous rock, the temperatures and pressures at which magmas crystallized can be determined. By combining *in situ* compositional and isotopic information with intensive parameters, distinct magmatic processes can be observed and distinguished from one another in both space, composition, and time. These datasets can ultimately be used to construct composition-pressure-temperature-time pathways for distinct magmatic events.

In this study, we combine *in situ* compositional, and isotopic information with temperature-pressure calculations to determine P-T-t pathway of the recharge magma that triggered the eruption of the Cerro Chascon lava dome. We determine the relative crystallization sequence of the ascending recharge magma from >25 km depth to the surface and evaluate how magmatic processes occurring at multiple levels in the crust control the compositions and textures of what ultimately erupted at the surface. We also show the recharge magma was initially a tholeiitic basalt prior to extensive fractionation at ~20 km depth, and explore the composition of an enriched mantle source for some CVZ magmas.

3.3 GEOLOGIC BACKGROUND

The Purico-Chascon Volcanic Complex (PCVC) is one of the youngest eruptive centers associated with the Altiplano-Puna Volcanic Complex (APVC; de Silva, 1989), a 10 to 1 Ma series of nested calderas and extensive ignimbrite sheets (>10,000 km^3) erupted between 21 and 24 degrees S in the Central

Volcanic Zone (CVZ) of the Andean mountain chain (Fig 1A). Activity initiated at the Purico-Chascon volcanic complex ~ 1.0 Ma with the eruption of the 80-100 km^3 Purico ignimbrite (Francis et al, 1984; de Silva, 1991; Schmitt et al., 2001). Following the climactic eruption, volcanic activity became more effusive resulting in the formation of a summit complex (<10 km^3) of intermediate lava domes (Hawkesworth et al., 1982; Francis et al., 1984; Schmitt et al., 2001), the youngest being the <0.18 Ma Cerro Chascon and Cerro Aspero domes (Figure 1B, C, D; Hawkesworth et al., 1982; Francis, 1984; de Silva, 1991; Schmitt et al., 2001). Cerro Chascon is a crystal-rich, high-K dacite lava (Figure 1D, Figure 2) with significant (up to 20 vol.%) variably quenched basaltic-andesite inclusions (Hawkesworth et al., 1982; Francis, 1984; Davidson et al., 1990).

Davidson et al., (1990) analyzed a suite of mafic inclusions from Cerro Chascon and characterized the compositional and isotopic variations from the interior of an inclusion across the inclusions-host interface and into the dacite host and determined that the Cerro Chascon dacite represents a hybrid mixture of the basaltic-andesite recorded in the mafic inclusions and previously emplaced ignimbrite basement. In their model, the basaltic andesite ascended from depth and pooled against the Purico ignimbrite basement. The transfer of heat from the basaltic-andesite lava into the ignimbrite basement resulted in the rapid crystallization of the basaltic-andesite with the simultaneous melting of the ignimbrite basement generating a rhyolite melt. Eventually, crystallization of the basaltic-andesite leads to overturn and the mixing of the two magmas. Davidson

et al., (1990) also recognized that during the mixing processes crystals from both magmas are exchanged and proposed that large, high $^{87}Sr/^{86}Sr$ plagioclase, low-Mg amphiboles, and possibly biotite and quartz were derived from the ignimbrite basement. In contrast, olivine, pyroxene, and high-An plagioclase (>An60) crystallized within the mafic magma when it pooled against the ignimbrite. In this study, we focus on the chemistry of individual crystalline phases from the two Cerro Chascon lavas. We test the model of Davidson et al. (1990) and generate a time-integrated (relative) cross section of the upper ~30 km of crust during the recharge event. We also use olivine-hosted melt inclusions and thermodynamic modeling to investigate the presence of a true primitive magma in the central Andes.

3.4 ANALYTICAL METHODS

We obtained bulk rock major and trace element concentrations from the Cerro Chascon dacite and basaltic-andesite (n = 2) using a Thermo-ARL automated X-ray fluorescence spectrometer (XRF) and an Agilent 7700 inductively coupled plasma mass spectrometer (ICP-MS) at the Washington State University Geoanalytical Laboratory (http://soe.wsu.edu/facilities/geolab/technotes/icp-ms_method.html). For detailed description of methods see Johnson et al. (1999). *In situ* major and trace element abundances in plagioclase and amphibole were measured at Oregon State University (OSU) using a Cameca SX100 electron microprobe with five

wavelength dispersive spectrometers, including two high-sensitivity large diffraction crystals for trace element analyses. Analyses where conducted using an accelerating voltage of 15 KeV with a beam current of 30 nA and focused 1 μm beam for plagioclase, amphibole, olivine, clinopyroxene, K-feldspar and spinel, and de-focused 5 μm beam for glass. Volatile element migration was corrected using a 0-time intercept correction. Corrected elements include Na, K, and Si. Count times ranged from 10 s for major elements to 60s for minor or trace elements. Specific crystal configurations, count times, and standard reproducibility are given in the supplementary materials. Generally, the error associated with major elements is < 2% (relative to average standard values). To determine the major and trace element variations within texturally distinct zones in individual crystals, detailed (~5 μm step) transects were conducted through the distinct zones.

In situ isotopic analyses were conducted using two methods. Following EMP analyses selected crystals were sampled using a NuWave computer-automated micro-drill at OSU (see Charlier et al., 2006), and sampled aliquots were sent to New Mexico State University (NMSU) where elemental Sr was separated using low blank, cation-exchange chromatography (Ramos, 1992). Once separated, $^{87}Sr/^{86}Sr$ ratios of individual plagioclase crystals were measured using thermal ionization mass spectrometry (TIMS) at NMSU (Ramos, 1992; Charlier et al., 2006). *In situ* isotopic analyses were also conducted using a Photon Machine Analyte G2 laser-ablation unit and a Nu Plasma multi-collector

inductively coupled plasma mass spectrometer (MC-ICP-MS) at OSU. For a detailed comparison of the two methods and analytical methods for LA-ICP-MS analyses, see Burns et al, (2014).

3.5 PETROLOGY

We collected a suite (n = 20) of variably quenched, basaltic-andesite inclusions ranging from ~5 to 30 cm in diameter, and their respective hosts. Three mafic inclusions and the host were selected for detailed petrological (**Table 3.1**) and geochemical characterization and are discussed below.

Basaltic-andesite inclusions from Cerro Chascon are fine-grained and porphyritic consisting of plagioclase, amphibole, clinopyroxene, olivine, oxides, and rare quartz and biotite (15 vol.% phenocrysts) in a finely crystalline, moderately vesicular (27 vol.%) groundmass of plagioclase and amphibole microphenocrysts (50 vol.%) and rhyolite glass (75 wt.% SiO_2). Phenocrysts are typically large (>1 mm), subhedral to anhedral, and have prevalent disequilibrium textures including resorbed quartz with clinopyroxene mantles, dusty sieved plagioclase, and olivine mantled with amphibole (**Figure 3.2**).

Dacite lavas from Cerro Chascon are coarse-grained, crystal-rich (66 vol.% crystals), and porphyritic, containing plagioclase, amphibole, biotite, quartz, orthopyroxene, clinopyroxene, olivine, k-feldspar, oxides, and accessory zircon, apatite, and sphene in a finely crystalline, moderately vesicular (24 vol.%) groundmass consisting of amphibole microphenocrysts in high-silica rhyolite

glass (76 wt.% SiO_2). Phenocrysts are typically large (>1 mm) and range from euhedral to subhedral and clear (**Figure 3.2**). Disequilibrium textures are less abundant, but similar to textures in the mafic inclusions. These textures include resorbed quartz with clinopyroxene mantles, dusty sieved plagioclase, and olivine with amphibole rims.

3.6 BULK ROCK COMPOSITIONS

In order to put the *in situ* compositional and isotopic information discussed in this study in context with the rest of the PCVC we analyzed the magmas from which our crystals resided for major and trace element abundances. These variations are discussed in the following sections and compared with previously analyzed samples from the same units. We did not analyze bulk rock isotopes as part of this study. However, we have included a brief discussion on the bulk rock isotope ratios previously reported from Cerro Chascon.

We analyzed a mafic inclusion (CH09013) and host (CH09014) from Cerro Chascon for major element abundances and the results are presented in Table 3.2. The mafic inclusion is basaltic-andesite (56 wt.% SiO_2) with relatively high concentrations of CaO, MgO, and TiO_2 and low K_2O (**Figure 3.3**). Our results are well within the range of mafic inclusion compositions reported by Hawkesworth et al., (1982) and Schmitt et al., (2001) for all elements (**Figure 3.3**). The crystal-rich host we analyzed is dacite (63 % SiO_2). The dacite host has significantly lower concentrations of CaO, MgO, and TiO_2 than the basaltic-andesite and

higher K_2O. Similar to the basaltic-andesite, our dacite compositions are within the range reported by Hawkesworth et al. (1982) and Schmitt et al. (2001). Importantly, the dacite lavas show some broad compositional similarities to the Purico ignimbrite. In contrast, the basaltic-andesite lavas are much more primitive (higher CaO and MgO and lower SiO_2 and K_2O) than dacite lavas and compositions from the Purico ignimbrite. A key feature of the combined major element whole rock dataset is the pronounced compositional gap between the two lavas.

Trace element abundances were also measured in a basaltic-andesite inclusion and host dacite and the results are presented in Figure 3.4. The basaltic-andesite (**Figure 3.4A**) defines a relatively flat REE pattern (La/Yb_N= 4.1) with a Eu anomaly of 23.3. The host dacite (**Figure 3.4B**) has a much steeper REE slope (La/Yb_N=8.4) with a slightly lower Eu anomaly (22.7). Our results are similar to the values reported by Hawkesworth et al. (1982) and Schmitt et al. (2001) who reported La/Yb_N from 2.8 to 4.2 for the basaltic-andesite and 7.8 to 15 for the dacite host and Eu anomalies of 21.2 to 24.4 and 16.0 to 30.5, respectively. By comparison, the basaltic-andesite has significantly lower LREE and higher HREE than the Purico ignimbrite, whereas the dacite is broadly similar.

Hawkesworth et al. (1982) analyzed bulk rock radiogenic isotopic ratios and those results are summarized below. The dacite host and basaltic-andesite inclusions from Cerro Chascon have very distinct isotopic signatures (**Figure 3.5**).

The basaltic-andesite inclusions have significantly lower $^{87}Sr/^{86}Sr$ and higher $^{143}Nd/^{144}Nd$ than the host dacite and overlap data from Quaternary stratovolcanoes on the CVZ arc-front. The dacite host lavas define a roughly linear trend, spanning the isotopic gap between much higher $^{87}Sr/^{86}Sr$ ratios typical of ignimbrites of the APVC and CVZ stratovolcanoes. The radiogenic isotopic signatures of the regional ignimbrites represent high degrees of crustal assimilation during a regional magmatic flare-up (de Silva, 1989). Note that even the most primitive bulk rock analyses are significantly displaced from island arc tholeiitic compositions reflecting variable degrees of crustal contamination. The distinct isotopic signature of the upper crustal magmas associated with the ignimbrite flare-up and typical magmas associated with the CVZ arc make Cerro Chascon the ideal location for identifying the sources of crystal cargo and understanding the processes, dynamics, and timing of mafic recharge in silicic magmatic systems.

3.7 CRYSTAL TEXTURES AND COMPOSITIONS

In this section we report the textural, compositional, and isotopic variations observed in individual crystals within the Cerro Chascon lavas, and we discuss how the distributions of crystal types vary between the basaltic-andesite inclusions and the dacite host. Some of the plagioclase and amphibole chemistry have already been presented in Burns et al., (in review). We evaluate the textural, compositional, and isotopic variations in these crystals in context with the

magmatic recharge event that triggered the Cerro Chascon eruption and the source of magmas in the PCVC.

3.7.1 Plagioclase

Plagioclase is the most abundant phase in the Cerro Chascon lavas and makes up ~31% of mafic inclusions, and ~36% of the crystal-rich host. Mafic inclusions are dominated by (30 vol. %) small (<500 μm), tabular, subhedral, clear, plagioclase microphenocrysts (**Figure 3.6B; Table 3.3**). The microphenocrysts have relatively high An and MgO contents (An_{72-77} and 400-700 ppm, respectively) and low $^{87}Sr/^{86}Sr$ isotope ratios (0.7062-0.7064; **Figure 3.6D, E, F**). Larger plagioclase crystals (~500-1500 μm) are also present in the mafic inclusions (**Figure 3.6A**), but they are less abundant (~1 vol.%) and are texturally, compositionally, and isotopically distinct from the microphenocrysts (**Figure 3.6D**, **E, F**). The phenocrysts have clear cores surrounded by a ~300 μm thick heavily sieved zone and a clear ~100 μm thick euhedral growth zone on the outermost edge of the crystal(s). The clear cores have relatively low An and MgO contents (An_{39-50} and <200 ppm, respectively) and high $^{87}Sr/^{86}Sr$ isotope ratios (0.7085-0.7091) with respect to the microphenocrysts. Plagioclase within the sieved zone and the outermost growth rims have significantly higher An and MgO contents (An_{65-85} and 400-800 ppm, respectively) that are similar to plagioclase microphenocryst compositions. Sr isotope ratios measured in the outermost

growth zones were significantly lower (0.7058-0.7065) than those in the clear cores and are also similar to plagioclase microphenocryst compositions.

The dacite host also contains two distinct types of plagioclase that are similar to plagioclase in the basaltic-andesite inclusions. The dacite is dominated (~20 vol. %) by large (500-2000 μm), euhedral to subhedral, clear phenocrysts (**Figure 3.6C**). The phenocrysts have low An and MgO contents (An_{39-50} and d.l.-200 ppm, respectively), and high $^{87}Sr/^{86}Sr$ (0.7085-0.7091) isotope ratios similar to large crystals in the mafic inclusions (**Figure 3.6D, E, F**). Some crystal rims do show slight increases in An contents and MgO in the outermost ~100 μm of the crystal, and have lower $^{87}Sr/^{86}Sr$ ratios (0.7065-0.7072). Some large crystals have variably thick sieved zones and reverse zoning on the outermost rims similar to phenocrysts in the mafic inclusions. Microphenocrysts are also present in the host dacite (~16 vol.%) and are texturally and compositionally similar (An_{72-77}) to microphenocrysts in the mafic inclusions. Optical limitations prevented us from analyzing Sr isotope ratios for the microphenocrysts.

3.7.2 Amphibole

Amphibole is second in abundance to plagioclase, making up ~26% of mafic inclusions and 16% of the host dacite. There are two types of amphibole in the Cerro Chascon lavas. Mafic inclusions are dominated by (~22 vol.%) small (<500 μm), euhedral to subhedral, clear, high Al_2O_3 (12-14 wt. %) amphibole microphenocrysts (**Figure 3.7B, C; Table 3.4**). Site-specific cation abundance calculations show that microphenocrysts have high ^{IV}Al, Mg#, and ^{C}Ti (**Figure**

3.7D, E, F). These amphiboles are tschermakites based on the classification scheme of Leake et al. (1997; **Figure 3.7D**). The second, less abundant (~5 vol. %) type of amphibole, found in basaltic-andesite inclusions, are large (> 1000 µm), subhedral, blocky to elongate and show no signs of disequilibrium (**Figure 3.7A, C**). These crystals have significantly lower Al_2O_3 (7-8.5 wt.%), ^{IV}Al, ^{C}Mg, ^{C}Ti, and are magnesiohornblendes according to the classification of Leake et al. (1997). The dacite host contains two populations of amphibole that are compositionally identical to those in the mafic inclusions. However, the dacite contains fewer high-Al tschermakites (~11 vol. %). Importantly, the amphiboles in Cerro Chascon define two completely distinct populations similar to observations made in other continental arc mixed magma systems (e.g., Koleszar et al., 2012; Walker et al., 2012; Angelis et al., 2013).

3.7.3 Olivine, olivine-hosted melt inclusons, and Cr-spinel

Olivine is present in both the basaltic-andesite inclusions and dacite host (~3 vol.% and <1 vol.%, respectively). Olivines range in size from ~500-1500 µm and are typically subhedral with resorbed rims surrounded by ~50-100 µm thick high-Al amphibole rims (**Figure 3.8A, B**). Crystal cores are relatively Mg-rich (Fo_{81} to Fo_{84}) and become more Fe-rich toward the rim (Fo_{75} to Fo_{76}; **Figure 3.8C**). NiO concentrations are low (<1000 ppm) and show no significant variations between crystal cores and rims. In contrast, CaO ranges from ~1000 to 2300 ppm (mostly between 1000-1600 ppm) and shows a strong negative

correlation with Fo contents, increasing rim-ward. Olivine crystals also contain rare basaltic melt inclusions (44-48 wt.% SiO_2) and Cr-spinel mineral inclusions (**Figure 3.8A**). The melt inclusions are generally glassy and spherical, ~110-140 μm in diameter, but small olivine rims at the melt-crystal boundary indicate that the melts partially crystallized. Analyses of two melt inclusions are presented in table 3.6. Melt inclusions have variable Mg# (53-67) with Al_2O_3 (13-16 wt.%), CaO (9-11 wt.%), and TiO_2 (6000-8000 ppm). These compositions are similar to the bulk rock compositions of late Miocene and younger back-arc basalts and basaltic andesites in the central Andes (Risse et al., 2013) and primitive basalts from other continental arcs (e.g., Cascade Range western United States; Conrey et al. 1997). Cr spinels are small (10-50 μm), subhedral, and have Cr# ranging from 57 to 59. Al_2O_3 and TiO_2 range from 11.90 to 13.89 and 1.52 to 1.84 (**Figure 3.15**; **Table 3.7**), respectively.

3.7.4 Clinopyroxene

Clinopyroxene crystals are also found in both the basaltic-andesite inclusions and the host dacite (~5 vol.% and ~3 vol.%, respectively) and are euhedral to subhedral, Mg-rich augite (**Figure 3.9**). There are two distinguishable types of augite. The dominant type is euhedral to subhedral, ranges in size from <500 to ~1000 μm, is relatively clear, and occurs as both individual crystals and clumps of crystals (**Figure 3.9A, B**). These crystals often form rims surrounding resorbed quartz crystals (**Figure 3.9B**). The second type

of augite is considerably larger (>1 mm) and have coarsely sieved cores surrounded by ~300 μm thick euhedral growth zones (**Figure 3.8C**). The two populations show no systematic variations in Wo, En, or Fs contents ($Wo_{36-42}En_{43-50}Fs_{11-19}$); however, large sieved cores have slightly higher Mg# (Mg_{80} vs. Mg_{77}) and Cr_2O_3 (4000 vs. ~2000 ppm) and lower FeO (7.71 vs. ~8.65 wt.%) concentrations than the smaller clear crystals.

3.7.5 K-Feldspar

K-feldspar is present in both the dacite host and basaltic-andesite inclusions (both <1 vol. %; **Figure 3.10A, B**). These crystals are large (up to 4000 μm), clear (no perthitic texture), euhedral, display prominent Carlsbad twinning, and contain inclusions of plagioclase, amphibole, quartz, biotite, and magnetite (**Figure 3.10A**). Crystal interiors have a restricted range of compositions ($An_{<1}Ab_{19-21}Or_{78-80}$) with an average of ~ $An_1Ab_{21}Or_{78}$ (**Figure 3.10B**). In contrast, there are distinct ternary feldspar ($An_{30}Ab_{63}Or_{7)}$ rims on the outermost ~100 μm of the oikocrysts. Texturally, the inclusions of plagioclase, amphibole, biotite, and quartz are indistinguishable from crystals in the dacite host groundmass. In addition, analyses of multiple plagioclase crystals within the sanidine are identical to low An plagioclase crystals in the groundmass of the host dacite (An_{38-52}).

3.7.6 Magnetite

The only oxide found in the groundmass of lavas from Cerro Chascon is titano-magnetite. Magnetite crystals are generally small (<100 um) and subhedral and appear to be randomly dispersed throughout the mafic inclusions and dacite host.

3.8 DISCUSSION

In this section, we use crystal and glass chemistry to determine the magmatic conditions in which the crystals found in the Cerro Chascon lavas crystallized. We also combine textural, compositional, and isotopic information from individual crystalline phases to evaluate the magmatic processes occurring at multiple levels of the crust prior to the eruption of the Cerro Chascon lava dome. Lastly, the datasets are integrated to reconstruct the crystallization sequence that gave rise to the basaltic-andesite magma during ascent through the CVZ crust and explore the composition a mafic parental melt.

3.8.1 Intensive Parameters

We determined magmatic temperatures and pressures for the crystalline phases within the Cerro Chascon lavas using a variety of thermometers and barometers. Amphibole and plagioclase-amphibole pairs were modeled using the amphibole thermobarometer of Ridolfi et al., (2010) and the plagioclase-amphibole thermometer of Holland and Blundy (1994); the results are shown in

Figure 3.11. Low-Al amphibole crystals (magnesiohornblendes) from basaltic-andesite and dacite lavas yield temperatures between 796 and 841± 25 °C (Ridolfi et al., 2010), similar temperatures were obtained using the edenite-richterite exchange thermometer of Holland and Blundy (1994) for touching magnesiohornblende-An_{45} plagioclase pairs (788-821± 25°C), and reported by Schmitt et al. (2001) for the Cerro Chascon dacite host (830°C). High-Al amphiboles (tschermakites) yield much higher temperatures ranging from ~928-1001 ± 25°C (Ridolfi et al., 2010). Similar, but slightly more variable temperatures (925-973 ± 40°C) were calculated applying the thermometer of Holland and Blundy (1994) to touching tschermakite-plagioclase microphenocryst pairs. Amphibole crystallization pressures were determined using the amphibole thermobarometer of Ridolfi et al. (2010) and the Al-in-amphibole barometer of Anderson and Smith (1995). Low-Al amphiboles (magnesiohornblendes) from the Cerro Chascon dacite appear to have crystallized between 94 and 153 MPa (Ridolfi et al., 2010), similar pressures (105-199 MPa) were estimated using the barometer of Anderson and Smith (1995) and reported by Schmitt et al. (2001) for the Cerro Chascon dacite. High-Al amphiboles (tschermakites) from Cerro Chascon lavas yield significantly higher pressures of 396-580 MPa (~15-20 km in depth), with 80% of crystals between 396 and 550 MPa (**Figure 3.11**). Al-in-amphibole pressures were not calculated for the high-Al tschermakites as their crystallization temperatures far exceeded the temperatures at which the Anderson and Smith (1995) barometer is calibrated.

Temperatures and pressures recorded in amphibole and plagioclase crystals from Cerro Chascon lavas record two distinct magma reservoirs in the crust. Large, low-Al amphibole crystals record an upper crustal magma reservoir between ~4 and 8 km deep at temperatures of ~800 to 850°C. These conditions are similar to the temperatures and pressures reported by Schmitt et al. (2001) for the Purico ignimbrite. In addition, large, high $^{87}Sr/^{86}Sr$-plagioclase, and large quartz crystals in the Cerro Chascon lavas are texturally and compositionally similar to crystals within the Purico ignimbrite. We suggest that the sieved plagioclase grains and the resorbed quartz crystals record the intrusion of a hotter, more mafic magma from depth interacting with the residual magma in the Purico magma reservoir. Thermobarometric calculations indicate the recharge magma ascended from depth and underwent significant crystallization in the crust between 15 and 20 km (~400-550 MPa) below the surface. In addition to crystallization in the mid-crust, olivine crystals with Cr-spinel and basaltic melts provide evidence for a deeper magmatic component. The resorbed edges of olivines and high-Al amphibole rims indicate that olivines grew prior to reaching the mid-crust.

We also modeled temperatures using olivine-melt thermometry on olivine and olivine-hosted melt inclusions. Melt inclusion compositions were corrected for post entrapment crystallization and/or Fe^{2+} diffusion prior to calculating temperatures. To determine the extent to which post-entrapment crystallization (PEC) may have modified the inclusion glass compositions, host olivine

compositions were compared with equilibrium olivine-melt compositions predicted using the accepted equilibrium partitioning values ($K_D^{ol/liq}$) of 0.3 (Roeder and Emslie, 1970; **Figure 3.11**). To correct for PEC we used the PETROLOG software of Danyushevsky and Plechov (2011). Initial melt inclusion compositions were calculated using the "Reconstruct MI composition" algorithm. The algorithm works by simulating Fe-Mg exchange between melt and olivine during re-equilibration, and partially melting or crystallizing olivine to achieve equilibrium. Once equilibrium is reached, modeled FeO* contents are equilibrated with user input FeO* of the melt inclusion by increasing or decreasing the temperature. We also modeled the initial melt composition by simply removing olivine from the melt (**Figure 3.12**). The resulting calculated liquids of both methods were compositionally identical within analytical error for most elements. The calculated initial melt composition is given in Table 3.10.

Olivine-melt temperatures calculated using two independent geothermometers (**Figure 3.13; Table 3.11**; Putirka, 2007; Beattie, 1993) yielded temperatures ranging from 1275°C to 1282°C, well within the ~30°C error estimated for both thermometers (**Figure 3.13**; Putirka, 2008). Melt temperatures were also calculated using two liquid thermometers (equations 14 and 15 of Putirka, 2008) and yielded lower temperatures (1246-1263±50°C; **Figure 3.13; Table 3.11**). However, factoring in the errors associated with these models, these temperatures are similar. Magmatic temperatures were also determined using the MELTS software of Ghiorso and Sack (1995). The most primitive melt

composition was modeled at mid-crustal conditions (T=1,400-1,000°C; P=1000-300 MPa) while varying water contents from 0-1.25 wt.%. Fo_{77-82} olivine was on the solidus at temperatures ranging from 1224-1282°C. Although pressure estimates are not readily available for the olivine-melt system, the high-Al amphibole rims and resorbed rims indicate that the olivines had formed prior to emplacement into the mid-crust (~20 km), and MELTS modeling, although less robust, indicates pressures in excess of 450 MPa (~17km). In addition to olivine temperature-composition relationships, at higher water contents (0.75-1.25 wt.%), MELTS also predicts that An_{77-84} plagioclase (the range of plagioclase microphenocryst compositions in Cerro Chascon lavas) will crystallize at temperatures (1093-1050°C) and pressures (390-400 MPa) which is slightly higher than the crystallization conditions for the high-Al amphibole crystals.

3.8.2 Petrological and Geochemical Evidence for Magma Recharge

3.8.2.1 Bimodal crystal populations and intra-crystalline isotopic zoning

Two texturally, compositionally, and isotopically distinct populations of both plagioclase and amphibole in Cerro Chascon record the mixing of two distinct magmas. Large, low An, high $^{87}Sr/^{86}Sr$ plagioclase crystals and large low-Al amphiboles are compositionally and isotopically indistinguishable from crystals within the Purico ignimbrite, and they record low magmatic pressures and temperatures consistent with the inferred Purico ignimbrite magma reservoir. In contrast, high An, low $^{87}Sr/^{86}Sr$ plagioclase microphenocrysts and high-Al

amphibole record crystal growth in a much hotter, less evolved magma with less crustal isotopic signatures. High-Al amphibole and plagioclase-amphibole pairs record temperatures and pressures consistent with crystallization in the mid-crust. MELTS modeling conducted using PEC corrected olivine-hosted melt inclusion data (basalt) also predicts that An_{77-84} plagioclase is consistent with mid-crustal (~400 MPa), high temperature (1093-1050 °C) plagioclase crystallization from a basaltic magma.

Along with the bimodal crystal populations, sieved textures (e.g., Tsuchiyama, 1985), and compositional and isotopic zoning in individual plagioclase crystals also record mixing and crystal growth in a mixed magma. Experimental work conducted by Tsuchiyama (1985) showed that sieved or “dusty” rims form via partial melting when Na rich plagioclase crystals are immersed in a Ca rich melt. In addition, Davidson and Tepley (1997) recognized that rim-ward decreases in $^{87}Sr/^{86}Sr$ were characteristic of crystal growth following mafic recharge into an evolved felsic magma body. Large core-to-rim isotopic variations in plagioclase crystals from Cerro Chascon record the incorporation of radiogenic upper crustal ignimbrite material into the ascending mafic magma. During this process, plagioclase reacted with the hotter, more mafic melt, and it was partially resorbed, and then grew a rim in equilibrium with the surrounding mafic magma. Rare plagioclase with sieved rims in the Cerro Chascon dacite host were likely incorporated into the mafic magma before being re-introduced to the dacite, probably during a later stage of the mixing process. Similar variations in phase

chemistry and inferred magmatic processes have been described in the Chaos Crags lava domes in Lassen Volcanic National Park (Clynne, 1999; Tepley et al., 1999).

3.8.2.2 Clinopyroxene Rims on Quartz

Clinopyroxene rims on resorbed quartz crystals form as a result of the incorporation and reaction of residual quartz into the mafic, Cerro Chascon recharge magma. Sato (1975) proposed that alkali diffusion into the silicic boundary layer surrounding quartz crystals incorporated into a mafic magma increases the chemical potential of CaO relative to the groundmass resulting in clinopyroxene growth even in magmas where clinopyroxene is not saturated. In the Cerro Chascon lavas, we suggest that ascending mafic magma reheated the Purico ignimbrite magma that resulted in the transfer of crystalline material, including quartz, into the recharge magma. Once incorporated, the quartz crystals were resorbed, and clinopyroxene rims grew. Individual clinopyroxene crystals in the Cerro Chascon groundmass (**Figure 3.8B**) are texturally and compositionally indistinguishable from crystals mantling quartz crystals and may represent clinopyroxene rims disaggregated during the mixing process (Clynne, 1999). Clumps of clinopyroxene may represent parts of disaggregated rims or remnants of rims from small quartz crystals that have been completely reacted away. Similar features were observed in mixed lavas from Clear Lake, California (Stimac and Pearce, 1992).

3.8.2.3 Sanidine Oikocrysts and Ternary Feldspar Rims

Although sanidine crystals are rare in the Cerro Chascon lavas, their presence and textural and compositional features provide critical insights into the development and evolution of the Purico-Chascon magmatic system. Sanidine crystals with plagioclase rims (rapakivi texture) are similar to textures commonly observed in plutonic rocks (e.g., Hibbard, 1981; Stimac and Wark, 1992). These textures suggested that the dacite magma that was at an advanced crystalline state that was then recharged by a new pulse of mafic magma (Vernon, 1986, 1990; Bussy, 1990). The plagioclase rims on sanidine in Cerro Chascon lavas have significantly lower anorthite contents than plagioclase from the basaltic-andesite recharge magma (microphenocrysts and high anorthite rims on plagioclase phenocrysts) consistent with sandine-melt reactions and formation of dissolution boundaries (e.g., Stimac and Pearce, 1992; Bussy; 1990) rather than equilibrium plagioclase growth. The driving mechanism for the dissolution was likely the incorporation of the sanidine crystals into the ascending mafic magma. The large size (up to 5 cm) of the sanidine crystals in the Cerro Chascon lavas, along with the presence of mineral inclusions that are texturally and compositionally identical to minerals in the groundmass, are evidence for late-stage crystallization of K-rich interstitial melt in the early stages of pluton formation (Watts et al., 1999). The apparent lack of perthitic texture indicates that the magma temperature never reached the two feldspar solvus (Bowen and

Tuttle, 1950). Therefore, it is likely that the magma experienced a protracted (~800 ky) history as an upper crustal, near-solidus (>600 °C) crystal mush. Extended crustal residence times (>10^5 years) are common in silicic magma systems (Reid et al., 1997; Vazquez and Reid, 2002).

3.8.2.4 Olivine, Cr-Spinel, and Basaltic Glass Inclusions

Olivine, Cr-spinel, and olivine-hosted basaltic melt inclusions record the presence of a primitive mafic magma in the Cerro Chascon system. Spinel inclusions in olivine indicate that spinel crystallized first followed by olivine and the entrapment of olivine-hosted melt inclusions. MELTS thermodynamic modeling using basaltic melt inclusions as the starting composition is in agreement with this observed crystallization sequence. MELTS modeling indicates that clinopyroxene joins olivine at temperatures in excess of 1,100°C. In support of this, crystallization experiments conducted by Blatter et al. (2013) showed that at 400 MPa (consistent with mid-crust) $Wo_{41}En_{46}Fs_{13}$ clinopyroxene crystallizes between 1025 and 975°C. These compositions are consistent with the large clinopyroxene crystals in Cerro Chascon with sieved cores (**Figure 3.8C**). The high Mg# and Cr_2O_3 of the sieved crystals are also consistent with clinopyroxene crystallization from a more mafic magma.

3.8.2.4 Amphibole Rims on Olivine

Amphibole rims on olivine record multi-stage crystal growth in an evolving mafic liquid during ascent through the mid-crust. Amphibole rims on olivine are commonly attributed to peritectic reactions between olivine and an evolving melt during the basalt-to-andesite crystallization sequence (Sisson and Grove, 1993). During crystallization, the fractionation of anhydrous minerals (i.e. olivine, clinopyroxene, and plagioclase) effectively increases the water content of the melt until the amphibole stability field is reached (e.g., Cawthorn & O'Hara, 1976; Grove et al., 2003; Zimmer et al., 2010). In the Cerro Chascon lavas, the non-radiogenic isotopic composition of plagioclase crystals along with petrographic evidence for plagioclase and high-Al amphibole growing concurrently indicate that it was likely the rapid crystallization of plagioclase in the mid-crust that initiated amphibole growth. Experiments conducted by Blatter et al. (2013) investigated the crystallization of arc-related magnesian basalts (2 wt.% H_2O) at 400 MPa and temperatures ranging from 1,200 to 975°C. Their results show that plagioclase crystallization (An_{72}) commences at ~1,125°C, and that ~30-40 % crystallization occurs before amphibole crystallization begins at ~1,000°C. The abundance of plagioclase microphenocrysts (~45 vol.%) in the groundmass of mafic inclusions from Cerro Chascon is consistent with the amount of crystallization observed in the experiments of Blatter et al. (2013). Coombs and Gardner (2004) showed that amphibole rims grow on olivine if olivine crystals are incorporated into relatively cool (800-850°C), low-pressure (150 MPa) high-silica melts. However, phase equilibria and thermodynamic modeling discussed here

indicates that high-Al amphibole grew at much higher pressures and the model of Coombs and Gardner (2004) does not apply.

3.8.3 Recharge Model for Cerro Chascon

New geochemical and thermobarometric data allow us to modify the previous recharge model for Cerro Chascon of Davidson et al. (1990) and create a detailed P-T-t pathway for the recharge event that triggered the eruption of Cerro Chascon. Our data indicate that olivine, clinopyroxene, plagioclase ($>An_{60}$), and high-Al amphibole crystallized in the mid-crust prior to interaction with the Purico ignimbrite basement. In contrast, Davidson et al., (1990) proposed that olivine, clinopyroxene, and plagioclase ($>An_{60}$) crystallized in the mafic magma after it ponds in the upper crust. Davidson et al. (1990) also recognized that large, high $^{87}Sr/^{86}Sr$ plagioclase, low-Al amphibole, and possibly quartz and biotite in the Cerro Chascon lavas are phenocrysts from the Purico ignimbrite. We agree with this interpretation, and add that significant clinopyroxene growth occurs at the expense of quartz in the upper crust. Additionally, sanidine crystals show that the Purico magmatic system existed as a near eutectic (>600°C) crystalline mush prior to the recharge event not as solid crystalline basement.

Based on our numerous thermobarometric constraints, we present a detailed model for the recharge event at Cerro Chascon. Mafic magmas, likely derived from a lower-crustal melting, assimilation, storage, and homogenization zone (MASH; Hildreth and Moorbath, 1988) beneath the CVZ ascended into the

mid-crust. Cr-spinel was the first phase to crystallize, followed by olivine. The exact crystallization depth is unknown, but petrological relationships and thermodynamic modeling indicate olivine crystallized at depths >20 km (**Figure 3.14A**). Upon further ascent high Mg# clinopyroxene crystallized followed by high-An plagioclase at ~20 km. After ~45% crystallization and a significant increase in H_2O content, amphibole joined plagioclase on the liquidus (Figure 14B). The increase in H_2O content associated with plagioclase crystallization may have also stabilized magnetite (e.g., Osborn, 1959; Gill, 1981; Sisson & Grove, 1993). Crystallization of amphibole and magnetite continue in the mid-crust. It is plausible that the removal of olivine and pyroxene at this level eventually decreased the density of the magma until positive buoyancy was achieved and the magma ascended into the upper crust (Sparks and Huppert, 1984). The magma, now containing abundant plagioclase and amphibole ascended into the upper crust where it ponded beneath the remnant crystal-rich mush of the Purico ignimbrite magma body (**Figure 3.14C**). Upon ponding, the large temperature contrast between the two magmas (>100°C) led to the reheating and subsequent partial melting of the ignimbrite crystal mush. Individual crystalline phases record the partial melting event including isotopically zoned sieved plagioclase, resorbed quartz with clinopyroxene rims, and sanidine with plagioclase rims.

Davidson et al. (1990) proposed that following the ponding of the mafic magma and reheating of the Purico ignimbrite basement, further mafic input

resulted in the breakdown of the mafic-felsic interface and the entrainment of mafic inclusions into the overlying felsic material via viscous decoupling. We agree, but add that density instabilities resulting from gas expansion and exsolution of the highly vesicular mafic magma (>25 vol% vesicles) may have aided in inclusion formation furthering the reaction (Eichelberger, 1980). There is also evidence (i.e. sieved plagioclase and clinopyroxene rims on quartz in the host dacite) that during this time some hybrid mafic inclusions disaggregated and their contents were re-distributed within the host dacite (e.g., Tepley et al., 1999).

Mafic recharge is a common process cited for triggering silicic eruptions (e.g., Sparks et al., 1977; Eichelberger, 1978; Huppert et al., 1982; Carrigan and Eichelberger, 1990; de Silva et al., 1994; Watts et al., 1994). Recharge may be the result of increased hydraulic pressure resulting from the input of additional volume into the silicic magma reservoir (Blake, 1981, 1984), exsolution of volatiles from the silicic melt in response to recharge-induced superheating (Sparks et al., 1977), or by vapor phase exsolution of an ascending mafic magma when it cools upon establishing contact with a cooler felsic magma (Huppert et al., 1982; Tait et al., 1989; Pallister et al., 1992). In all of the scenarios described above, the over-pressurization of a magma chamber beyond the tensile strength of the surrounding wall-rock is the eruption trigger (Blake, 1981; Blake, 1984; Tait et al., 1989; Gregg et al., 2012). Davidson et al. (1990) recognized that an increase in fluid pressure resulting from the mafic recharge event may have triggered the eruption of Cerro Chascon. We agree that the recharge event likely

triggered the eruption(s), but add that vesiculation of the underlying mafic magma may have played a critical role in generating overpressure.

3.8.4 Source considerations for mafic magmas in the APVC

Most magmas that reach the surface in the APVC are highly differentiated and show variable high degrees of crustal contamination (e.g., de Silva, 1989; Davidson et al., 1991; Davidson and de Silva, 1992; Lindsay et al., 2001; Schmitt et al., 2001; Coira and Kay, 1993; Ort et al., 1996; Kay et al., 2010) owing to assimilation during ascent through ~70 km of continental crust. Davidson and de Silva (1992) investigated a suite of Quaternary minor volcanic centers from the CVZ back arc and found the most primitive lavas (picrobasalts from Chiar Kkollu) are high-Mg basalts with trace element (La/Yb and Zr/Nb) affinities that resemble enriched ocean island basalt-like compositions. However, Davidson and de Silva (1992) noted that even the most mafic compositions may record storage and modification in a deep crustal MASH zone. Enriched mantle has also been proposed for the source of mafic magmas to the south in the Puna region of the Andean plateau (Kay et al., 1999; Drew et al., 2009; Risse et al., 2013). Drew et al. (2009) proposed that the enrichments in large ion lithophile elements and LREEs in basalts from S. Puna plateau represent basalt magma genesis from long-lived (since Cretaceous), metasomatically enriched sub-continental lithospheric mantle. They also explain the high $^{87}Sr/^{86}Sr$ isotope ratios (>0.7055) observed in these lavas to the same enriched lithospheric mantle source.

Alternatively, Kay et al. (1999) and Risse et al. (2013) propose that the high $^{87}Sr/^{86}Sr$ isotope ratios (>0.7055) and high elemental Sr (>700 ppm) observed in back-arc basalts from the southern Puna plateau in Argentina record partial melting of depleted mantle that was re-enriched in the Miocene by crustal addition during subduction erosion of the forearc. Risse et al. (2013) determined that ~13% partial melting of lherzolite at ~60 km depth (depth of Moho in the region) could explain the compositions of the most mafic back-arc lavas in the southern Puna. Kay et al. (2011) measured $\delta^{18}O$ values from the samples utilized by Risse et al. (2013) and noted that even the most primitive olivine crystals (Fo_{88} and ~5000 ppm Ni) have elevated $\delta^{18}O$ values (up to 6.8 per mil) indicating that the mafic magmas were contaminated by crustal material prior to olivine growth.

Spinel compositions reported in this study plot in a field characteristic of crystal growth in an enriched mantle source. However, the high-Mg olivine compositions reported herein (Fo_{82}) are too low to represent primary mantle-derived olivine (i.e. > Fo_{88}). In addition, it is generally accepted that mantle-derived magmas contain >5000 ppm Ni. The Ni concentrations of olivine from Cerro Chascon (<1000 ppm) are consistent with crystallization from magma with <100 ppm Ni (assuming a Kd_{Ni} of 10; Mysen, 1979). Thus, although olivine and basalt melt inclusions are recording true mafic magmas it is likely that these magmas have been modified prior to the crystallization of olivine. These results are in agreement with the olivine crystals discussed by Kay et al. (2011) in the

southern Puna back-arc. Davidson and de Silva (1992) proposed that compositional and isotopic baseline for magmas erupted in the CVZ since the Miocene are largely controlled by interactions of mafic magma in the lowermost crust in a lower crustal MASH zone. The lower Fo and Ni contents of olivine in Cerro Chascon along with similar features in olivine from the southern Puna are consistent with crystallization following magma modification in the lower crust. In addition, the enriched isotope ratios ($^{87}Sr/^{86}Sr$ >0.7055) observed in mafic magmas throughout the CVZ, including Cerro Chascon and the southern Puna back-arc, are consistent with the MASH zone isotopic baseline proposed by Davidson et al. (1991) and Davidson and de Silva (1992).

Interestingly, our data indicates that the mafic magma crystallization extensively at ~20 km depth. Extensive plagioclase crystallization resulted an ~2-fold increase in water content and subsequently stabilized amphibole and possibly magnetite (Zimmer et al., 2010). The isotopic character of plagioclase microphenocrysts indicates that when crystallization occurred at ~20 km, the mafic magma had not been modified significantly by crustal assimilation. Quantifying the total amount of assimilation is not possible due to a lack of isotopic constraints on the mantle end member (see Kay et al., 2010 for discussion), but a conservative estimate would be between 0 and 10% crustal material. The lowest $^{87}Sr/^{86}Sr$ isotope ratios recorded in individual crystals in Cerro Chascon (~0.7057) consistent with the enriched mantle of Kay et al. (2010) and/or the MASH zone of Davidson and de Silva (1992). Further studies of

olivine-hosted melt inclusions including detailed isotopic and trace element information are needed to better constrain the composition and role of mantle derived magmas in these systems.

CONCLUSIONS

Detailed textural, compositional, and isotopic data from individual crystalline phases within arc lavas reveals critical information about the ascent, storage, and mixing of magmas in continental arc magmatic system. Deep crustal magmas invisible at the bulk rock scale are recorded in olivine-hosted spinel inclusions, olivine phenocrysts, and olivine-hosted melt inclusions. These magmas crystallize extensively in the mid-crust (~20 km depth) resulting in the formation of crystal-rich basaltic–andesite magmas that are texturally and compositional akin to crystal-rich mafic inclusions found in subduction related lavas worldwide. Crustal anatexis and mixing do not appear to play a significant role in evolution of ascending mafic magmas in the mid-crust, but are important processes once magmas rise into the uppermost 4-8 km of the crust. The mixing of these deeper, lower-crustal magmas with magmas stored in the upper crust results in the bimodal character common in arc magmas. Future work is needed to constrain the true composition of the lower crustal magma. This work will include a more robust characterization of the basaltic melt inclusions including REE and isotopic characterization. In addition, now that we understand the locations, processes, and relative timing of the recharge event at Cerro Chascon,

crystal growth and diffusion-based trace element modeling can be used to estimate the timescales associated with the recharge event.

REFERENCE

Andersen, D.J., Lindsley, D.H., & Davidson, P.M. (1993). QUILF: A Pascal program to assess equilibria among Fe–Mg–Mn–Ti oxides, pyroxenes, olivine, and quartz. *Computers & Geosciences* 19, 1333-1350.

Anderson J.L., & Smith D.R. (1995). The effects of temperature and 102 on the Al-in-hornblende barometer. *American Mineralogist* 80, 549-559.

Beattie, P. (1993). Olivine melt and orthopyroxene melt equilibria. *Contributions to Mineralogy and Petrology* 115, 103-111.

Blake, S. (1981). Volcanism and the dynamics of open magma chambers. *Nature* 289, 783-785

Blake, S. (1984). Volatile oversaturation during the evolution of silicic magma chambers as an eruption trigger. *Journal Of Geophysical Research* 89, 8237-8244.

Blatter, D.L., Sisson, T.W., & Hankins, W.B. (2013). Crystallization of oxidized, moderately hydrous arc basalt at mid- to lower-crustal pressures: implications for andesite genesis. *Contributions to Mineralogy and Petrology* 166, 861-886.

Bowen, N.L. & Tuttle, O.F. (1950). The system $NaAlSi_3O_8$-$KAlSi_3O_8$-H_2O. *Journal of Geology* 58, 489-511.

Bussy, F. (1990). The rapakivi texture of feldspars in a plutonic mixing environment: A dissolution-recrystallization process? *Geological Journal* 25, 319-324.

Carrigan, C. & Eichleberger, J. (1990). Zoning of magmas by viscosity in volcanic conduits. *Nature* 343, 248-251.

Cawthorn, R.G. & O'Hara, M.J. (1976). Amphibole fractionation in calc-alkaline magma genesis. *American Journal of Science* 276, 309-329.

Charlier, B. L. A., Ginibre, C., Mogan, D., Nowell, G. M., Pearson, D. G., Davidson, J. P., and Ottley, C. J. (2006). Methods for the microsampling and high-precision analysis of strontium and rubidium isotopes at single crystal scale for petrological and geochronological applications. *Chemical Geology* 232, 114–133.

Clynne, M. & Borg, L. (1997). Olivine and chromian spinel in primitive calc-alkaline and tholeiitic lavas from the southernmost Cascade Range, California; a reflection of relative fertility of the source. *Canadian Mineralogist* 35, 453.

Coombs, M. & Gardner, J. (2004). Reaction rim growth on olivine in silicic melts: Danyushevsky, L.V. & Plechov, P. (2011). Petrology Users Manual, 1–23.
Davidson, J.P. & de Silva, S. (1992). Volcanic rocks from the Bolivian Altiplano: Insights into crustal structure, contamination, and magma genesis in the central Andes. *Geology* 20, 1127.
Davidson, J.P., de Silva, S., Holden, P., & Halliday, A. (1990). Small-Scale Disequilibrium in a Magmatic Inclusion its More Silicic Host. *Journal of Geophysical Research 95*, 17661–17675.
Davidson, J.P., Harmon, R., & Worner, G. (1991). The source of central Andean magmas; Some considerations. *Geological Society of America Special Paper* 265, 233–245.
Davidson, J.P., Hora, J., Garrison, J., Dungan, M. (2005). Crustal forensics in arc magmas. *Journal of Volcanology and Geothermal Research* 140, 157–170.
Davidson, J.P. & Tepley, F.J.T. (1997). Recharge in volcanic systems: evidence from isotope profiles of phenocrysts. *Science* 275, 826.
Davidson, J.P., Turner, S., Handley, H., Macpherson, C., & Dosseto, Anthony. (2007a) Amphibole “sponge” in arc crust? *Geology* 35, 787.
Davidson, J.P., Morgan, D.J., & Charlier, B.L. (2007b). Isotopic Microsampling of Magmatic Rocks. *Elements* 3, 253–259.
de Silva, S. (1989). Altiplano-Puna volcanic complex of the central Andes. *Geology* 17, 1102.
de Silva, S. (1991). Styles of zoning in central Andean ignimbrites; Insights into magma chamber processes. *Geological Society of America Special Paper* 265, 217–232.
de Silva, S., Salas, G., & Schubring, S. (2008). Triggering explosive eruptions—The case for silicic magma recharge at Huaynaputina, southern Peru. *Geology* 36, 387.Implications for magma mixing. *American Mineralogist* 89, 748.
de Silva, S., Self, S., Francis, P., Drake, R., & Carlos, R. (2007). Effusive silicic volcanism in the Central Andes: The Chao dacite and other young lavas of the Altiplano-Puna Volcanic Complex. *Journal Of Geophysical Research* 99, 17805–17825.
Drew, S.T., Ducea, M.N., & Schoenbohm, L.M. (2009). Mafic volcanism on the Puna Plateau, NW Argentina: Implications for lithospheric composition and evolution with an emphasis on lithospheric foundering. *Lithosphere* 1, 305–318.
Eichelberger, J.C. (1978). Andesitic volcanism and crustal evolution. *Nature* 275, 2l-27.
Frost, T. & Mahood, G. (1987). Field, chemical, and physical constraints on mafic-felsic magma interaction in the Lamarck Granodiorite, Sierra Nevada, California. *Geological Society of America Bulletin* 99, 272–291.
Ghiorso, M.S. & Sack, R.O. (1995). Chemical Mass Transfer in Magmatic Processes IV. A revised and internally consistent thermodynamic model for the interpolation and extrapolation of liquid-solid equilibria in magmatic

systems at elevated temperatures and pressures. *Contribution to Mineralogy and Petrology* 119, 197-212.

Gill, J.B. (1981). Orogenic Andesites and plate tectonics. Springer, Berlin, p 390

Grove, T.L., Elkins-Tanton, L.T., Parman, S.W., Chatterjee, N., Muntener, O. & Gaetani, G.A. (2003). Fractional crystallization and mantle-melting controls on calc-alkaline differentiation trends. *Contributions to Mineralogy and Petrology* 145, 515-533.

Hammarstrom, J.M., & Zen, E. (1986). Aluminum in hornblende: An empirical igneous geobarometer. *American Mineralogist* 71, 1297-1313.

Hawkesworth, C., Hammill, M., Gledhill, A., van Calsteren, P., & Rogers, G. (1982). Isotope and trace element evidence for late-stage intra-crustal melting in the High Andes. *Earth and Planetary Science Letters* 58, 240–254.

Helz, R.T. (1982). Phase relations and compositions of amphiboles produced in studies of the melting behavior of rocks. In: Ribbe P (ed) Amphiboles; petrology and experimental phase relations. *Mineralogical Society of America*, Washington, DC, pp 279–353.

Hibbard, M.J. (1981). The magma mixing origin of mantled feldspars. *Contributions to Mineralogy and Petrology* 76,158-170.

Hildreth, W. & Moorbath, S. (1988). Crustal contributions to arc magmatism in the Andes of central Chile. *Contributions to Mineralogy and Petrology* 98, 455–489.

Holland, J.D. & Blundy, T.J.B. (1994). Calcic amphibole equilibria and a new amphibole±plagioclase geothermometers, *Contributions to Mineralogy and Petrology* 104, 208-224.

Huppert, H.E. Sparks, R.S.J., and Turner, J.S., (1982). Effects of volatiles on mixing in calc-alkaline magma systems. *Nature* 297, 554-557.

Johnson, D.M., Hooper, P.R., and Conrey, R.M. (1999). XRF analysis of rocks and minerals for major and trace elements on a single low dilution Li-tetraborate fused bead. *Advances in X-ray Analysis* 41, 843-867.

Kamenetsky, V.S., Crawford, A.J., & Meffre, S. (2001). Factors controlling chemistry of magmatic spinel: an empirical study of associated olivine, Cr-spinel and melt inclusions from primitive rocks. J*ournal of Petrology* 42, 655–671.

Kay, S.M., Coira, B.L., Caffe, P.J., & Chen, C-H. (2010). Regional chemical diversity, crustal and mantle sources and evolution of central Andean Puna plateau ignimbrites. *Journal of Volcanology and Geothermal Research* 198, 81–111.

Lindsay, J., Schmitt, A., Trumbull, R., de Silva, S., Siebel, W., & Emmerman, R.(2001). Magmatic evolution of the La Pacana caldera system, central Andes, Chile: Compositional variation of two cogenetic, large-volume felsic ignimbrites. *Journal of Petrology* 42, 459–486.

Osborn, E.F. (1959). Role of oxygen pressure in the crystallization and differentiation of basaltic magma. *American Journal of Science* 257, 609–647.

Pallister, J.S., Hoblitt, R.P., & Reyes, A.G. (1992). A basalt trigger for the 1991 eruptions of Pinatubo volcano? *Nature* 356, 426–428.

Putirka, K.D. (2008). Thermometers and barometers for volcanic systems, *in* Putirka, K.D., and Tepley, F.J., eds., Minerals, inclusions and volcanic processes. *Reviews in Mineralogy and Geochemistry* 69, 61–120.

Putirka, K.D., Perfit, M., Ryerson, F.J., & Jackson, M.G. (2007). Ambient and excess mantle temperatures, olivine thermometry, and active vs. passive upwelling. *Chemical Geology* 241, 177-206.

Ramos, F.C. (1992). Isotope Geology of the Metamorphic Core of the Central Grouse Creek Mountains, Box Elder County, Utah. University of California Los Angeles.

Reid, M., Coath, C., Harrison, T., & McKeegan, K. (1997). Prolonged residence times for the youngest rhyolites associated with Long Valley Caldera: 230Th--238U ion microprobe dating of young zircons. *Earth and Planetary Science Letters* 150, 27–39.

Ridolfi, F., Renzulli, A., & Puerini, M. (2010). Stability and chemical equilibrium of amphibole in calc-alkaline magmas: an overview, new thermobarometric formulations and application to subduction-related volcanoes. *Contributions to Mineralogy and Petrology* 160, 45–66.

Risse, A., Trumbull, R., & Kay, S.M.,Coira, B., & Romer, R. (2013). Multi-stage Evolution of Late Neogene Mantle-derived Magmas from the Central Andes Back-arc in the Southern Puna Plateau of Argentina. *Journal of Petrology* 54, 1963–1995.

Roeder, P.E., Emslie, R.F. (1970). Olivine-liquid equilibrium. *Contributions to Mineralogy and Petrology* 29, 275–289.

Ruprecht, P. & Wörner, G. (2007). Variable regimes in magma systems documented in plagioclase zoning patterns: El Misti stratovolcano and Andahua monogenetic cones. *Journal of Volcanology and Geothermal Research* 165, 142–162.

Sato, H. (1975). Diffusion coronas around quartz xenocrysts in andesites and basalts from Tertiary volcanic region in north eastern Shikoku, Japan. *Contributions to Mineralogy and Petrology* 50, 40-64.

Schmitt, A., de Silva, S., Trumbull, R., & Emmermann, R. (2001). Magma evolution in the Purico ignimbrite complex, northern Chile: evidence for zoning of a dacitic magma by injection of rhyolitic melts following mafic recharge. *Contributions to Mineralogy and Petrology* 140, 680–700.

Sisson, T.W. & Grove, T.L. (1993a). Experimental investigations of the role of H2O in calc-alkaline differentiation and subduction zone magmatism. *Contributions to Mineralogy and Petrology* 113, 143-166.

Sparks, R.S.J. & Huppert, H.E. (1984). Density changes during the fractional crystallization of basaltic magmas: fluid dynamic implications. *Contributions to Mineralogy and Petrology* 85, 300–309.

Sparks, S. & Sigurdsson, H. (1977). Magma mixing: a mechanism for triggering acid explosive eruptions. *Nature* 267, 315–318.

Stimac, J.A. & Pearce, T.H. (1992). Textural evidence of mafic-felsic magma interaction in dacite lavas, Clear Lake, California. *American Mineralogist* 77, 795-809.

Stimac, J.A. & Wark, D.A. (1992). Plagioclase mantles on sanidine in silicic lavas, Clear Lake, California: Implications for the origin of rapakivi texture. *Geological Society of America Bulletin* 104, 728-744.

Tait, S., Jaupart, C., & Vergniolle, S. (1989). Pressure, gas content and eruption periodicity of a shallow, crystallising magma chamber. *Earth and Planetary Science Letters* 92, 107-123.

Tsuchiyama, A. (1985). Dissolution kinetics of plagioclase in the melt of the system diopside-albite-anorthite, and origin of dusty plagioclase in andesites. *Contributions to Mineralogy and Petrology* 89, 1-16.

Vazquez, J.A. & Reid, M.R. (2002). Time scales of magma storage and differentiation of voluminous high-silica rhyolites at Yellowstone caldera, Wyoming. *Contributions to Mineralogy and Petrology* 144, 274–285.

Vernon, R.H. (1990). Crystallization and hybridism in microgranitoid enclave magmas: Microstructural evidence. *Journal of Geophysical Research* 95, 17849-17859.

Watts, R., de Silva, S., Croudace, G. (1999). Effusive eruption of viscous silicic magma triggered and driven by recharge: a case study of the Cerro Chascon-Runtu Jarita Dome Complex in Southwest Bolivia. *Bulletin of Volcanology* 61, 241–264.

Yernon, R.H. (1986). K-feldspar megacrysts in granites-phenocrysts, not porphyroblasts. *Earth Science Reviews* 23,1-63.

Zimmer, M.M., Plank, T., Hauri, E.H., Yogodzinski, G., Stelling, P., Larsen, S., Singer, B., Jicha, B., Mandeville, C., & Nye, C. (2010). The Role of Water in Generating the Calc-alkaline Trend: New Volatile Data for Aleutian Magmas and a New Tholeiitic Index. *Journal of Petrology* 51, 2411–2444.

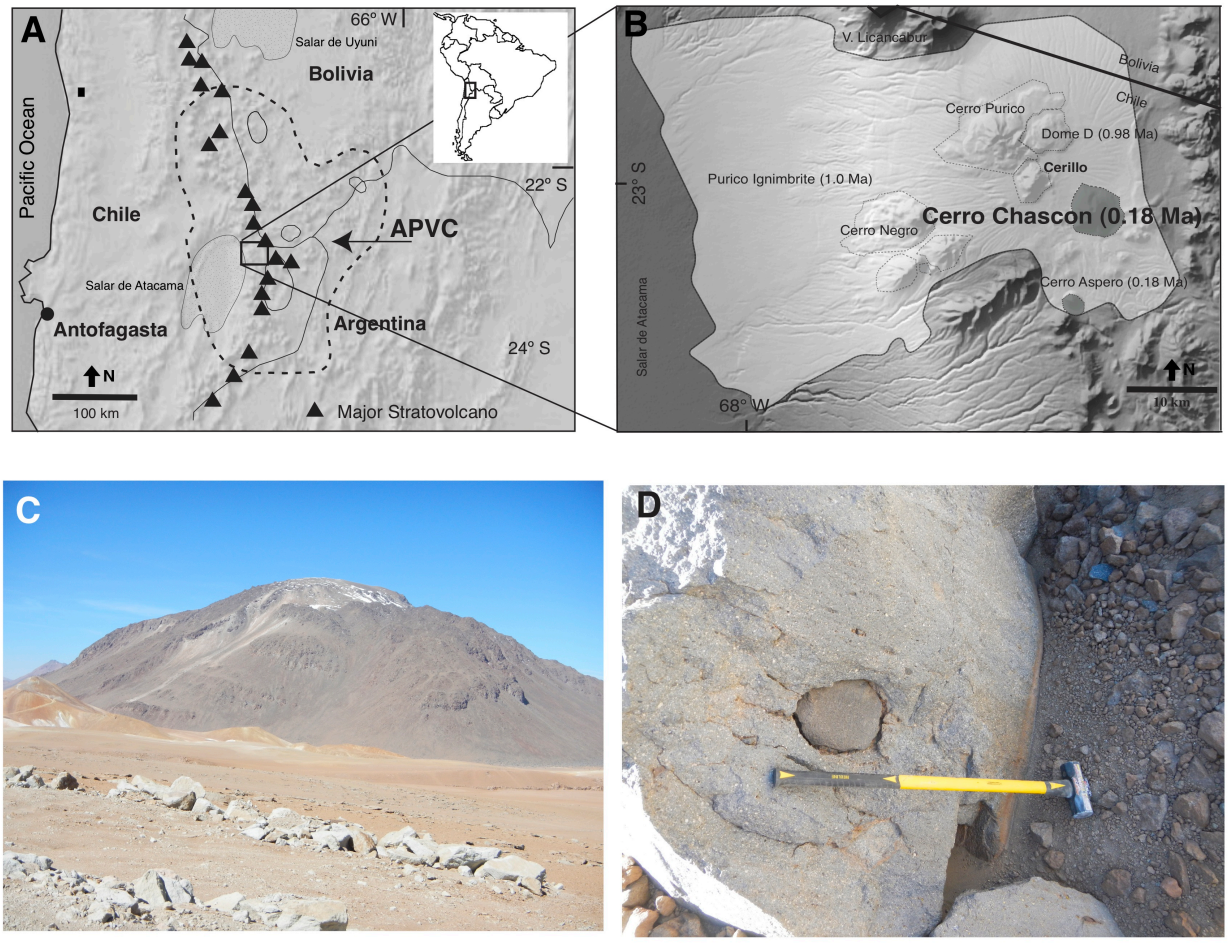

Figure 3.1. (A) Map shows the location of the Purico-Chascon volcanic complex in South America. Dashed field marks the extent of the Altiplano-Puna volcanic complex (APVC). The circular fields represent the locations of APVC calderas (Salisbury et al., 2010) and stippled fields represent salars. (B) Map shows the features of the 1.0 to recent Purico-Chascon volcanic complex. This study is focused on the Cerro Chascon lava dome. (C) Photograph shows the Cerro Chascon viewed from the SW. (D) Photograph of typical Cerro Chascon outcrop showing a quenched basaltic-andesite inclusion hosted in crystal-rich dacite (hammer handle is ~1 m).

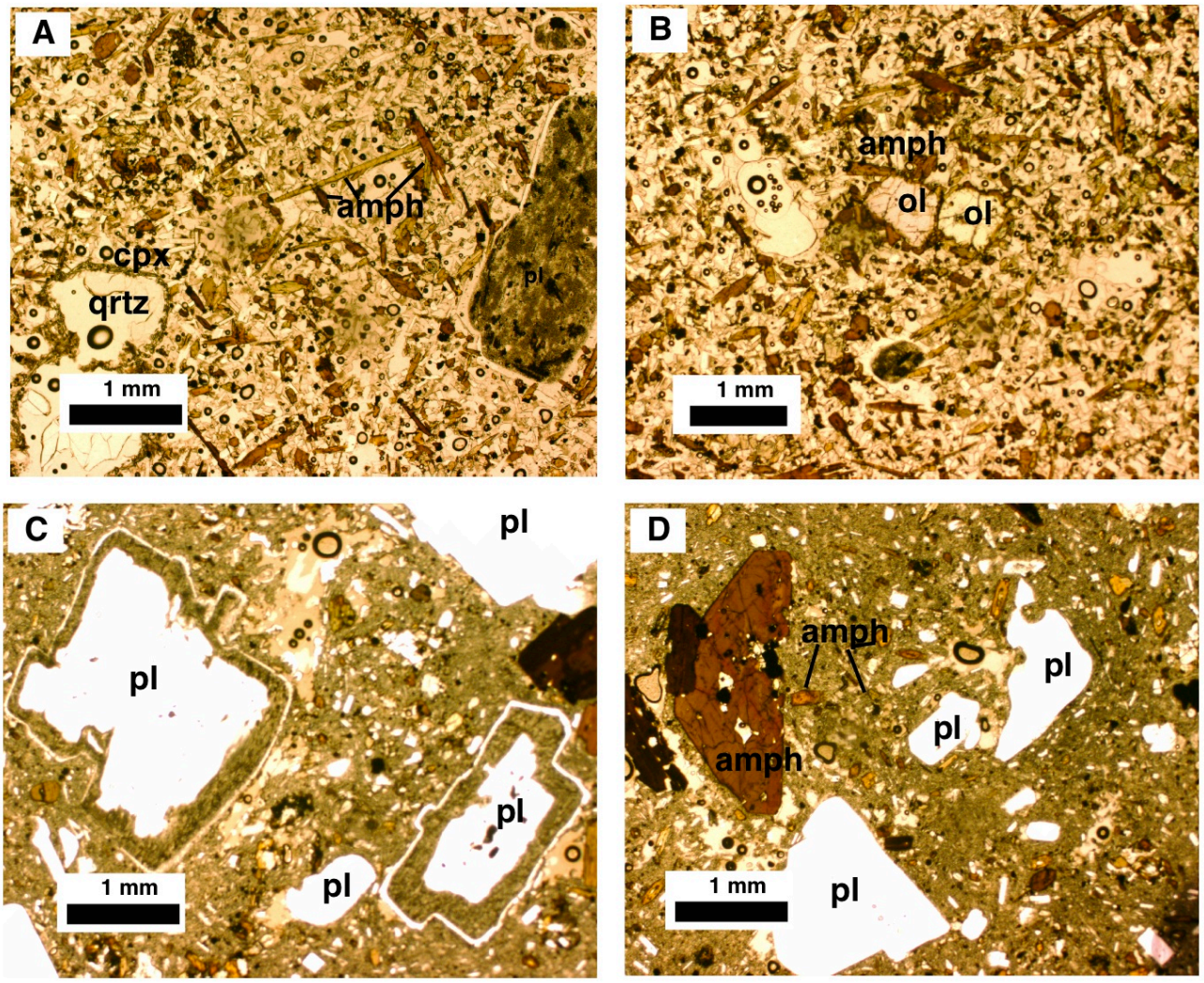

Figure 3.2. Photomicrographs show the textures and crystal contents of mafic inclusions (A, B) and host dacite (C, D). Note the resorbed quartz rimmed with clinopyroxene and the heavily sieved plagioclase crystal (A), olivine crystals with amphibole rims (B,C), dusty sieved and clear plagioclase in the same section, and two distinct amphibole size populations (D).

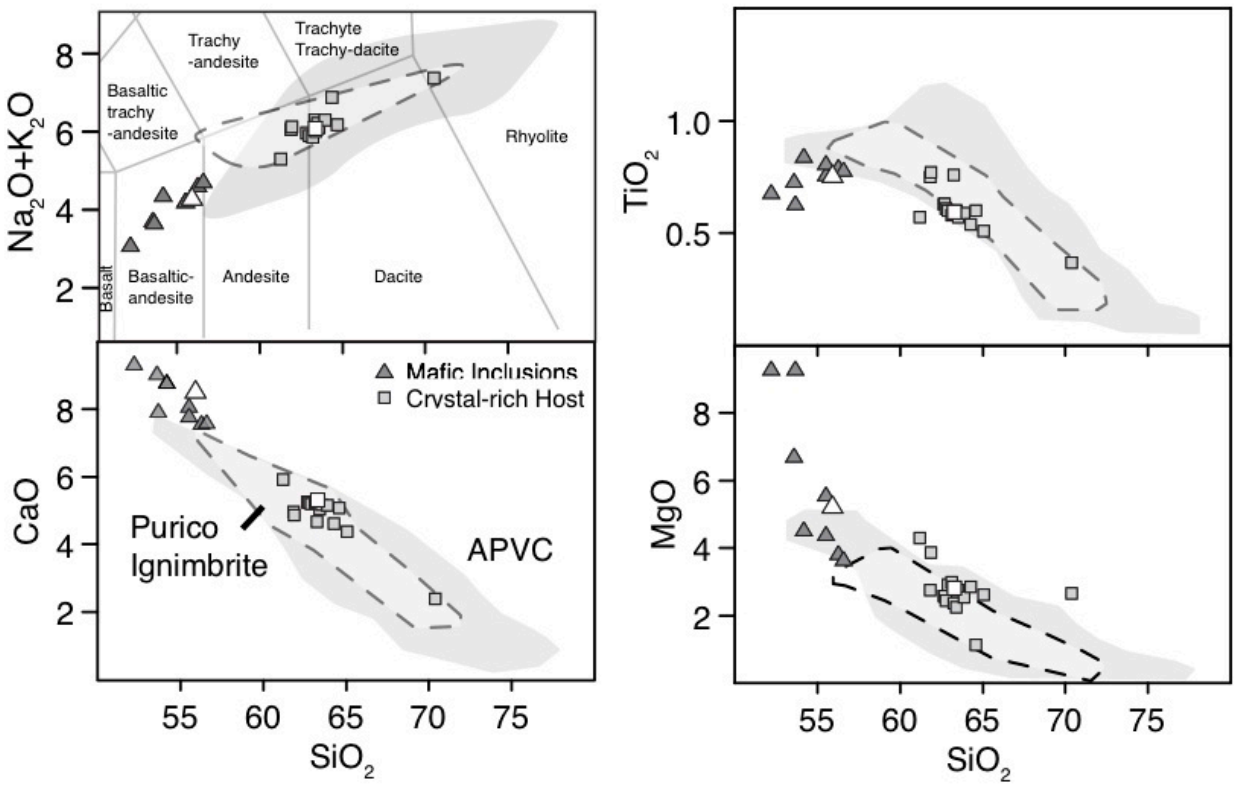

Figure 3.3. Major element Harker and TAS diagrams for the Cerro Chascon lava dome (wt.% oxides). Grey data points represent data from the literature and white data points are new to this study. Data from the Purico ignimbrite (white field with dashed lines) and the volcanic centers from the APVC (grey field) are included for reference, see figure for details. Data sources include Hawkesworth et al., (1982), Schmitt et al., (2001), and de Silva et al., (2006).

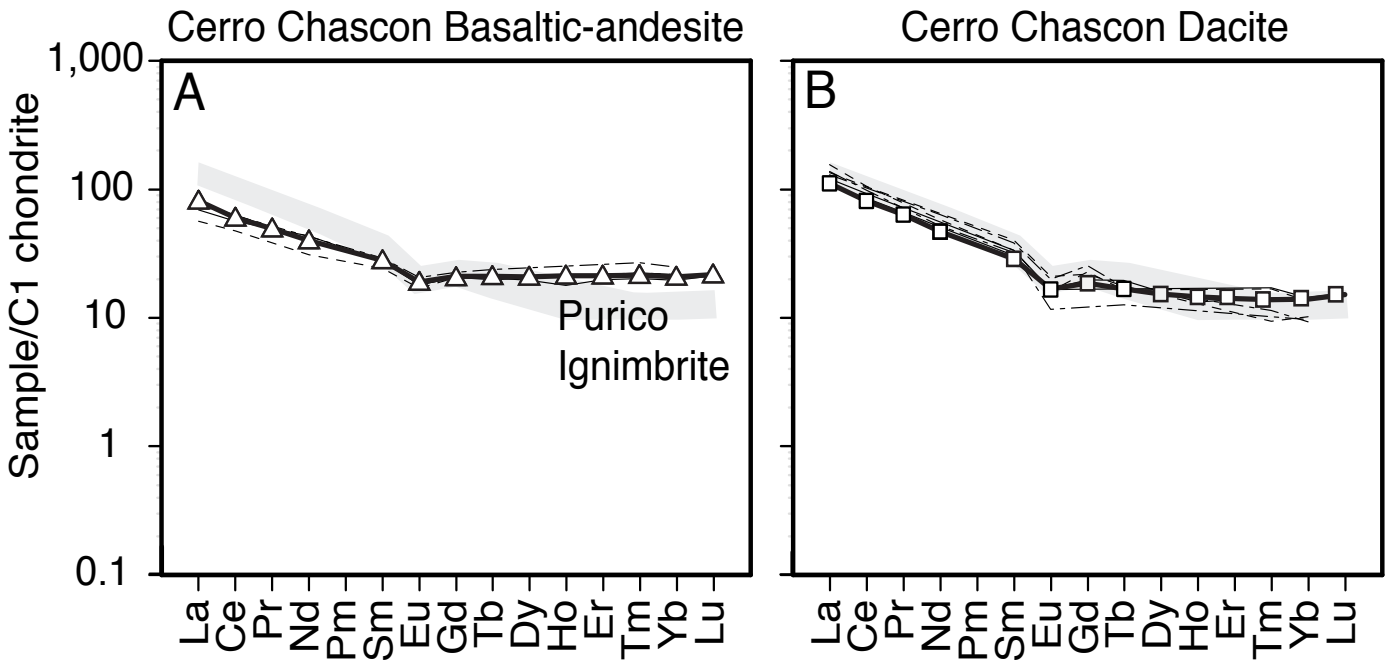

Figure 3.4. C1 chondrite normalized REE diagrams show the normalized concentration of REE in basaltic-andesite and dacite lavas from Cerro Chascon. The dashed lines represent data from the Cerro Chascon lavas reported by Hawkesworth et al., (1982) and Schmitt et al., (2001). The grey field represents analyses of Purico ignimbrite reported by Schmitt et al., (2001). C1 chondrite data is from Sun and McDonough (1989).

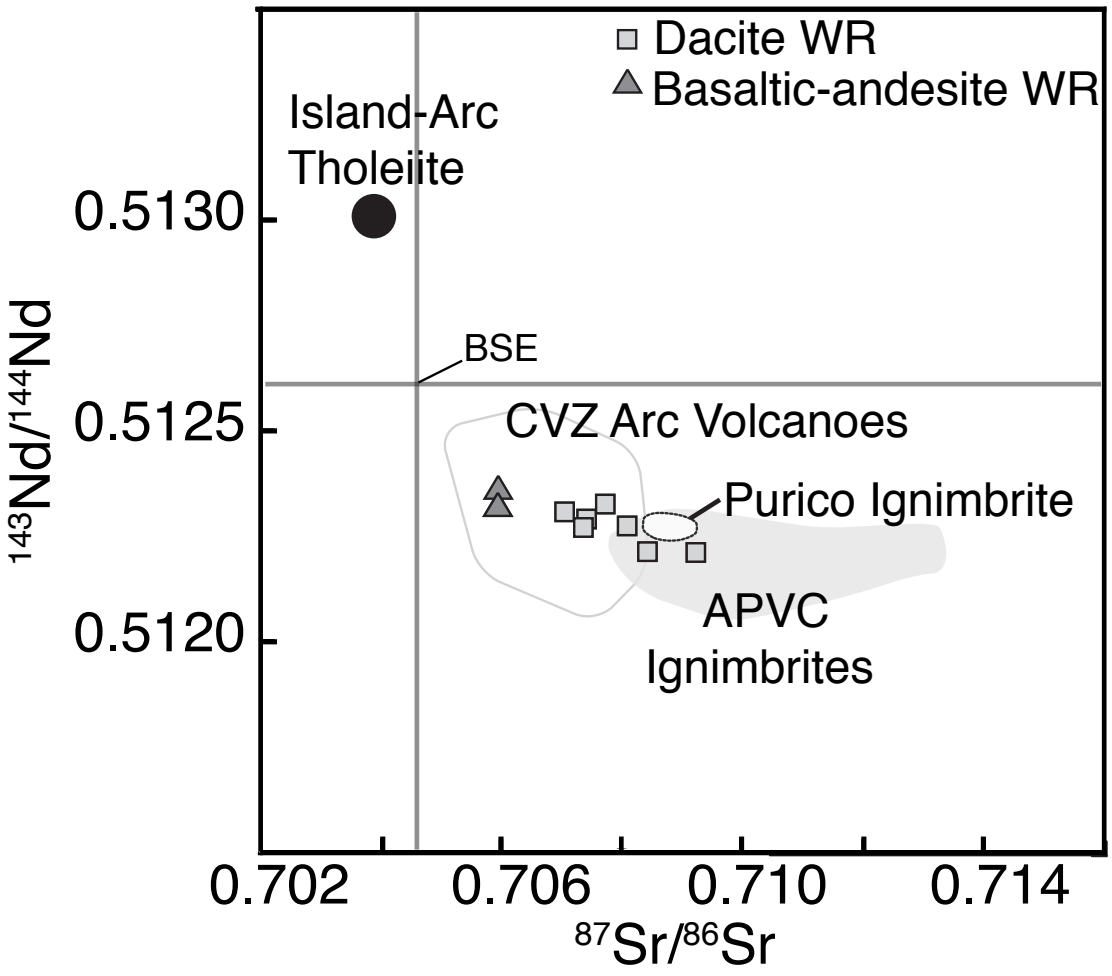

Figure 3.5. Plot shows whole rock $^{87}Sr/^{86}Sr$ vs. $^{143}Nd/^{144}Nd$ for lavas from Cerro Chascon. Included are data from the Purico ignimbrite, recent lavas (<1 Ma) from the CVZ arc-front, and ignimbrites and lavas from the APVC (10-1 Ma). Diagram also includes the average composition of island-arc tholeiites and bulk silicate Earth (BSE). Data sources include Schmitt et al., (2001), Hawkesworth et al., (1982), de Silva et al., 2006; Lindsay et al., 2001; Jacobsen and Wasserburg, 1984; Zindler and Hart, 1986).

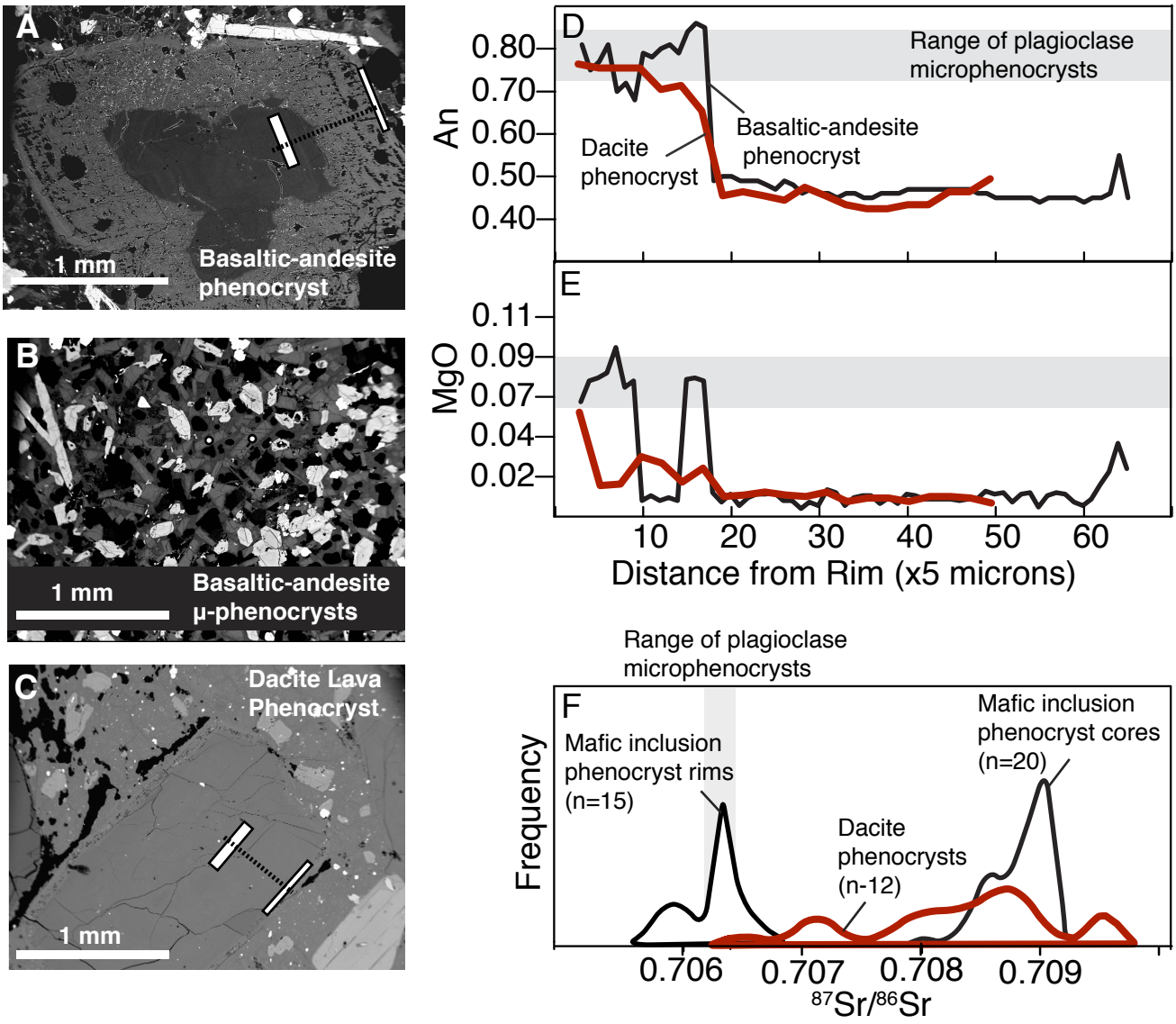

Figure 3.6. (A-C) Back-scattered electron images show plagioclase populations discussed in the text. The black dashed lines show the location of EMP transects and the white boxes and points show the locations sampled for isotopes using LA-MC-ICP-MS. Major and trace element data are from crystals shown. (D-E) Plots show core to rim An and MgO variations from phenocrysts within the basaltic-andesite and dacite lavas. The black and red lines show compositional variations along the transects shown on the basaltic-andesite and dacite phenocrysts, respectively. The grey field represents the compositional range of plagioclase microphenocrysts from the Cerro Chascon lavas (n=35 crystals). Note the overlap between plagioclase phenocryst rims and the microphenocrysts. (F) Frequency curves from Burns et al., (2014) show the distribution of $^{87}Sr/^{86}Sr$ isotope ratios of plagioclase crystals from both Cerro Chascon lavas. Crystals from the basaltic-andesite are separated into core and rim analyses to show the distinct isotopic character of each area. The grey field represents the isotopic range of plagioclase microphenocrysts (n=4 crystals).

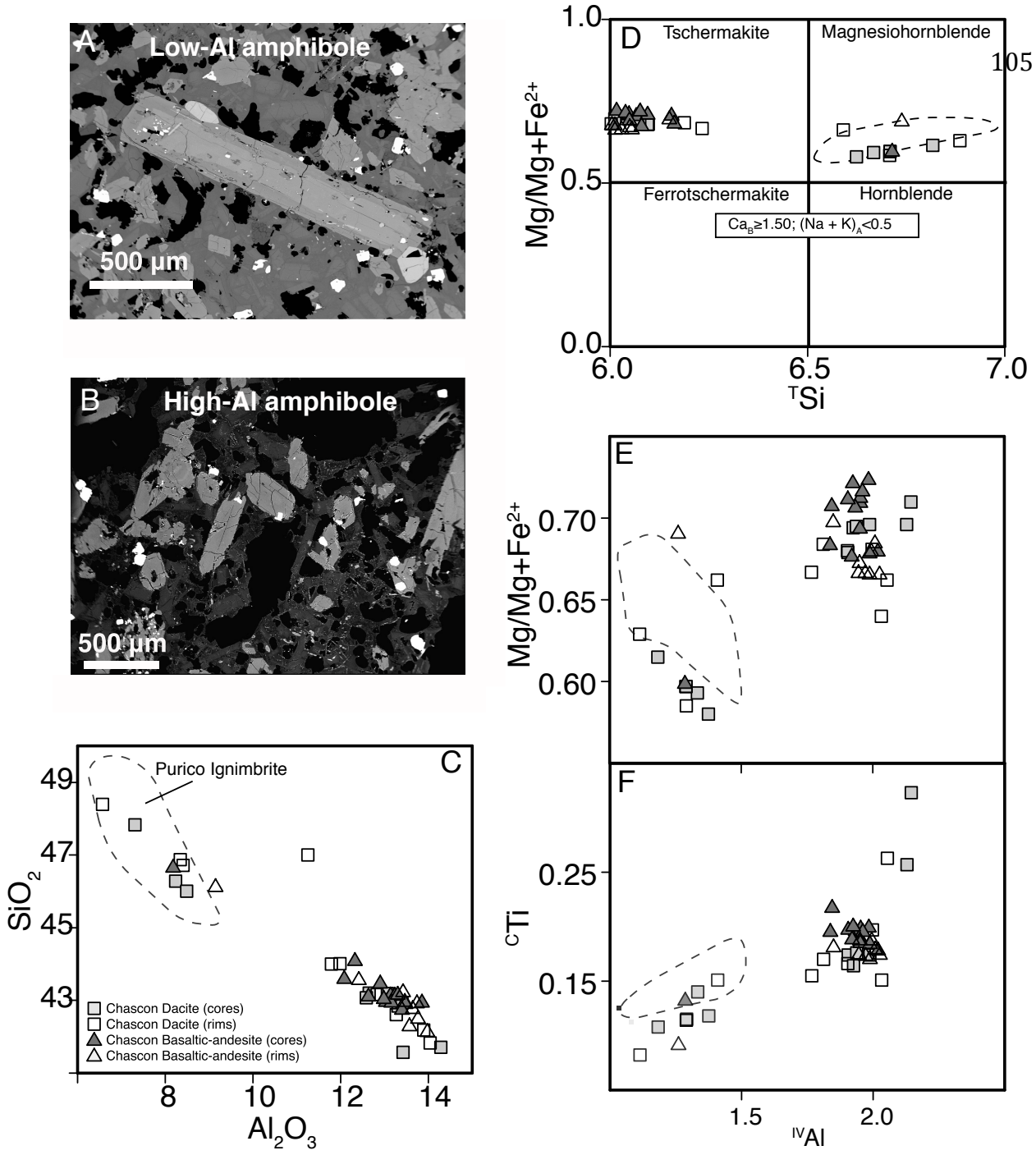

Figure 3.7. (A, B) Back-scattered electron images of representative low-Al and high-Al amphibole crystals in the Cerro Chascon lavas. (C) Al_2O_3 vs. SiO_2 diagram compares high and low Al amphiboles from the Purico ignimbrite and Cerro Chascon lavas. Note the similarity between low-Al amphibole in the Purico ignimbrite pumice and Cerro Chascon lavas. Also, note the compositional gap between high- and low-Al amphiboles (~9-12 wt.% Al_2O_3). (D) Amphibole classification diagram following Leake et al., (1997) shows Si per formula unit vs. Mg# [Mg/(Mg+Fe^{2+}]. Low-Al amphibole in the Purico ignimbrite and Cerro Chascon lavas are magnesiohornblendes. High-Al amphiboles in the Cerro Chascon lavas are tschermakites. (E, F) Diagrams show tetrahedral coordinated Al vs Mg# and Ti in the c-lattice site. Note the large compositional gaps between the two groups indicating the two amphibole types grew in distinct pressure-temperature environments.

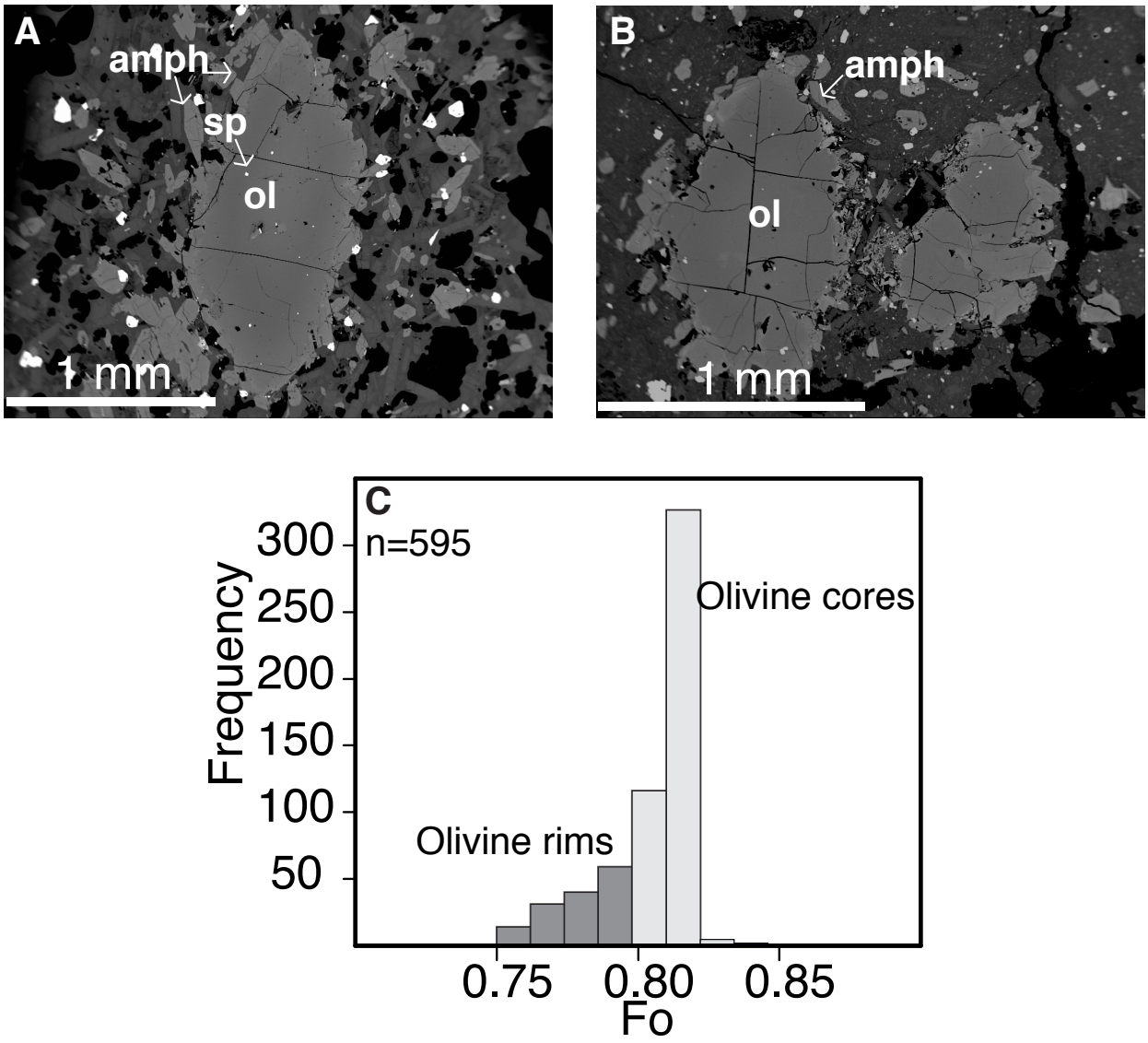

Figure 3.8. (A-B) BSE images show representative olivine crystals from the basaltic-andesite (A) and dacite (B) lavas from Cerro Chascon. Highlighted in the images is Cr-spinel inclusions and high-Al amphibole. Also note that the olivine in A contains a basaltic melt inclusion near the center of the crystal. (C) Histogram shows the distribution of Fo contents in olivine from Cerro Chascon.

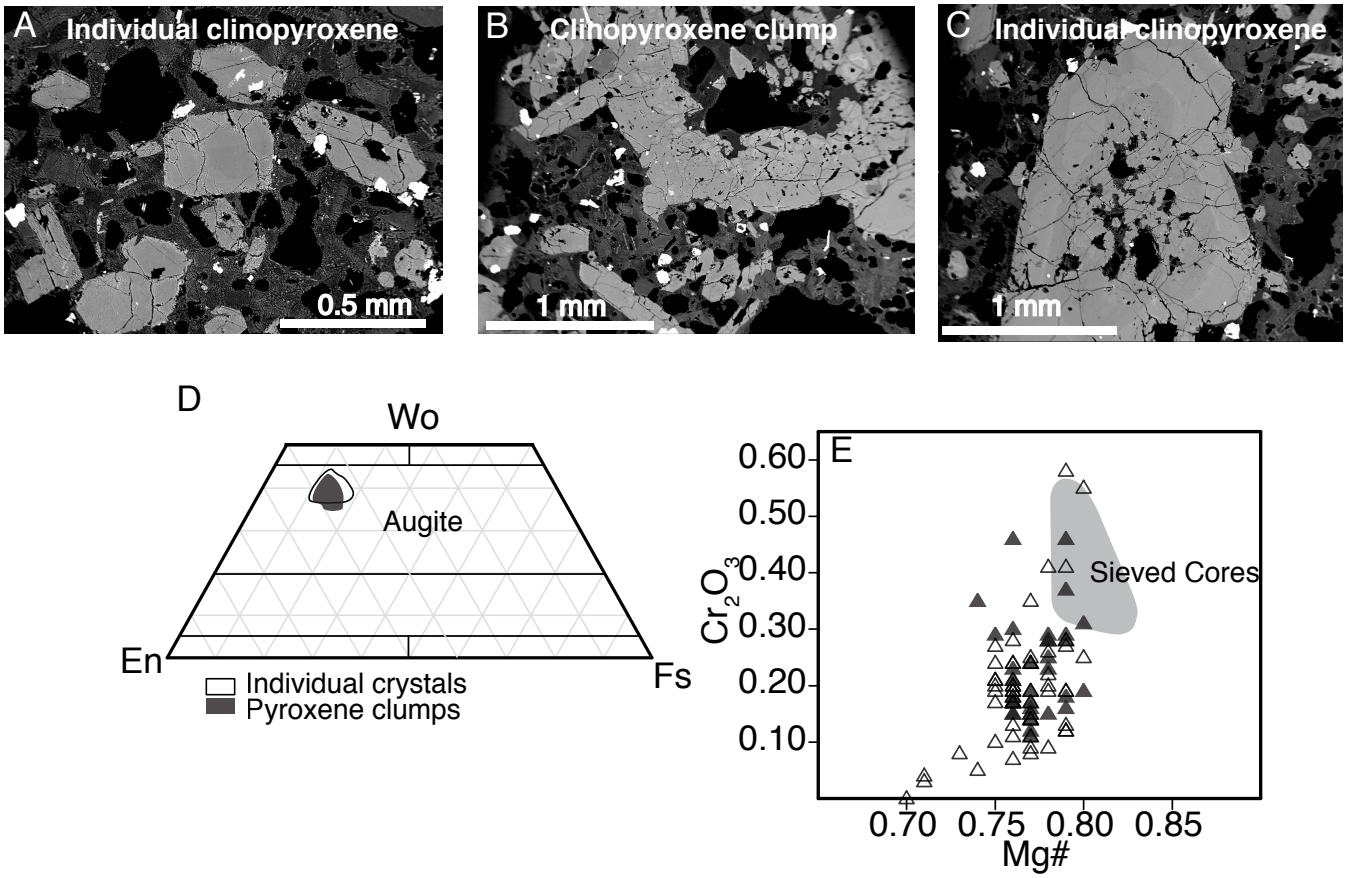

Figure 3.9. (A-C) BSE images show the clinopyroxene types described in the text. (D) Ternary diagram shows the composition of individual pyroxene crystals in the groundmass and crystal clumps, some surrounding resorbed quartz. Note the apparent lack of variability between the types. (E) Bi-variate plot shows Mg# ($Mg_{atomic}/[Mg_{atomic}+Fe_{atomic}]$) versus Cr_2O_3. Note that clinopyroxene with sieved cores have high Mg# and Cr_2O_3.

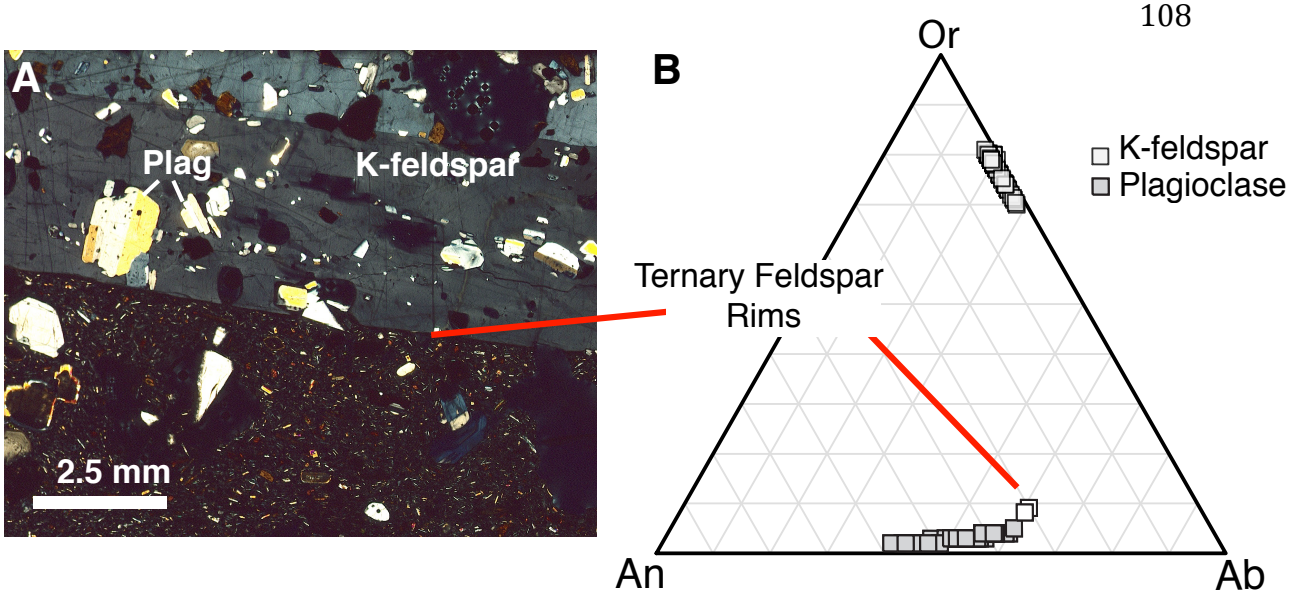

Figure 3.10. (A) Photomicrograph shows a large K-feldspar oikocryst containing phenocrysts of plagioclase and amphibole. (B) Ternary diagram shows the composition(s) of K-feldspar and plagioclase inclusions. Note that the K-feldspar does not display perthitic texture, and that plagioclase compositions are identical to crystals within the Purico ignimbrite and cores of crystals within Cerro Chascon lavas.

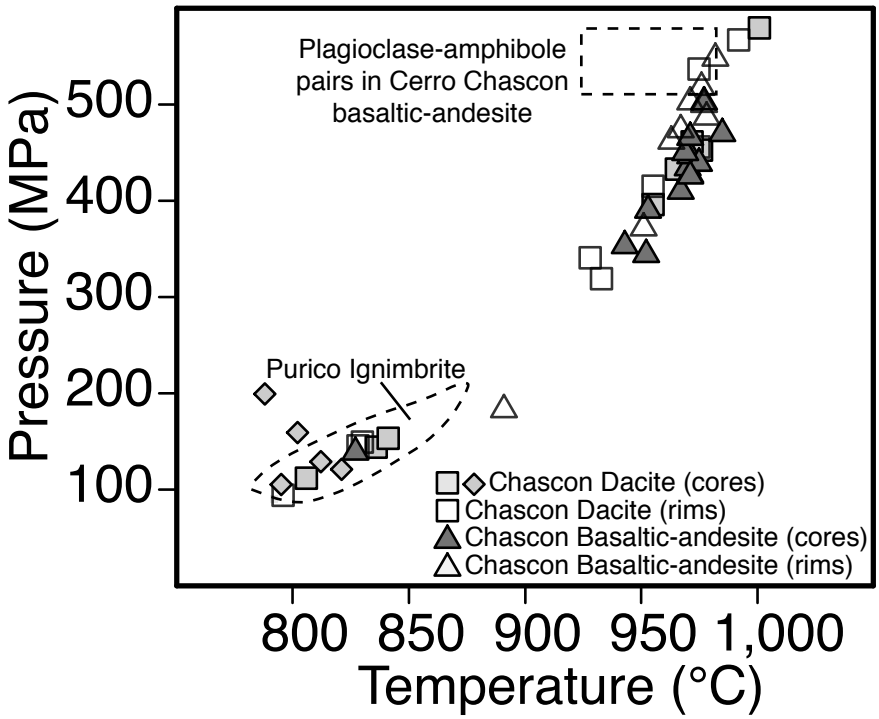

Figure 3.11. Magmatic temperatures and pressures calculated for the Cerro Chascon lavas. Triangles and squares represent temperatures calculated using the thermobarometer of Ridolfi et al., (2010). Diamonds represent temperatures calculated using the plagioclase-amphibole thermometer of Holland and Blundy (1994). Individual points represent averages of multiple analyses within the core or rim region of individual crystals (see supplementary data). The white dashed field represents temperatures from Purico ignimbrite dacite pumice. The dashed white box represents temperatures calculated for the Cerro Chascon basaltic-andesite using the plagioclase-amphibole thermometer of Holland and Blundy (1994). Magmatic pressures for plagioclase-amphibole pairs in the Cerro Chascon dacite were calculated using the Al-in-amphibole barometer of Anderson and Smith (1995). Plagioclase-amphibole temperatures from the Cerro Chascon basaltic-andesite were modeled using touching high-Al amphibole and plagioclase microphenocrysts pairs. Magmatic pressures were not calculated for these crystals as they crystallized at temperatures that exceed the calibration temperatures of Anderson and Smith (1995). Pressures were instead estimated (5.0-5.7 MPa) using regional seismic data (Chmielowski et al., 1999) and pressures obtained using the thermobarometer of Ridolfi et al. (2010). Temperatures from amphibole and plagioclase-ampibole pairs from both the Purico ignimbrite and Cerro Chascon basaltic-andesite overlap when uncertainties associated with both models are considered (±25 and ±50 °C, respectively) and clearly define two distinct pressure-temperature environments. Data sources include Abbot (2009) and Schmitt et al., (2001).

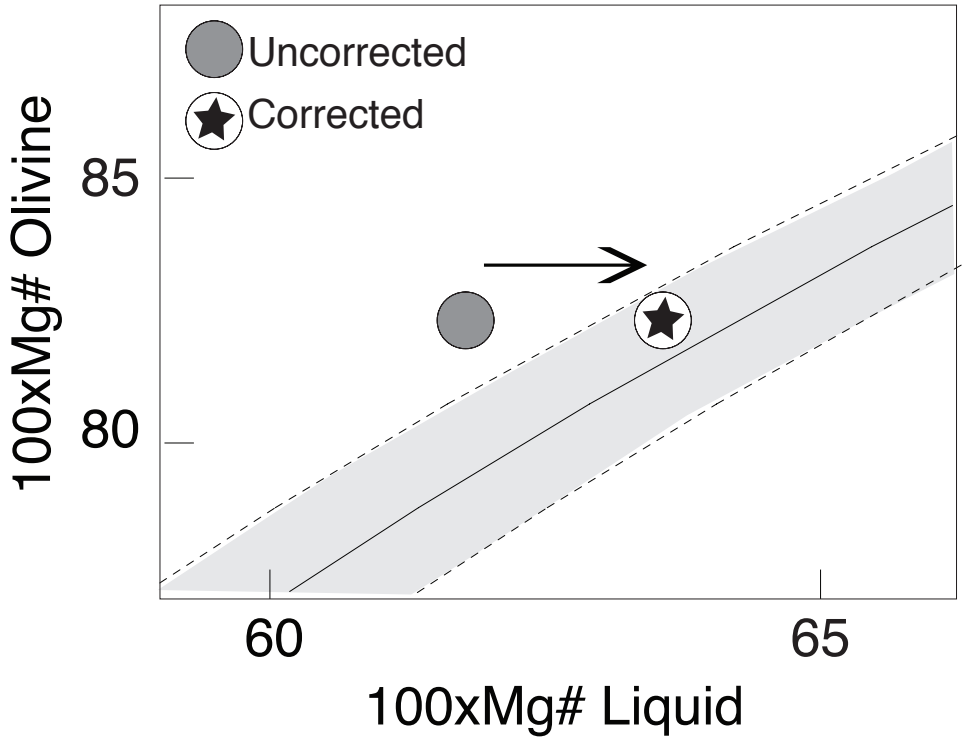

Figure 3.12. Comparison of uncorrected and corrected melt inclusion compositions from Cerro Chascon. Dashed bands represent represents crystal-melt equilibrium for K_D (Mg-Fe) values of 0.30± 0.03 (Roeder and Emslie, 1970).

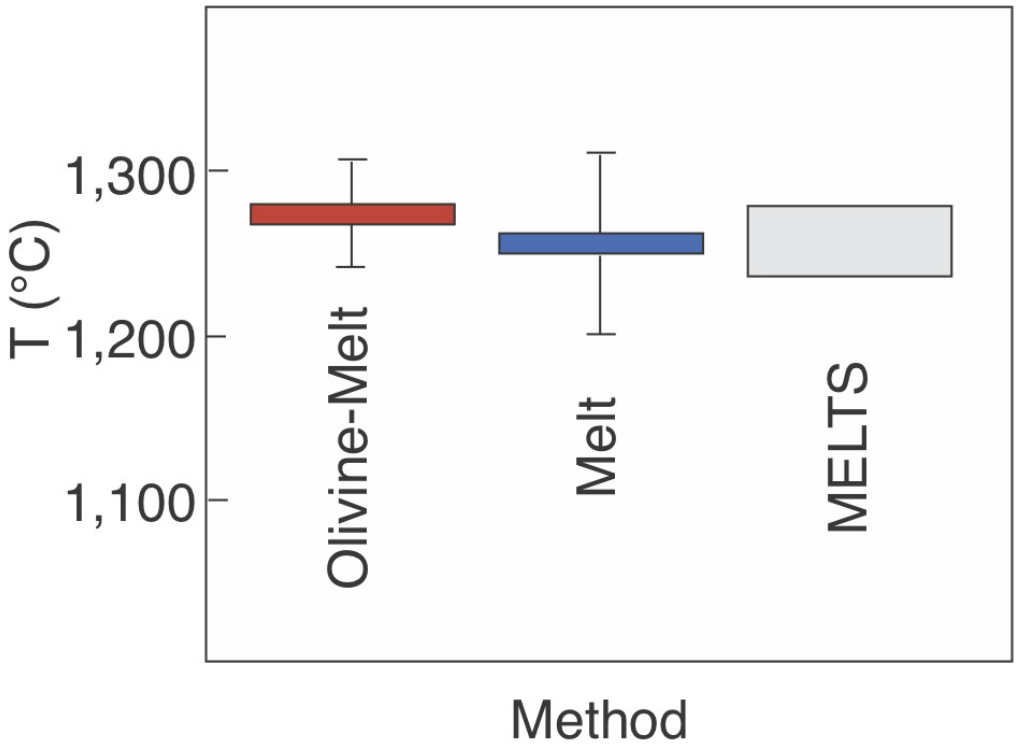

Figure 3.13. Comparison of olivine crystallization temperatures using multiple models. Olivine-melt temperatures were modeled using the thermometers of Beattie (1993) and Putirka (2007). Melt temperatures were modeled using equations 14 and 15 of Putirka (2008). MELTS olivine crystallization temperatures were obtained by modeling corrected melt inclusion compositions using the MELTS software of Ghiorso and Sack (1995). Note the general agreement between the three methods.

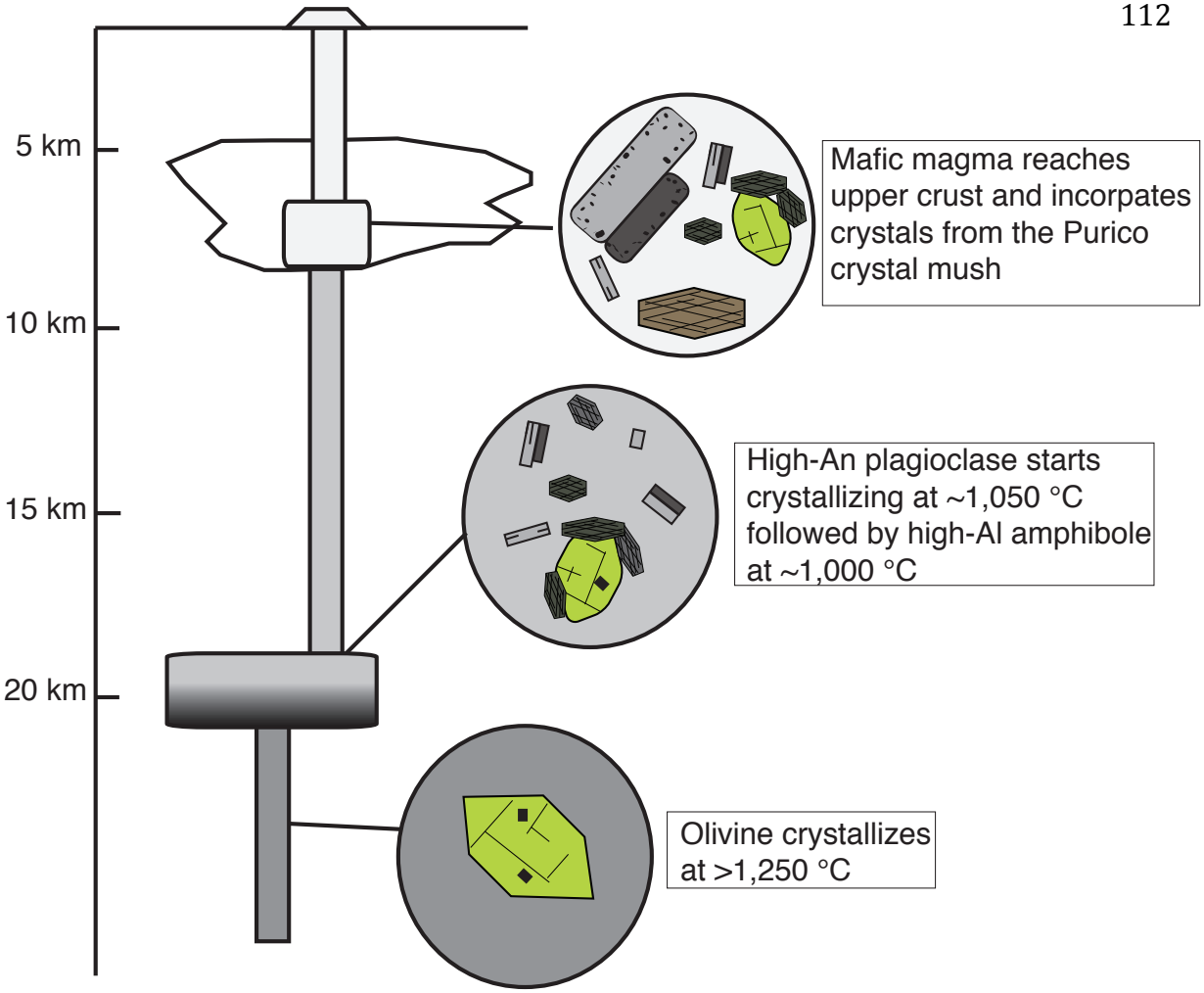

Figure 3.14. Schematic cross section shows ascent of mafic magma leading up to and triggering the eruption of the Cerro Chascon lava dome. Temperatures and pressures were determined using phase equilibria and crystal chemistry. Isotope ratios of individual magmas were determined using whole rock and intra-crystalline isotope measurements. The presence and isotopic composition of the MASH zone are in inferred following Davidson and de Silva (1992). The dashed box represents the proposed extent of the APMB (Chmielowski et al., 1999; de Silva et al., 2006).

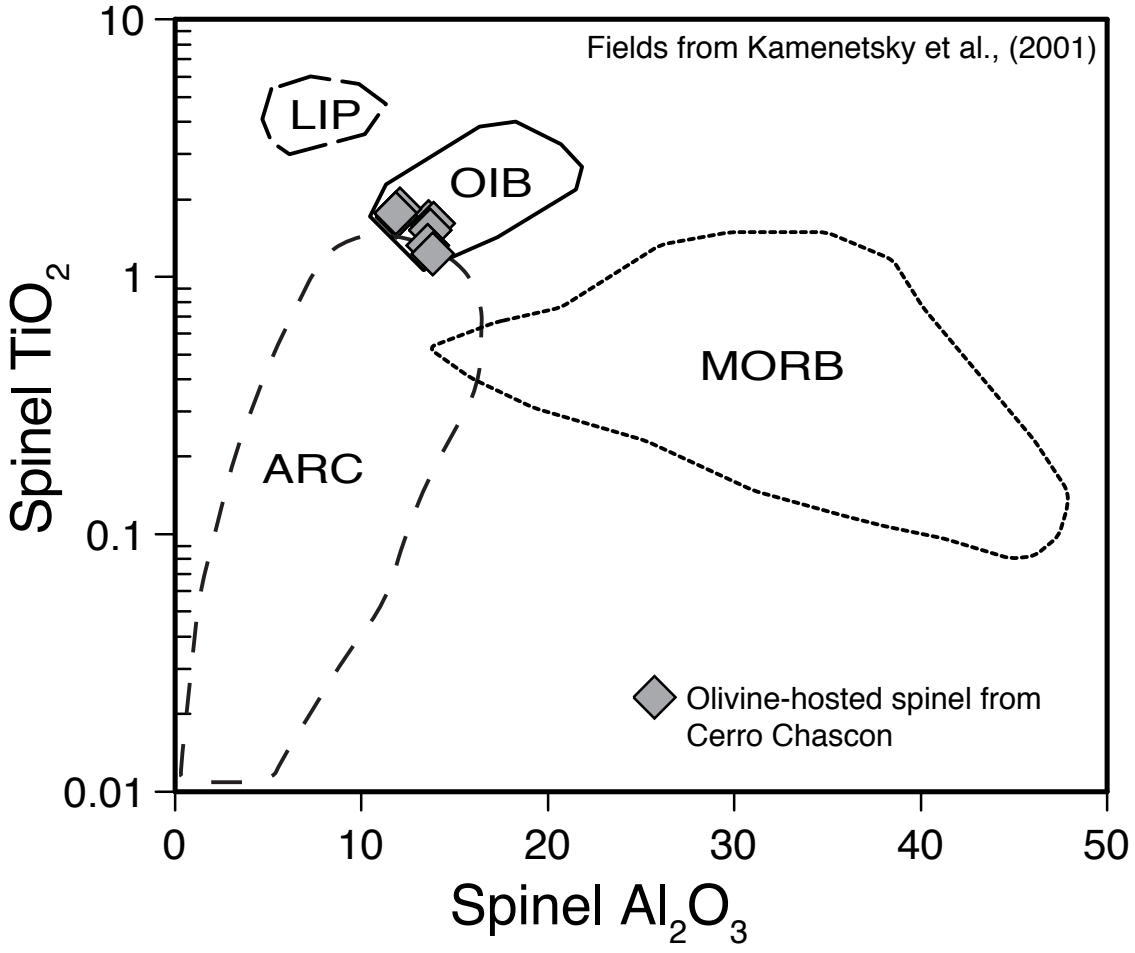

Figure 3.15. Plot shows Al_2O_3 versus TiO_2 in Cr-spinel hosted in olivine crystals. Fields are as discussed by Kamanetsky et al. (2001). Note that the composition(s) of spinel are consistent with enriched mantle values.

Table 3.1: Modal analyses of lavas from Cerro Chascon

	Cerro Chascon	
Unit	Basaltic-andesite	Dacite
Plagioclase	1.1	20.3
Amphibole	3.5	5.2
Clinopyroxene	4.7	3.2
Olivine	3.4	0.3
K-feldspar	<1.0	<1.0
Biotite	<1.0	2.6
Opaques	1.9	2.3
Accessories	<1.0	<1.0
µPlagioclase	29.6	15.5
µAmphibole	22	10.6
glass	16.2	30
vesicles	17.2	3.9
*vesicles	~27	-

Table 3.2:Whole-rock analyses of lavas from Cerro Chascon

Label	CH09013	CH09014
Unit	Basaltic-andesite	Dacite
SiO_2	55.91	63.27
TiO_2	0.76	0.58
Al_2O_3	16.29	15.58
FeO*	7.68	4.95
MnO	0.15	0.10
MgO	5.26	2.81
CaO	8.56	5.32
Na_2O	2.62	3.06
K_2O	1.71	2.94
P_2O_5	0.14	0.14
Sum	99.08	98.75
Ni	17.5	9.9
Cr	106.2	48.4
Sc	39.7	19.8
V	240.9	139
Ba	280	382.4
Rb	67.2	148.3
Sr	446.5	352
Zr	94.9	121.6
Y	29.6	21.3
Nb	7.2	10.1
Ga	16.6	17.7
Cu	30.1	24.9
Zn	73.9	65.6
Pb	10	18.7
La	18.20	24.60
Ce	39.10	53.00
Th	8.10	18.80
Nd	15.80	22.10
U	3.00	9.00
Cs	3.30	11.00
La	33.6	18.8
Ce	60.3	36.0
Pr	6.9	4.5
Nd	24.5	17.9
Sm	4.7	4.1
Eu	1.0	1.0
Gd	4.0	4.1
Tb	0.6	0.7
Dy	3.8	5.0
Ho	0.8	1.1
Er	2.1	3.3
Tm	0.3	0.5
Yb	2.0	3.3
Lu	0.3	0.5

Table 3.3: Representative compositions of plagioclase from Cerro Chascon lavas

unit	Basaltic-andesite			Dacite
	Phenocryst cores	Phenocryst rims	µPhenocrysts	Phenocrysts
sample	CH09016G_plag1	CH09016G_plag1	CH09016P_plag4	CH09014_plagE
Na_2O	6.08	2.54	2.74	5.74
MgO	0.001	0.050	0.06	0.00
SiO_2	57.65	50.00	49.45	57.25
Al_2O_3	27.35	32.12	32.09	26.77
FeO	0.21	0.55	0.47	0.23
CaO	8.58	14.57	15.18	8.55
K_2O	0.55	0.31	0.11	0.52
TiO_2	0.00	0.001	0.02	0.02
An	0.42	0.75	0.75	0.44
Total	100.40	100.14	100.13	99.08
$^{87}Sr/^{86}Sr$ (Ave.)	0.7088 (n=30)	0.7062 (n=14)	0.7063 (n=4)	0.7083 (n=18)

Table 3.4: Representative amphibole compositions from Cerro Chascon lavas

unit	Basaltic-andesite		Dacite	
type	Phenocryst	µPhenocrysts	Phenocrysts	µPhenocrysts
Sample	CH09013_amph6	CH09016H_amph6	CH09014_amph6	CH09014_amph8
SiO_2	47.17	43.16	45.98	43.21
TiO_2	1.21	1.79	1.06	1.56
Al_2O_3	7.91	13.14	8.48	13.27
Cr_2O_3	-	-	-	-
FeO	15.91	11.22	16.53	11.80
MnO	0.49	0.13	0.54	0.19
MgO	13.26	15.61	12.79	14.95
CaO	11.69	11.37	11.74	11.47
Na_2O	1.25	1.96	1.59	2.03
K_2O	0.82	0.66	0.89	0.76
F	0.12	0.00	0.18	0.09
Cl	0.08	0.02	0.10	0.02
^{IV}Al	1.16	1.83	1.29	1.81
^{VI}Al	0.19	0.38	0.17	0.39
^{C}Mg	2.87	3.33	2.79	3.24
$^{C}Fe^{2+}$	1.61	0.70	1.60	0.79
^{C}Ti	0.13	0.19	0.12	0.16
Si^{T}	6.84	6.17	6.71	6.19
T (°C)	820	970	842	968
P (MPa)	131	436	153	456

Table 3.5: Representative olivine compositions for Cerro Chascon lavas

Unit	Basaltic-andesite	Dacite
sample	CH09013_ol6r	CH09014_ol1
SiO2	38.69	38.67
Al2O3	0.02	0.03
K2O	0.01	0.00
MnO	0.28	0.28
FeO	17.29	17.27
NiO	0.07	0.06
Na2O	-	-
MgO	43.34	43.02
CaO	0.15	0.13
Cr2O3	0.02	0.00
TiO2	0.00	0.00
Fo %	0.82	0.82
Total	99.87	99.45

Table 3.6: Melt inclusion compositions from Cerro Chascon

unit	Basaltic-andesite	
type	MI1	MI2
SiO_2	45.54	47.72
TiO_2	0.86	0.62
Al_2O_3	16.43	12.59
FeOt	13.10	15.10
MnO	0.20	0.28
MgO	8.45	13.59
CaO	11.04	8.69
Na_2O	2.29	0.89
K_2O	0.87	0.22
Cr_2O_3	0.00	0.00
P_2O_5	0.17	0.18
Total	98.96	99.90

Table 3.7: Representative clinopyroxene compositions for Cerro Chascon lavas

unit	Basaltic-andesite		
type	Individual xls	xl clumps	sieved cores
sample	CH09016P_cpx1	CH09016P_clump1	CH09016D_cpx1
SiO_2	50.90	51.02	51.94
Al_2O_3	4.40	4.39	3.67
K_2O	-	-	0.02
FeO	7.93	8.06	7.89
Na_2O	0.28	0.28	0.29
MgO	15.97	15.98	16.92
TiO_2	0.41	0.43	0.34
CaO	19.50	19.16	18.70
NiO	0.04	0.05	0.01
MnO	0.19	0.17	0.20
Cr_2O_3	0.41	0.29	0.40
Mg#	0.78	0.78	0.79
Wo#	0.41	0.40	0.39
En#	0.46	0.47	0.49
Fs#	0.13	0.13	0.13
Total	100.05	99.85	100.35

Table 3.8: Representative olivine-hosted spinel compositions

unit	Basaltic-andesite	
type	Spinel	Spinel
sample	CH09013_ol1	CH09013_ol2
Na_2O	-	-
SiO_2	0.04	0.03
MgO	7.56	6.68
Al_2O_3	13.61	11.90
Cr_2O_3	27.64	25.94
TiO_2	1.64	1.72
CaO	0.01	0.02
FeO	45.73	48.91
MnO	0.34	0.35
V_2O_3	0.37	0.45
NiO	0.13	0.02
Cr#	57.7	59.40
Mg#	22.8	19.60

Table 3.9: Representative feldspar compositions from oikocrysts

unit	Dacite	
type	K-feldspar	Plagioclase
Na_2O	2.05	5.78
SiO_2	64.32	56.33
Al_2O_3	19.48	27.39
FeO	0.11	0.19
CaO	0.12	8.88
K_2O	12.97	0.45
An %	0.64	99.03
Ab %	19.22	44.66
Or %	80.13	52.65
Total	99.05	2.69

Table 3.10: Comparison of uncorrected and corrected melt inclusions

unit	Basaltic-andesite	
type	uncorrected	corrected
SiO_2	45.54	45.90
TiO_2	0.86	0.86
Al_2O_3	16.43	16.49
FeOt	13.10	11.76
MnO	0.20	0.20
MgO	8.45	8.78
CaO	11.04	11.08
Na_2O	2.29	2.30
K_2O	0.87	0.87
Cr_2O_3	0.00	0.10
P_2O_5	0.17	0.17
Total	98.96	98.51

Table 3.11: Comparison of olivine thermometers

Method	Calibration	T (°C)	uncertainty (°C)
olivine-melt	Putirka, 2007	1275	±30
olivine-melt	Beattie, 1993	1282	±30
melt	Putirka, 2008 (eq 14 & 15)	1246-1263	±50
MELTS	Ghiorso and Sack, 1995	1224-1882	

Using intra-crystalline isotopic variations to determine the cause of compositional zonation in the Purico ignimbrite, northern Chile

Dale H. Burns

Shanaka L. de Silva

Frank Tepley III

Matthew W. Loewen

In preparation:

Journal of Volcanology and Geothermal Research

4.1 Abstract

The ~1 Ma Purico ignimbrite is an 80-100 km^3 compositionally zoned ignimbrite in the central Andes of northern Chile. Compositional zoning is characterized by an up-section transition from rhyolite to dacite to andesite pumice. Multiple models have been proposed for the cause of compositional zoning in the Purico ignimbrite with processes including fractional crystallization, assimilation, and magmatic recharge. In this study we combine *in situ* compositional and isotopic data from plagioclase crystals to investigate the cause of compositional zoning in the Purico ignimbrite. Andesite pumice contains two isotopically distinct types of plagioclase, high MgO (130-490 ppm) low $^{87}Sr/^{86}r$ crystals (0.7076-0.7084) that record a hot (>900 °C) andesite magma derived from an ~20 km deep magma reservoir, and low MgO (90-240 ppm), high $^{87}Sr/^{86}Sr$ (0.7096-0.7114) plagioclase that appear to be derived from the lower temperature (crystallized at ~800-900 °C), upper crustal (<10 km) plutonic basement. Dacite pumice also contains two texturally and compositionally (An) distinct types of plagioclase. However, both types have very restricted MgO (b.d.l.-200 ppm) and $^{87}Sr/^{86}Sr$ (0.7085-0.7095) and grew at significantly lower temperatures (<850 °C) than the plagioclase in the andesite pumice. These crystals are also significantly larger than plagioclase from the andesite pumice and have clear euhedral rims. Rhyolite pumice also contains two texturally, compositionally, and isotopically distinct types of plagioclase. One type has MgO (b.d.l.-240 ppm) and $^{87}Sr/^{86}Sr$ isotope ratios (0.7088-0.7095) consistent with

being derived from the dacite magma. In contrast, the second type has significantly higher $^{87}Sr/^{86}Sr$ ratios (0.7095-0.7103) consistent with the upper crustal ignimbrite basement. By combining these new data with previous bulk rock compositional and isotopic data and thermo-barometric modeling, we show that the compositional variability seen in the Purico ignimbrites represents a combination of crustal assimilation, crystallization, and melt extraction all initiated by mafic recharge.

4.2. Introduction

Compositionally zoned ignimbrites are thought to result from the eruption of compositionally zoned silicic magma reservoirs (e.g., Smith, 1979; Hildreth, 1981; Eichelberger et al., 2006). Although these types of eruptions are common in continental magmatic systems, the magmatic processes responsible for the formation of these zoned magma bodies are not fully agreed upon. Fractional crystallization is perhaps the most commonly cited (e.g., McBirney, 1980; Sparks, 1984; Grunder and Mahood, 1988; de Silva, 1991); however, processes such as progressive crustal melting (Huppert and Sparks, 1988), assimilation (Grunder and Mahood, 1988; de Silva, 1991), cyclic injections of new magma (Sparks and Huppert, 1984; Schmitt et al., 2001; Watanabe et al., 2006), and interstitial melt extraction (e.g. Sisson and Bacon, 1999; Lindsay et al., 2001; Bachmann and Bergantz, 2004) are also frequently proposed. The processes ultimately responsible for the compositional zoning in ignimbrites have major implications

for how magmas are stored, generated, and evolve in the Earth's crust, along with how large silicic eruptions are triggered. For example, compositional zoning via fractional crystallization would require a large initial input of parental magma and sufficient time to develop compositional zoning. In this case, crystallization-induced volatile exsolution may generate local overpressure great enough to trigger an eruption (Blake, 1984). In contrast, if compositional zoning forms in response to magmatic recharge, volumetric increase due to the emplacement of the recharge magma into a previously emplaced magma reservoir and/or due to the melting of previously emplaced material could potentially generate the overpressure to trigger an eruption. These differences have major implications for the cause and timing of triggering explosive silicic eruptions.

Most studies that have addressed the cause of compositional zoning in magma reservoirs have been largely based on bulk rock compositional and isotopic variations. The ability to determine the isotopic ratios of individual crystalline phases and portions of individual crystalline phases has proved to be a great tool in understanding the evolution of magmatic systems (e.g. Davidson and Tepley, 1997; Tepley et al., 1999; Davidson et al., 2005; Ramos et al., 2005; Charlier et al., 2007; Martin et al., 2010). Individual crystals can record the isotopic identity of the magmas/sources from which they were derived even after mixing and hybridization have homogenized magmas at the bulk rock scale.

In this study, we use *in situ* crystal chemistry and intra-crystalline $^{87}Sr/^{86}Sr$ isotope ratios from plagioclase crystals to determine the cause of compositional

zoning in the Purico ignimbrite in northern Chile. Previous work on the Purico ignimbrite has led to multiple models for the cause of compositional zoning in the ignimbrite. Francis et al. (1984) and de Silva (1991) proposed that fractional crystallization with minor assimilation were the processes responsible for the compositional variations. In contrast, Schmitt et al. (2001) concluded that the zoning formed following a magmatic recharge event. We analyze plagioclase crystals from three compositionally distinct types of pumice and determine the genetic relationships between individual crystal populations and consequently the magmatic processes that led to the formation and eruption of a chemically heterogeneous magma. We show that fractional crystallization alone cannot account for the compositional variations in the Purico ignimbrite and that open system processes occurring at multiple levels in the crust are required.

4.3 Geologic Background

The Purico ignimbrite is the dominant unit of the 1.0 Ma to recent Purico-Chascon volcanic complex (PCVC) in northern Chile (**Figure 4.1**). The PCVC is the last major eruptive center associated with the Altiplano-Puna volcanic complex (APVC; de Silva, 1989; **Figure 4.1A**), a large silicic volcanic field comprised of multiple large volume (>1000 km^3) ignimbrite sheets that erupted as part of a regional magmatic flare-up between 10 and 1 Ma. The ignimbrite flare-up initiated ~10 Ma following a period of intense uplift and crustal thickening that began ~25 Ma (Allmendinger et al., 1997) in response to lithoshperic

delamination/slab foundering in response to a steepening of the subducting slab. High mantle power input into the crust resulting from one or both of these processes resulted in the large volumes of mantle-derived magmas ascending into the crust and the generation of large volumes of magma in the upper crust (e.g. de Silva, 1989; de Silva and Gosnold, 2007). The crust beneath the CVZ is dominated by Paleozoic granites and gneisses with high $^{87}Sr/^{86}Sr$ isotope ratios (up to ~0.750; Lucassen et al., 2001); thus, ignimbrites from the APVC have distinctly higher $^{87}Sr/^{86}Sr$ than typical arc lavas and tuffs from the CVZ (Figure. 3B; Hawkesworth et al., 1982; de Silva, 1991; Davidson et al., 1992; Coira and Kay, 1993; Ort et al., 1996; Lindsay et al., 2001; Schmitt et al., 2001; Kay et al., 2005; de Silva et al., 2006; Wörner et al., 1992; Mamani et al., 2010) Activity during the flare-up occurred in three major pulses at ~8, 6, and 4 Ma, with the peak of magmatism occurring ~4 Ma. Since 4 Ma ignimbrite activity has declined, with the last major eruptions occurring ~1 Ma at the PCVC. Isotopically, ignimbrites erupted during the peak of the flare-up (e.g. Atana, Toconao, and Tara ignimbrites) tend to have the highest $^{87}Sr/^{86}Sr$ isotope ratios (0.7103-0.7132; Lindsay et al., 2001) reflecting the highest proportion of crustally derived material.

The ~80-100 km^3 Purico ignimbrite (**Figure 4.2**) is a single cooling unit comprised of three distinct flow units (de Silva, 1991; Schmitt et al., 2001). The two lowermost and most extensive flow units (LPI I and LPI II from Schmitt et al., 2001) are non-welded crystal-rich (~50 % crystals) dacites typical of other

ignimbrites in the APVC (de Silva et al., 1989b; Schmitt et al., 2001). The lowermost flow unit (LPI I) is texturally and compositionally homogenous throughout, containing exclusively dacite pumice. In contrast, the overlying flow unit (LPI II) is texturally and compositionally heterogeneous comprised of a basal rhyolite fall deposit overlain by massive crystal-rich dacite, with the upper one-third of the unit containing abundant dark andesite and banded pumice (**Figure. 4.2; Figure. 4.3**; de Silva, 1991; Schmitt et al., 2001). The uppermost and least voluminous unit of the Purico ignimbrite (UPI of Schmitt et al., 2001) is a welded crystal-rich dacite compositionally similar to the lowermost unit.

The LPI II contains three distinct types of pumice (**Figure 4.2, 4.3**). The basal tephra fall unit of the LPI II is comprised of crystal-poor (<10% crystals) rhyolite pumice (**Figure. 4.2; 4.3**). Importantly, the rhyolite pumice is exclusive to this unit. Phenocrysts in the rhyolite are typically small and consist of plagioclase, biotite, quartz, and oxides in a groundmass of highly vesicular (72 vol.%), non-indurated rhyolite glass (71 wt.% SiO_2). The most abundant type of pumice, making up the majority of the LPI II flow unit is crystal-rich dacite (~50% crystals; **Figure 4.2, 4.3**). The dacite contains phenocrysts of plagioclase, amphibole, biotite, quartz, minor orthopyroxene, and clinopyroxene in a groundmass of fresh, vesicular (~65 vol.%), moderately indurated rhyolite glass (~74 wt.% SiO_2). The third pumice type, present in the upper third of LPI II, is mingled dacite-andesite and andesite pumice. The andesite pumice (**Figure. 4.2C; 4.3**) is crystal-rich (~50 % crystals) containing phenocrysts of plagioclase, hornblende (usually

rimmed with opaques), orthopyroxene, clinopyroxene, and Fe-Ti oxides in a groundmass of less vesicular (39 vol.%), dark dacite glass (67 wt.% SiO_2).

Compositionally, the andesite, dacite, and rhyolite pumice define major element arrays characterized by increasing K_2O and decreasing CaO and Fe_2O_3 with increasing SiO_2 (**Figure 4.4; Table 1**), which de Silva (1991) interpreted to represent progressive fractionation of the observed phenocryst phases (i.e. plagioclase, orthopyroxene, clinopyroxene, and/or hornblende). However, trace elements among the three pumice types have divergent trends that cannot be explained by simple crystal fractionation (**Figure 4.5; Table 1**). Sr and Rb trends in the andesite and rhyolite pumice are steeper than in the dacite consistent with magmas with different Sr and Rb bulk mineral-melt distribution coefficients. The rhyolite pumice is also significantly more enriched in Ba and Zr than the dacite. If progressive fractionation were occurring, Ba and Zr would be expected to decrease from the dacite to the rhyolite owing to the compatibility of the elements in biotite and zircon (both present in the dacite pumice). Isotopically, all three pumice types in the Purico ignimbrite define a very restricted range of $^{87}Sr/^{86}Sr$ and $^{143}Nd/^{144}Nd$ ratios ranging from ~0.7087 to 0.7090 and 0.51222 to 0.51229, respectively (**Figure. 4.6; Table 1**). Andesite and rhyolite pumice have slightly higher $^{87}Sr/^{86}Sr$ than the dacite pumice also precluding simple fractional crystallization for the origin of the compositional variations.

There are also significant variations between matrix glass (**Figure 4.4; 4.5**) and plagioclase and quartz hosted melt inclusions and crystal chemistries

between the pumice types (see Schmitt et al., 2001). Matrix glass from the andesite and rhyolite pumice has broadly similar major and trace element abundances. In contrast, matrix glass from the dacite has significantly higher K_2O and Rb, and lower Sr, Zr, and Ba. Similarly, melt inclusions hosted in quartz and plagioclase from the rhyolite are enriched in compatible elements (i.e. Ba, Sr, and Zr) relative to the melt inclusions in the dacite. In additional, melt inclusions trapped in sequential growth zones in plagioclase from the rhyolite pumice become progressively more evolved from core to rim (i.e. decreasing MgO and Sr), whereas melt inclusions trapped in sequential growth zones in plagioclase from the dacite pumice remain constant indicating unique crystallization histories (Schmitt et al., 2001). Thermo-barometric calculations for crystals from the three pumice types indicate that the three magmas crystallized at different temperatures not consistent with a progressive fractionation (Schmitt et al., 2001). The andesite magma crystallized at the highest temperature (~880-965 °C), but interestingly, the rhyolite appears to have crystallized at significantly higher temperatures than the dacite (~835-850 °C vs. ~770-800 °C; Table 4.1). The apparent progressive fractionation trend recorded in major element variations and lack of significant isotopic variability in the Purico ignimbrite pumices, and the compositional variability observed trace elements, glass chemistry, and thermo-barometric calculations have led to multiple proposed models for the processes responsible for compositional zoning in the Purico ignimbrite. In the following

section, we review those models and discuss how we plan to evaluate those models and determine the cause of compositional zoning in the Purico ignimbrite.

4.4. Previous Models for Purico Magma Reservoir

There are two previous models that have been proposed for the cause of compositional zonation in the Purico magma reservoir. de Silva (1991) proposed that the major element trends (appear to be fractionation trends) and lack of bulk rock isotopic variability (0.7087-0.7091) between the pumice types in LPI II indicated the distinct compositions sampled in the Purico ignimbrite formed in response to closed-system fractionation of the andesite magma and the formation of a large compositionally gradational magma reservoir. However, de Silva (1991) also recognized that trace element variations were not completely consistent with fractional crystallization and proposed that crystallization was accompanied by minor assimilation of roof rock to produce the rhyolite. In contrast, Schmitt et al. (2001) proposed that bulk rock trace element variations (andesite and rhyolite pumice have steeper Sr and Rb slopes and rhyolite pumice has higher Ba and Zr than the dacite pumice), matrix glass compositions (i.e. dacite pumice has higher K_2O and Rb, and lower Sr, Zr, and Ba than the rhyolite), melt inclusions compositions (i.e. rhyolite is enriched in Ba and Zr relative to the dacite and melt inclusions trapped in sequential growth zones in plagioclase record crystallization histories not consistent with plagioclase in the dacite), and thermo-barometric calculations indicate that the rhyolite and andesite magmas

related to one another, but not to the dacite. Schmitt et al., (2001) proposed that the andesite magma represents a deeper, hotter andesite that ascended into previously emplaced upper crustal (4-8 km depth) dacite magma reservoir. Rapid and efficient fractionation of the andesite resulted in the extraction of a hot, low density, low viscosity rhyolite melt, which ascended through the dacite magma reservoir and ponded at the top of the magma chamber. In this study, we further investigate the two models for the cause of compositional zoning in the Purico ignimbrite using *in situ* crystal chemistry and intra-crystalline $^{87}Sr/^{86}Sr$ isotope variations in the andesite, dacite, and rhyolite pumice from LPI II.

4.5. Methods

Samples of the Purico andesite and rhyolite pumice were collected during field seasons in the central Andes in 2009 and 2012. Dacite pumice samples were from the collections of coauthor de Silva. Only clean individual pumice clasts were collected and analyzed. Matrix samples were not collected in order to minimize mechanical fractionation. Bulk rock major elements, trace elements, and isotope ratios were not measured in this study, as these have been studied extensively and large datasets are available (de Silva, 1991; Davidson et al., 1990; Schmitt et al., 2001).

In situ major and trace element abundances in plagioclase and amphibole were measured at Oregon State University using a Cameca SX100 electron microprobe with five wavelength dispersive spectrometers, including two high-

sensitivity large diffraction crystals for trace element analyses. Analyses where conducted using an accelerating voltage of 15 KeV with a beam current of 30 nA and focused 1 um beam for both plagioclase and amphibole. Volatile element migration was corrected using a 0-time intercept correction. Corrected elements include Na, K, and Si. Count times ranged from 10 s for major elements to 60s for trace elements. Specific crystal configurations and count times presented in the supplementary materials. Prior to measuring unknowns, plagioclase calibrations were checked using the USNM 115900 (LABR) standard. Average values for replicate analyses and associated error is presented in supplementary materials. Generally, the error associated with major elements is typically less than 2% (see supplementary materials for details).

In situ isotopic analyses where conducted using two methods. Selected crystals were sampled using a NuWave computer-automated micro-drill at OSU (see Charlier et al., 2006), and sampled aliquots where sent to New Mexico State University (NMSU) where elemental Sr was separated using cation-exchange chromatography. $^{87}Sr/^{86}Sr$ was then measured using thermal ionization mass spectrometry (TIMS) at NMSU (see Ramos, 1997 for details). $^{87}Sr/^{86}Sr$ ratios were also measured using laser ablation multicollector inductively coupled plasma mass spectrometry (LA-MC-ICP-MS) in the W.M. Keck Collaboratory for Plasma Mass Spectrometry at Oregon State University using a NuPlasma MC-ICP-MS and Photon Machines G2 Excimer laser system. General analyses followed the techniques outlined in Miller and Kent (2009). We also followed the

method of Woodhead et al. (2005) to correct for potential krypton and rubidium (Rb) interferences and to monitor calcium argide and dimer formation. Background interferences by krypton isotopes and contributions from any other gas species present within the plasma and sweep gas supplies were corrected by measuring an on-peak baseline prior to ablation, where measured backgrounds were subtracted from the intensities obtained during ablation. Mass biases were corrected by reference to an $^{86}Sr/^{88}Sr$ ratio of 0.1194, and we corrected for isobaric interference of ^{87}Rb on ^{87}Sr by measuring ^{85}Rb intensity and calculating the contribution of ^{87}Rb. For all plagioclase the calculated contribution of ^{87}Rb to the measured total mass 87 peak intensity was negligible (<< 1%). A deep-sea gastropod collected from the Gulf of Mexico was used as an in-house marine carbonate standard (solution measured $^{87}Sr/^{86}Sr$ = 0.709190 ± 0.000008 2se; Miller and Kent, 2009) and measurements of the gastropod were interspersed with measurement of unknowns throughout the analysis session. For all gastropod measurements throughout the analysis session $^{87}Sr/^{86}Sr$ = 0.709235 ± 0.000018 2se (n = 57). The small difference between our measured value for the gastropod and the solution measurement is common in this laboratory (e.g. Miller and Kent, 2009; Zimmerman et al. 2013) and as a result a small correction is applied to $^{87}Sr/^{86}Sr$ measured in unknowns. As an additional check of this correction we analyzed a natural clinopyroxene (BB-1) with solution measured $^{87}Sr/^{86}Sr$ = 0.70447 ± 0.00002 (2 se). Repeat analysis (n = 25) of this material throughout the analysis session returned a corrected value of $^{87}Sr/^{86}Sr$ =

0.70457 ± 0.00008 (2 se). Measurement of plagioclase and other materials were made using a laser spot size of 65 μm, a pulse frequency of 10 Hz and a translation rate of 5 μm/sec.

4.6. Results

Plagioclase dominates the mineral assemblage of the Purico andesite pumice making up ~56% of crystals. There are two compositionally and isotopically distinct types of plagioclase within the andesite pumice (AP1 and AP2; **Figure. 4.7A,B, 4.8A-C**). The first type (AP1) are generally small (<500 µm), subhedral, with variable An contents (An_{46-83}), high MgO and FeO contents (130-490 ppm and 250-630 ppm, respectively), and low $^{87}Sr/^{86}Sr$ isotope ratios (0.7079-0.7084). AP2 crystals are typically larger (>1,000 µm) and appear to be disaggregated fragments of larger crystals. These crystals show a similar range of An contents as AP1 crystals (An_{41-79}), but ~80% of crystals fall in a more restricted range from ~An_{39} and An_{55} and have lower MgO and FeO contents (90-240 ppm and 210-360 ppm, respectively), and significantly higher $^{87}Sr/^{86}Sr$ isotope ratios (0.7093-07114).

Plagioclase is also the dominant crystalline phase in the Purico dacite pumice (~70% of the crystals) and the dacite also contains two distinct types of plagioclase (DP1 and DP2; **Figure 4.7C,D; 4.8D-F**). The dominant plagioclase type (DP1) are large (1000-1500 µm) and subhedral to euhedral and tend to be fractured. Compositionally, DP1 crystals are homogeneous with restricted An

contents ranging from An_{39} to An_{55} and low, restricted MgO and FeO contents (b.d.l.-200 ppm and 200-300 ppm, respectively). Isotopically DP1 crystals define a restricted range of $^{87}Sr/^{86}Sr$ isotope ratios from 0.7088 to 0.7090. The second plagioclase type in the dacite pumice (DP2) is similar in size to DP1 crystals, but have clear evidence for dissolution in their cores surrounded by clear growth rims (**Figure 4.7D**). DP2 crystals have significantly more variable An contents than type DP1 crystals (An_{45-75}), but have indistinguishable MgO and FeO concentrations (b.d.l.-200 ppm and 200-300 ppm, respectively) and $^{87}Sr/^{86}Sr$ isotope ratios (0.7088).

Plagioclase makes up >90% of the crystalline phases in the Purico rhyolite pumice. There are two distinct plagioclase types in the rhyolite pumice (RP1 and RP2; **Figure 4.7E,F; 4.8G-I**). RP1 crystals are less than 1000 μm, subhedral, and have highly variable An contents ranging from An_{40} to An_{70} with low MgO and FeO abundances (b.d.l.-240 ppm and 190-490 ppm, respectively), and $^{87}Sr/^{86}Sr$ isotope ratios ranging from 0.7088 to 0.7095. The second type of plagioclase in the rhyolite pumice (RP2) is texturally indistinguishable from RP1 crystals, but define a larger range of An contents (An_{35-80}). RP2 crystals also have lower, more restricted MgO and FeO concentrations (b.d.l.-150 ppm and 210-380 ppm, respectively) and higher $^{87}Sr/^{86}Sr$ isotope ratios (0.7096 to 0.7103) than RP1 crystals.

In summary, each pumice type in the LPI II unit has two distinct types of plagioclase. Importantly, there are some very important similarities and

differences between the types of plagioclase in each pumice type (**Figure 4.7, 4.8**). Crystals with low MgO and FeO and lower $^{87}Sr/^{86}Sr$ isotope ratios in the rhyolite pumice (RP1) are indistinguishable from crystals from the dacite pumice (DP1; DP2). In contrast, RP2 crystals have significantly higher $^{87}Sr/^{86}Sr$ ratios and are isotopically similar to AP2 crystals from the andesite pumice. It is also important to note that plagioclase crystals in the andesite pumice with the highest An contents and MgO and FeO concentration and lowest $^{87}Sr/^{86}Sr$ isotope ratios (AP1) are exclusive to the andesite pumice and are the most primitive compositions recorded in the Purico ignimbrite.

4.7. Magmatic Dynamics/Conditions Recorded in Crystals from the Purico Ignimbrite

An analysis of trace element partitioning in plagioclase is presented in Figure 4.9. Experimentally derived partition curves for three different temperatures and trace element abundances representative of the range of magmas observed in the Purico ignimbrite are included (e.g Bindeman et al., 1998; Tepley et al., 2010). Plagioclase data will plot along a single partition curve if the compositional variations in a crystal, or population of crystals, is being controlled by closed system processes (i.e. temperatures, pressures, water contents; **Figure 4.9A**). In contrast, if open system processes are occurring, plagioclase data may plot on multiple distinct curves, or form a continuum between curves, thus, recording crystal growth in two compositionally distinct

magmas. In addition, because the shape and location of a partition curve is largely dependent on temperature, magmatic temperatures can be estimated based on the distribution of plagioclase compositions.

Crystals from the Purico andesite pumice record two distinct magmatic environments (**Figure 4.9B**). AP1 crystals plot along two distinct partition curves. Most crystals from AP1 plot along a 900 to 1,000 °C partition curve, consistent with the two-pyroxene temperatures (880-965 °C) reported by Schmitt et al., (2001) for the Purico andesite pumice (**Table 1**). However, there are some AP1 crystals that appear to have grown in a much higher temperature environment (1,100 and 1,200 °C). These are the highest magmatic temperatures ever recorded in the Purico ignimbrite. AP1 crystals also have significant compositional variations along their respective partitioning curve. These variations likely resulted from systematic changes in temperature, pressure and H_2O content as the andesite magma ascended and crystallized in the shallow crust (Schmitt et al., 2001). AP1 crystals also have the most primitive $^{87}Sr/^{86}Sr$ ratios recorded in the Purico ignimbrite (0.7079- 0.7084) consistent with more mafic andesite magma. AP2 crystals plot between the 750-800 and 900-1,000 °C partition curves, consistent with crystallization from a lower temperature (~800-900 °C), less mafic magma than AP1 crystals. These temperatures still partially overlap with the temperatures reported by Schmitt et al., (2001) for the andesite pumice (880-965 °C), but their significantly higher $^{87}Sr/^{86}Sr$ ratios (0.7093-07114)

are more consistent with crystallization from a radiogenic upper crustal magma (Figure 5).

Plagioclase crystals from the dacite pumice from the Purico ignimbrite shows evidence for crystallization in a single, homogeneous, low temperature environment (**Figure. 4.9C**). Both DP1 and DP2 crystals plot along a low temperature, 750-800 °C partitioning curve consistent crystallization from dacite magma. These temperatures are consistent with ~770-800 °C temperatures reported for the Purico dacite pumice using Fe-Ti oxide and plagioclase-amphibole temperatures (Schmitt et al., 2001). DP2 crystals do show significant variations in An content that correlate with the low temperature partition curve. These variations in An content indicate either 1) the Purico dacite magma only experienced closed system processes, or 2) open system processes did occur, but the magmas interacting were compositionally indistinguishable and evolved at approximately the same temperatures. $^{87}Sr/^{86}Sr$ isotope variations in plagioclase from the dacite pumice are also homogeneous, consistent with crystallization from an isotopically homogeneous evolved magma.

Rhyolite pumice from the Purico ignimbrite records crystallization in two distinct magmatic environments (**Figure. 4.9D**). RP1 plagioclase crystals span the entire compositional range between plagioclase from the dacite pumice and the andesite pumice with compositions plotting on both curves. This indicates crystals may have grown in both the dacite and andesite magmas. Isotopically, RP1 crystals have identical $^{87}Sr/^{86}Sr$ ratios to crystals from the dacite pumice

(**Figure 4.8**). The consistency in compositions, inferred storage conditions, and isotopic ratios indicate the RP1 plagioclase may be genetically related to crystals from the dacite magma. RP2 crystals differ slightly from RP1 crystals and appear to have crystallized between ~800 and 900 °C. These crystals are broadly similar to AP2 crystals except they define a much larger range of An contents. RP2 crystals also have distinct higher $^{87}Sr/^{86}Sr$ isotope ratios than RP1 crystals (0.7096- 0.7103 vs. 0.7088- 0.7095) and are broadly similar to AP2 crystals from the andesite pumice. It is likely that RP2 and AP2 crystals are genetically related.

4.8. Origin of Crystals in the Purico Ignimbrite

The high radiogenic isotope ratios recorded in bulk pumice samples (de Silva, 1989; Schmitt et al., 2001) and individual crystals from the Purico ignimbrite, are consistent with other upper crustal magmas from the APVC. Bulk rock trace element variations from APVC ignimbrites (Lindsay et al., 2001; Kay et al., 2010), including the Purico ignimbrite (Schmitt et al., 2001), indicate that significant crustal magma generation occurs between 35 and 15 km deep, and accumulates at ~20 km prior to ascent into the upper crust. This depth is consistent with a regional seismic low-velocity anomaly (Chmielowski et al., 1999; Zandt et al., 2003; Leidig and Zandt, 2003) that has been interpreted as the Altiplano-Puna Magma Body (APMB; Chmielowski et al., 1999; de Silva, 2006). It has been proposed that the APMB is predominantly andesitic to dacitic (de Silva and Gosnold, 2007) and that fractionation in the APMB results in the

separation and ascent of silicic magmas (mostly dacite) into the upper crust (de Silva and Gosnold, 2007; del Potro et al., 2013). Once in the upper crust the magmas fractionate to produce the crystal-rich dacite magmas that ultimately erupt in caldera forming eruptions (de Silva and Gosnold, 2007). Once emplaced in the upper crust, de Silva (1991) proposed that assimilation of upper crustal material serves to further modify the compositions of APVC magmas. Burns et al., (in review) combined bulk rock and *in situ* isotopic information with thermobarometry and argued that the APMB lies between ~17 and 20 km deep, and that during the formation of the Purico magmatic system magmas ascending from the APMB had baseline Sr isotope ratios >0.7080.

The compositional and isotopic variations observed in individual crystals within the Purico ignimbrite pumice indicate there are at least two distinct crustal levels where the Purico magmas inherit their compositional and isotopic character. High temperatures and low $^{87}Sr/^{86}Sr$ isotope ratios in AP1 crystals are consistent with crystal growth in deep, more mafic, hotter magma reservoir. Temperatures and pressures reported here and by Schmitt et al., (2001) for the andesite pumice are similar to the estimated temperature of the APMB reported by Burns et al., (in reveiw). In addition, the two pyroxene thermobarometry from lavas associated with Auchincilcha Volcanic Cluster (Grunder et al., 2006; Walker et al., 2012;) a long-lived volcanic system in northern Chile on the periphery of the APVC, record temperatures and pressures consistent with the APMB (~977-1,115 °C and ~300-750 MPa). Del Potro et al., (2013) proposed that the APMB is

compositionally and thermally zoned. Thus, the highest temperature AP1 crystals (>1000 °C) may represent crystals derived from a deeper in the APMB. Magmas within this reservoir would still have high $^{87}Sr/^{86}Sr$ ratios reflecting high degrees of crustal contamination. We propose that the low $^{87}Sr/^{86}Sr$ ratios observed in AP1 crystals (0.7079-0.7084) record the isotopic composition of the APMB at ~1 Ma when the Purico ignimbrite eruption was triggered. In contrast, we believe that higher $^{87}Sr/^{86}Sr$ AP2 crystals (0.7095-0.7115) reflect crystals that crystallized from a magma that had undergone further isotopic modification in the upper crust prior to 1 Ma. Importantly, these highest $^{87}Sr/^{86}Sr$ plagioclase crystals are isotopically indistinguishable from the range of bulk rock isotope ratios from the major APVC ignimbrites that erupted ~4-6 Ma during the peak of the flare-up (e.g. Atana, Toconao, Guacha, and Tara ignimbrites). In addition, the close proximity of the Purico ignimbrite shield to the calderas associated with those eruptions (i.e. La Pacana and Guacha) makes it probable that the remnant plutonic rocks from those systems would make up the upper crustal basement through which the Purico magmas ascended. The lower temperatures range recorded in AP2 crystals (800-900 °C) are slightly higher than the temperatures calculated for the Atana and Toconao magma reservoir (~730-790 °C). The temperature differences are not surprising, as the eruption likely sampled material from the uppermost portion of the magma reservoir, whereas the andesite magmas my have sampled material from deeper in the reservoir. These these temperatures

are similar to the temperatures (~870 °C) reported by Muir et al., (2014) for dacite lavas from Uturuncu volcano.

Plagioclase from the Purico dacite pumice lack the variability seen in plagioclase from the andesite pumice. The restricted range of $^{87}Sr/^{86}Sr$ ratios records crystal growth from a magma or magmas with very little isotopic variability. We propose the lack of variability records one of two possible scenarios: 1. The Purico dacite magma was emplaced in a single event during which a large volume of homogenous dacite magma ascended diapirically from the APMB (de Silva, 1989) and subsequently crystallized in the upper crust, or 2. The dacite magma reservoir formed through the episodic injection of dacite magma from APMB. In this case, the composition of magma being extracted from the APMB remained constant over the time period the dacite reservoir was assembled. We do not attempt to distinguish between these models, but we do note that the lack of high $^{87}Sr/^{86}Sr$ (>0.7095) plagioclase in the dacite pumice may indicate that either upper crustal assimilation (i.e. no crystals that overlap with the >0.7095 ratios recorded in the peak APVC ignimbrites) was less significant during the emplacement and evolution of the Purico dacite magma reservoir or that higher $^{87}Sr/^{86}Sr$ crystals are present in the Purico dacite, but were not sampled in this study.

Rhyolite pumice also contains high $^{87}Sr/^{86}Sr$ plagioclase crystals (RP2) that are consistent with high $^{87}Sr/^{86}Sr$ isotopes of ignimbrites erupted during the peak of the flare-up. Importantly, these crystals define a more restricted range of

$^{87}Sr/^{86}Sr$ isotope ratios than similar crystals from the andesite pumice (AP2). We interpret this to mean that the two magmas may have sampled slightly different materials, possibly distinct horizons within the upper crust.

4.9. Evaluation of Previous Magma Zoning Models for the Purico Ignimbrite

In situ compositional and isotopic information from plagioclase crystals presented herein coupled with previously published bulk rock compositional, isotopic, and thermo-barometric calculations for the Purico ignimbrite along with other ignimbrites in the APVC allow us to elucidate the magmatic processes responsible for causing compositional zonation in the Purico magma reservoir. The presence of at least three isotopically distinct plagioclase populations that differ between the three pumice types rules out fractional crystallization as the sole cause of compositional zoning in the Purico ignimbrite. Schmitt et al., (2001) proposed that the compositional zoning in the Purico ignimbrite originated when a hot, andesite magma (andesite pumice magma) recharged a previously emplaced dacite magma reservoir (dacite pumice magma). Schmitt et al. (2001) proposed that the rapid crystallization of the andesite magma resulted in the formation of a hot, low density, low viscosity rhyolite liquid that ascended to the top of the dacite magma reservoir. The *in situ* isotopic data presented here provides some support for the model of Schmitt et al., (2001), but also shows that the assimilation/incorporation of crystalline material from various levels in the crust during the ascent of magmas can play a significant role.

In our new model (**Figure 4.10**), at T = 0, andesite magm a, as recorded in the highest temperature (>1000 °C) plagioclase (AP1), separated and ascended from the APMB (AP1 +AL). The andesite magma continued to ascend until it reached the upper crust (<10 km depth) where it began incorporate crystalline material from the upper crustal basement (AP1+AP2+AL). The similarities between the isotopic ratios and crystallization temperatures of crystals from the basement and ignimbrites erupted during the peak of the flare-up ~4-6 Ma indicate the basement may represent residual peak flare-up magmas. At ~8 km depth (Schmitt et al., 2001), the andesite intercepted the previously emplaced Purico dacite magma reservoir. The dacite magma acted as a density and viscosity barrier ponding the andesite. The ~100 °C temperature difference between the two magma resulted in the rapid crystallization of the andesite magma. At this point, andesite melt compositions had not changes significantly since they were extracted from the APMB and the andesite contained two types of crystals: Low $^{87}Sr/^{86}Sr$ plagioclase derived from the APMB and high $^{87}Sr/^{86}Sr$ plagioclase from the upper crustal basement. At T=2, rapid and efficient crystallization of the andesite resulted in the formation of a buoyant, low density, low viscosity rhyolite melt that separates from the andesite and ascended through the dacite to the top of the magma reservoir (Schmitt et al., 2001). Schmitt et al., (2001) determined that ~30% crystallization of the andesite magma (plagioclase, clinopyroxene, orthopyroxene, and magnetite) could reproduce the trace element concentrations of the rhyolite magma. The rhyolite

melt (RL) that separated contained no identifiable crystalline phases; however, during ascent through the dacite, crystals were entrained into the rhyolite melt from the dacite magma (RL+RP1). At T = 3, once the rhyolite pooled at the top of the reservoir it interacted with the magma chamber roof incorporating high $^{87}Sr/^{86}Sr$ plagioclase (RP2) that are broadly similar, but more restricted than crystals in the andesite (RL+RP1+RP2).

Although crystal fractionation was not the sole cause for compositional zoning in the Purico ignimbrite, de Silva (1991) correctly identified magma chamber roof assimilation as a process occurring in the Purico magma reservoir. Schmitt et al., (2001) were correct in that the ultimate cause for compositional zoning in the Purico ignimbrite was magma recharge. *In situ* isotopes show that the there can be multiple processes that contribute to the development of compositional zoning in the Purico ignimbrite, but the all of the processes were ultimately driven by the injection if a hotter mafic magma from depth. Significantly, the Purico ignimbrite is one of the few APVC ignimbrites that show clear evidence for magmatic recharge as most of the largest ignimbrites show very little compositional variability (Hildreth, 1981). There have been a myriad of processes prescribed to explain the eruption of large homogeneous silicic ignimbrites. These processes include, but are not limited to, restricted sampling of a zoned magma reservoir (Smith, 1979; de Silva, 1991), thorough mixing and homogenization of an originally zoned upper crustal magma reservoir via convection (Dunbar et al., 1989), the eruption of thoroughly mixed mid- to lower-

crustal magmas without fractionation in the upper crust (Whitney and Stormer, 1985). de Silva (1991) argued that the largest APVC eruptions, tap sill-like magma reservoirs in which chamber wide convection is likely to eliminate compositional variability. Regardless of the process responsible for causing compositional zoning we have shown that the *in situ* isotopic methods discussed herein represent a method for elucidating components and processes not visible at the bulk rock-scale. Detailed studies of other large ignimbrites world-wide may reveal a variety of processes missed in previous studies.

4.10. Conclusions

This paper shows that *in situ* compositional and isotopic information collected in individual crystals represents a powerful tool for determining magmatic processes occurring in large silicic magmatic systems. The magmatic processes responsible for the development of compositional zonation in the Purico ignimbrite include mafic recharge, upper crustal assimilation, and fractional crystallization. Crystal-scale isotopic variations show the importance of an ~20 km deep regional magma reservoir in supplying andesite magmas into the upper crust prior to the Purico ignimbrite eruption. In addition, isotopically distinct crystals indicate that the recycling/assimilation of previously emplaced plutonic remnants from other regional ignimbrite eruptions play a role in the magmatic evolution of the Purico magmatic system. Although the compositional variability observed in the Purico ignimbrite is not unique, we emphasize that the

results presented herein do not necessarily apply to all other large silicic magma systems and individual systems should be assessed on a system-by-system basis. Recent and future advances in micro-analytical geochemistry are allowing for larger, more robust, *in situ* datasets to be collected. In future decades, the compositional and isotopic characterization of crystals from more continental arc magmatic systems should greatly improve our understanding of the development and evolution of large continental magmatic systems.

References

Allmendinger, R. W., Jordan, T. E., Kay, S. M., and Isacks, B., 1997. The evolution of the Altiplano-Puna Plateau of the Central Andes. *Annu. Rev. Earth Planet. Sci* 25: 139–174.

Bachmann, O., 2004. On the Origin of Crystal-poor Rhyolites: Extracted from Batholithic Crystal Mushes. *Journal of Petrology* 45: 1565–1582.

Charlier, B. L. A., Ginibre, C., Mogan, D., Nowell, G. M., Pearson, D. G., Davidson, J. P., and Ottley, C. J., 2006. Methods for the microsampling and high-precision analysis of strontium and rubidium isotopes at single crystal scale for petrological and geochronological applications. *Chemical Geology* 232: 114–133.

Charlier, B., Bachmann, O., Davidson, J., Dungan, M., and Morgan, D., 2007. The Upper Crustal Evolution of a Large Silicic Magma Body: Evidence from Crystal-scale Rb Sr Isotopic Heterogeneities in the Fish Canyon Magmatic System, Colorado. *Journal of Petrology* 48: 1875.

Chmielowski, J., Zandt, G., and Haberland, C., 1999. The Central Andean Altiplano-Puna magma body. *Geophys. Res. Lett.* 26: 783–786.

Davidson, J. and de Silva, S., 1992. Volcanic rocks from the Bolivian Altiplano: Insights into crustal structure, contamination, and magma genesis in the central Andes. *Geology* 20: 1127.

Davidson, J. and Tepley III, F. J. T., 1997. Recharge in volcanic systems: evidence from isotope profiles of phenocrysts. *Science* 275: 826.

Davidson, J., Hora, J., Garrison, J., and Dungan, M., 2005 Crustal forensics in arc magmas. *Journal of Volcanology and Geothermal Research* 140: 157–170.

de Silva, S., 1989a. Altiplano-Puna volcanic complex of the central Andes. *Geology* 17: 1102.

de Silva, S., 1989b. Geochronology and stratigraphy of the ignimbrites from the 21 o30's to 23 o30's portion of the Central Andes of northern Chile. *Journal of Volcanology and Geothermal Research* 37: 93–131.

de Silva, S., 1991. Styles of zoning in central Andean ignimbrites; Insights into magma chamber processes. *Geological Society of America Special Paper* 265: 217–232.

de Silva, S., Zandt, G., Trumbull, R., Viramonte, J. G. & Jimenez, G. S. N., 2006. Large ignimbrite eruptions and volcano-tectonic depressions in the Central Andes: a thermomechanical perspective. 1–17.

de Silva, S. and Gosnold, W., 2007. Episodic construction of batholiths: Insights from the spatiotemporal development of an ignimbrite flare-up. *Journal of Volcanology and Geothermal Research* 167: 320–335.

del Potro, R., Díez, M., Blundy, J., Camacho, A. G., and Gottsmann, J., 2013. Diapiric ascent of silicic magma beneath the Bolivian Altiplano. *Geophys. Res. Lett.* 40: 2044–2048.

Grunder, A. and Klemetti, E., 2006. Eleven million years of arc volcanism at the Aucanquilcha Volcanic Cluster, northern Chilean Andes: implications for the life span and emplacement of plutons. *Transactions: Earth …* .

Hawkesworth, C., Hammill, M., Gledhill, A., van Calsteren, P., and Rogers, G., 1982. Isotope and trace element evidence for late-stage intra-crustal melting in the High Andes. *Earth and Planetary Science Letters* 58: 240–254.

Hildreth, W., 1981. Gradientsin Silicic Magma Chambers Implications for Lithospheric Magmatism. *JOURNAL OF GEOPHYSICAL RESEARCH* 86: 10153–10192.

Huppert, H. 1988. The generation of granitic magmas by intrusion of basalt into continental crust. *Journal of Petrology,* 1–26.

Kay, S. M., Godoy, E., and Kurtz, A., 2005. Episodic arc migration, crustal thickening, subduction erosion, and magmatism in the south-central Andes. *Geological Society of America Bulletin* 117: 67.

Leidig, M. and Zandt, G., 2003. Modeling of highly anisotropic crust and application to the Altiplano-Puna volcanic complex of the central Andes. *Journal of Geophysical Research* 108: 2014.

Lindsay, J. Schmitt, A. K., Trumbull, R. B., de Silva, S. L., Siebel, W., and Emmermann, R., 2001. Magmatic evolution of the La Pacana calderan system, central Andes, Chile: Compositional variation of two cogenetic, large-volume felsic ignimbrites. *Journal of Petrology* 42: 459–486.

Lucassen, F., Becchioc, R., Harmond, R., Kasemanna, S., Franza, G., Trumbull, R., Wilkef, Hans-G., Romere, R. L., Dulski, P., 2001. Composition and density model of the continental crust at an active continental margin—the Central Andes between 21 and 27 S. *Tectonophysics* 341: 195–223.

Mamani, M., Worner, G., and Sempere, T., 2010. Geochemical variations in igneous rocks of the Central Andean orocline (13S to 18S): Tracing crustal

thickening and magma generation through time and space. *Geological Society of America Bulletin* 122:162–182.

Martin, V., Davidson, J., Morgan, D. & Jerram, D., 2010. Using the Sr isotope compositions of feldspars and glass to distinguish magma system components and dynamics. *Geology*.

Ort, M. H., Coira, B. L., and Mazzoni, M. M., 1996. Generation of a crust-mantle magma mixture: magma sources and contamination at Cerro Panizos, central Andes. *Contrib Mineral Petrol* 123: 308–322.

Schmitt, A., de Silva, S., Trumbull, R., and Emmermann, R., 2001. Magma evolution in the Purico ignimbrite complex, northern Chile: evidence for zoning of a dacitic magma by injection of rhyolitic melts following mafic recharge. *Contrib Mineral Petrol* 140: 680–700.

Sisson, T. and Bacon, C., 1999. Gas-driven filter pressing in magmas. *Geology* 27: 613.

Smith, R. L., 1979. Ash-flow magmatism. *Geological Society of America* Special Paper 180: 1–23.

Sparks, R., Huppert, H., Turner, J., Sakuyama, M., and O'Hara, M., 1984. The fluid dynamics of evolving magma chambers [and discussion]. *Philosophical Transactions of the Royal Society of London. Series A, Mathematical and Physical Sciences* 310: 511–534.

Tepley III, F. J. T., Davidson, J. P., and Clynne, M. A., 1999. Magmatic Interactions as Recorded in Plagioclase Phenocrysts of Chaos Crags, Lassen Volcanic Center, California. *Journal of Petrology* 40: 787–806.

Tepley III, F. J. T., Lundstrom, C. C., Mcdonough, W. F., and Thompson, A., 2010. Trace element partitioning between high-An plagioclase and basaltic to basaltic andesite melt at 1 atmosphere pressure. *LITHOS* 118: 82–94.

Tepley III, F. J. T., de Silva, S., and Salas, G., 2013. Magma Dynamics and Petrological Evolution Leading to the VEI 5 2000 BP Eruption of El Misti Volcano, Southern Peru. *Journal of Petrology* 54: 2033–2065.

Walker, Jr., B. A., Klemetti, E. W., Grunder, A. L., Dilles, J. H., Tepley III, F. J. T., Giles, D., 2012. Crystal reaming during the assembly, maturation, and waning of an eleven-million-year crustal magma cycle: thermobarometry of the Aucanquilcha Volcanic Cluster. *Contrib Mineral Petrol* 165: 663–682.

Wörner, G., Moorbath, S., and Harmon, R., 1992. Andean Cenozoic Volcanic Centers Reflect Basement Isotopic Domains. *Geology* 20: 1103–1106.

Zandt, G., Leidig, M., Chmielowski, J., Baumont, D., and Yuan, X., 2002. Seismic Detection and Characterization of the Altiplano-Puna Magma Body, Central Andes. *Pure appl. Geophys* 160: 787–807.

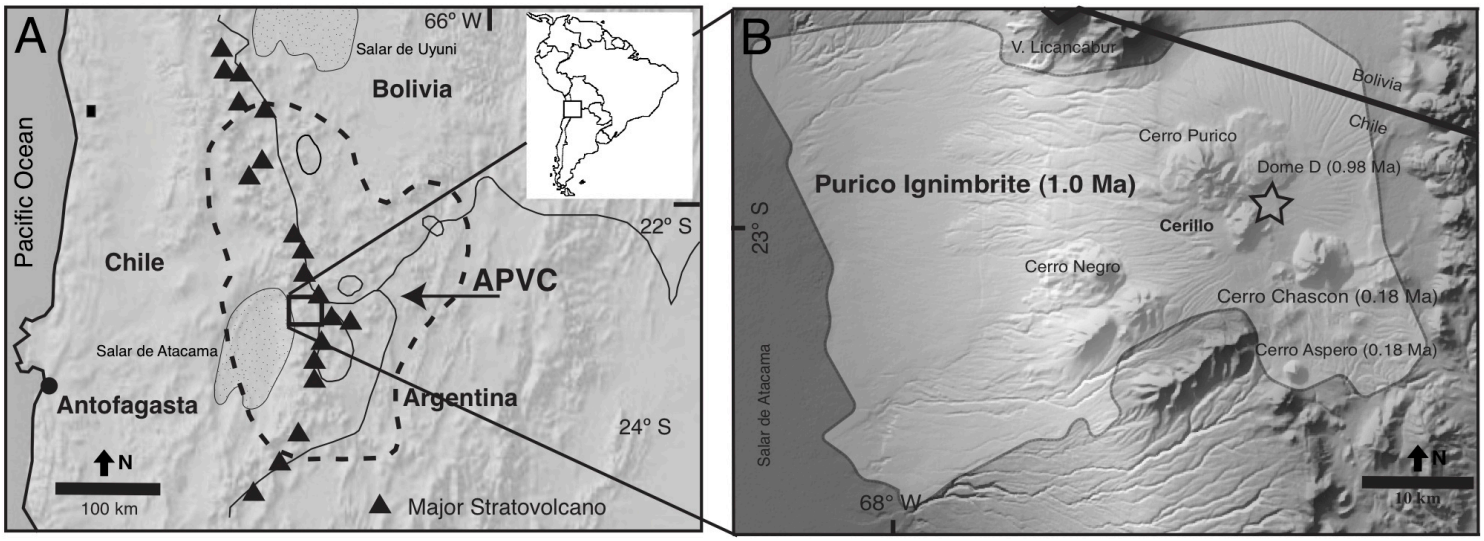

Figure 4.1. (A) Map shows the location of the Purico-Chascon Volcanic Complex in northern Chile. The dashed line field shows the extent of the Altiplano-Puna Volcanic Complex (APVC; de Silva, 1989). The circular fields represent the locations of 10-1 Ma APVC caldera complexes (Salisbury et al., 2011), the stippled fields represent salars, and the black triangles show the location of stratovolcanoes along the CVZ arc. (B) Map the distribution of the Purico ignimbrite and other lavas associated with the PCVC. The start represents the proposed vent from which the Purico ignimbrite erupted. Map modified from Francis et al. (1984) and Schmitt et al. (2001).

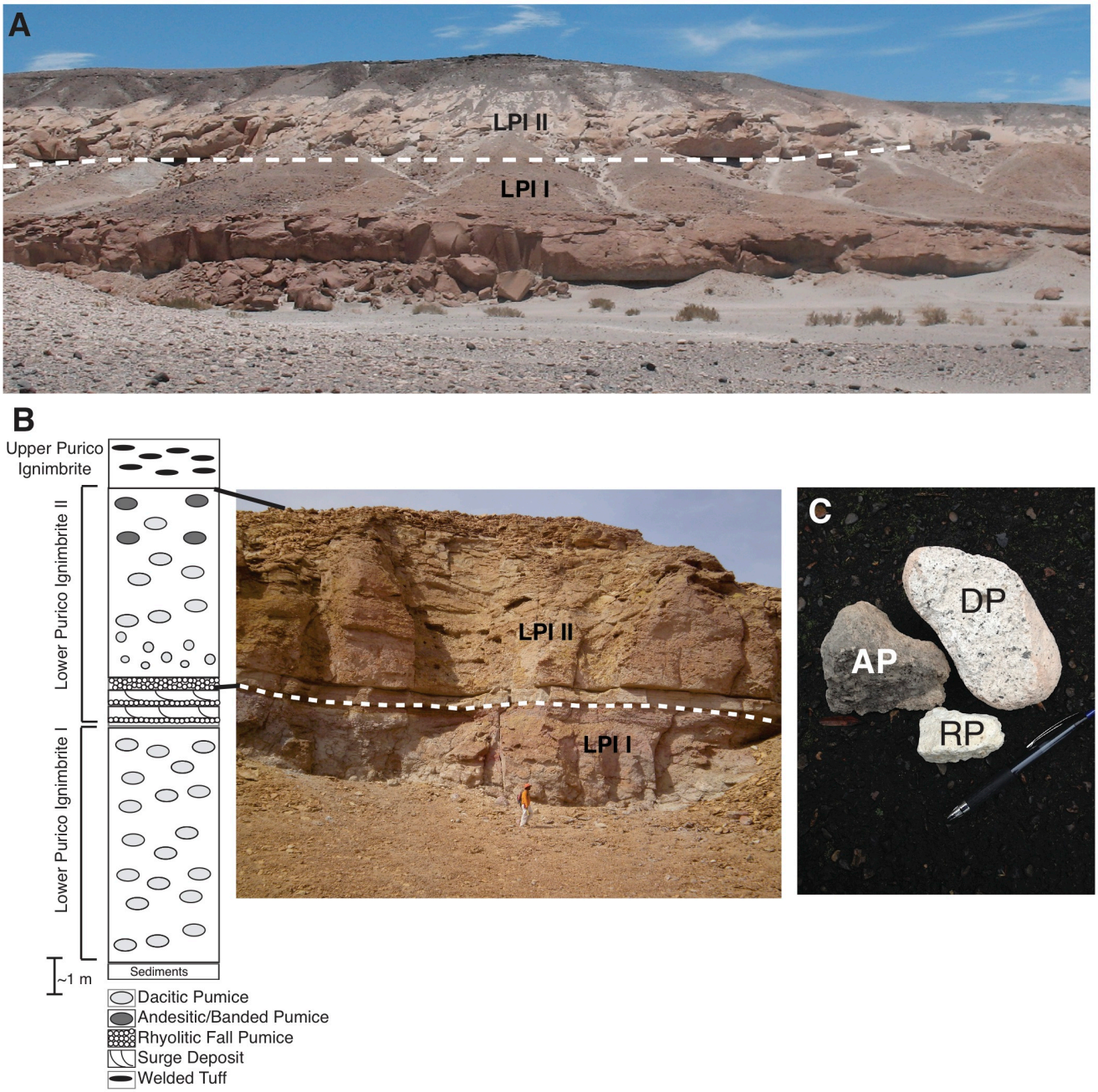

Figure 4.2. (A) Photograph shows outcrop of the lower Purico ignimbrite. Dashed line shows the contact between the LPI I and LPI II flow units of Schmitt et al. (2001). (B) Schematic stratigraphic section and photograph show the general stratigraphy of the Purico ignimbrite. (C) Image shows hand samples of the three pumice types in the Purico ignimbrite (AP: andesite pumice; DP: dacite pumice; RP; rhyolite pumice).

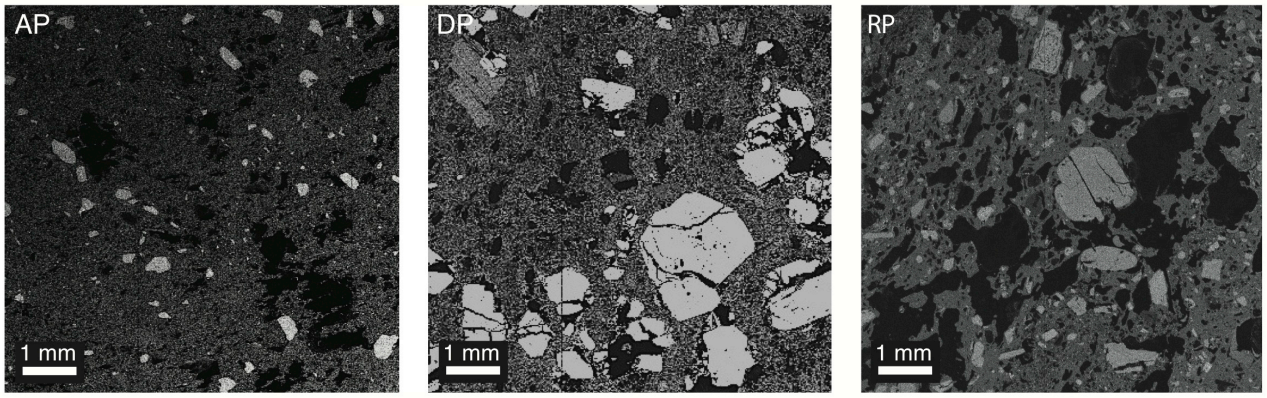

Figure 4.3. Aluminum X-ray maps show the groundmass textures and Al-rich phenocrysts in pumice from the LPI II (andesite pumice: AP; dacite pumice: DP; rhyolite pumice: RP).

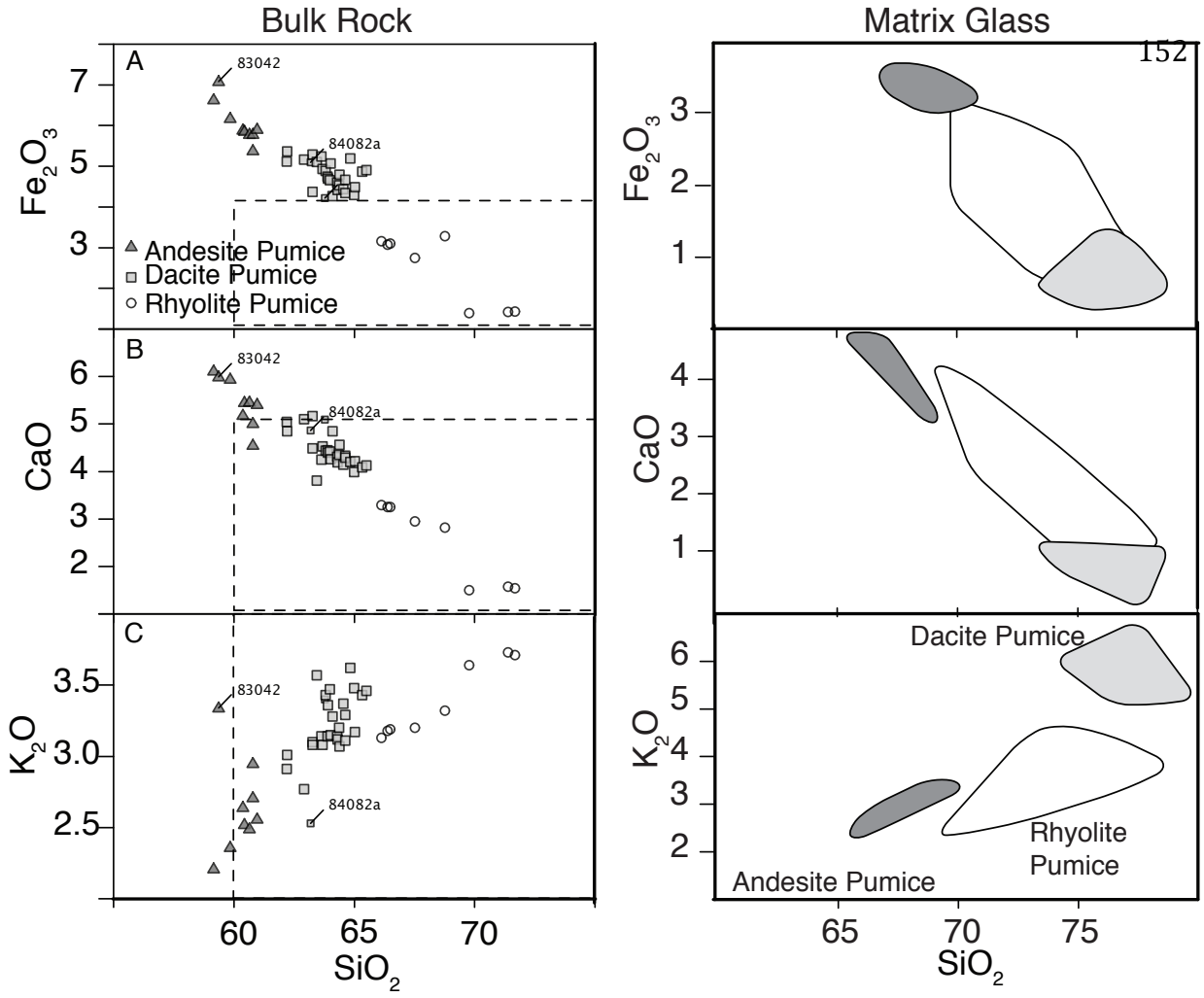

Figure 4.4. SiO_2 versus selected major elements for bulk rock and matrix glass samples from the three pumice types in the Purico ignimbrite. Dashed boxes in bulk rock diagrams represent the range of defined in the matrix glass plots. Matrix glass from the pumice has significantly higher K2O than bulk rock samples. Note that bulk rock major element arrays define broadly linear trends with increasing SiO_2, whereas the matrix glass from the dacite pumice has higher SiO_2 and K_2O and lower CaO and Fe_2O_3 than the rhyolite pumice. Data sources include de Silva (1991) and Schmitt et al. (2001).

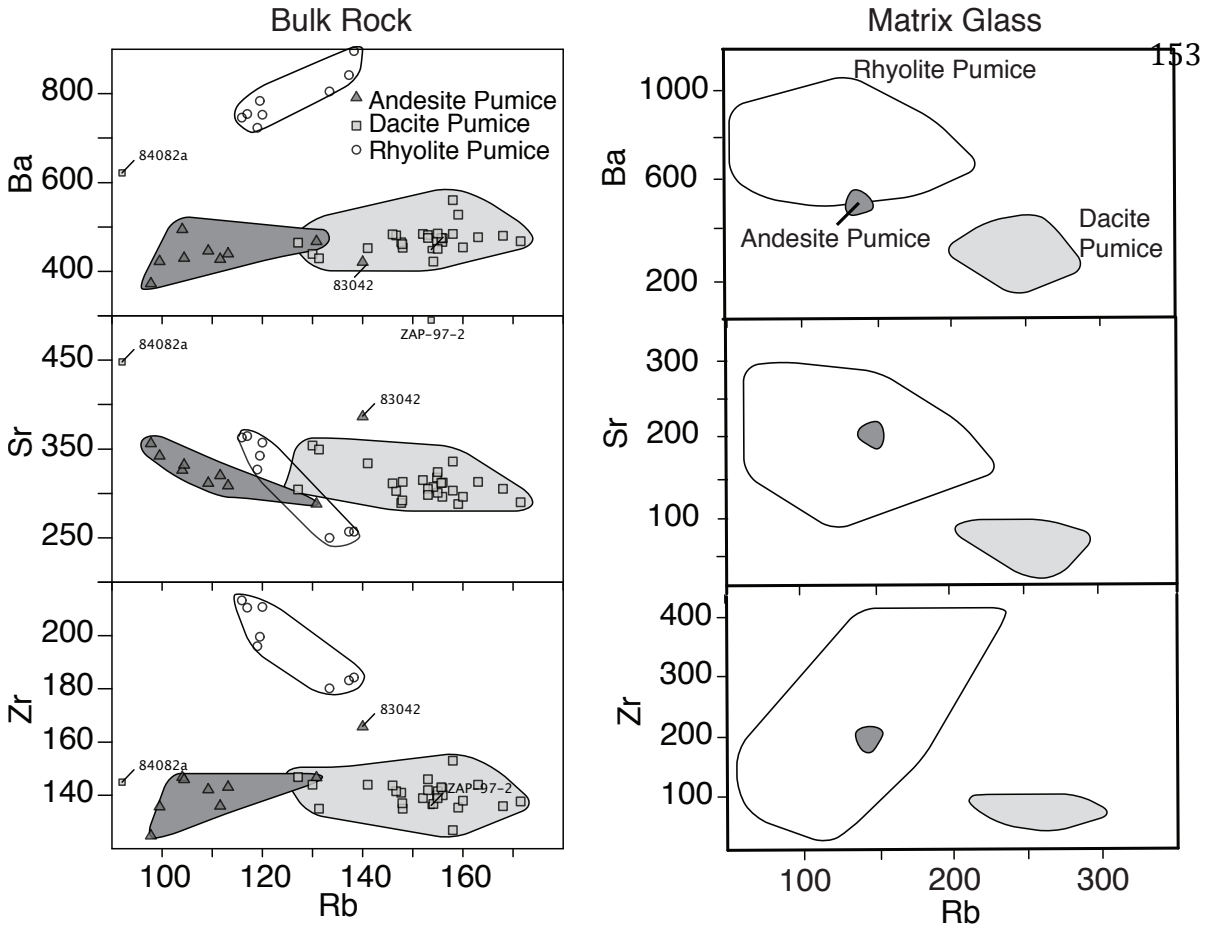

Figure 4.5. Bulk rock and matrix glass Rb versus selected trace elements in the Purico pumice types. Note that the bulk rock rhyolite pumice has significantly more Ba and Zr and less Rb than the dacite pumice. Additionally matrix glass from the dacite pumice has higher Rb and lower Ba, Sr, and Zr than matrix glass from the rhyolite pumice. Data sources include de Silva (1991) and Schmitt et al. (2001).

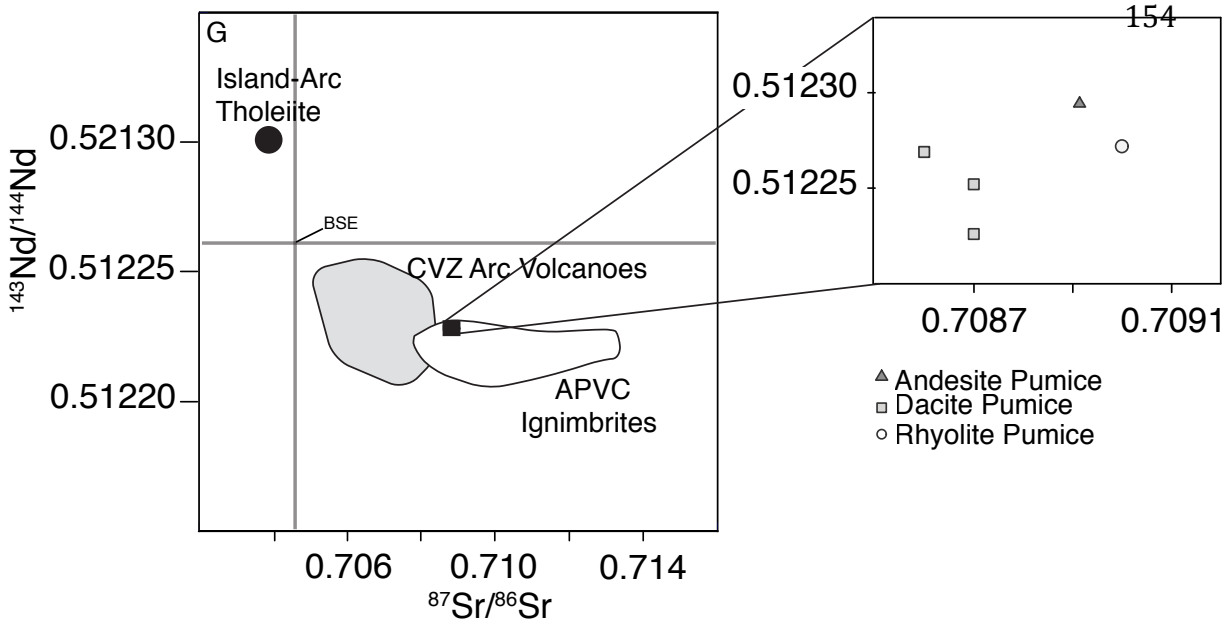

Figure 4.6. Diagram shows bulk rock Sr versus Nd isotope ratios for the Purico ignimbrite pumice types. Fields for other ignimbrites of the APVC, CVZ arc volcanoes erupted in the past 1 Ma, and the composition of island-arc tholeiites are included for comparison. Note that the high Sr isotope ratios in all three Purico ignimbrite pumice types, and the slightly higher Sr isotopic character of the rhyolite and andesite pumice relative to the dacite pumice. Data sources include de Silva, (1991); Schmitt et al., (2001); de Silva et al., (2006); and Mamani et al., (2010).

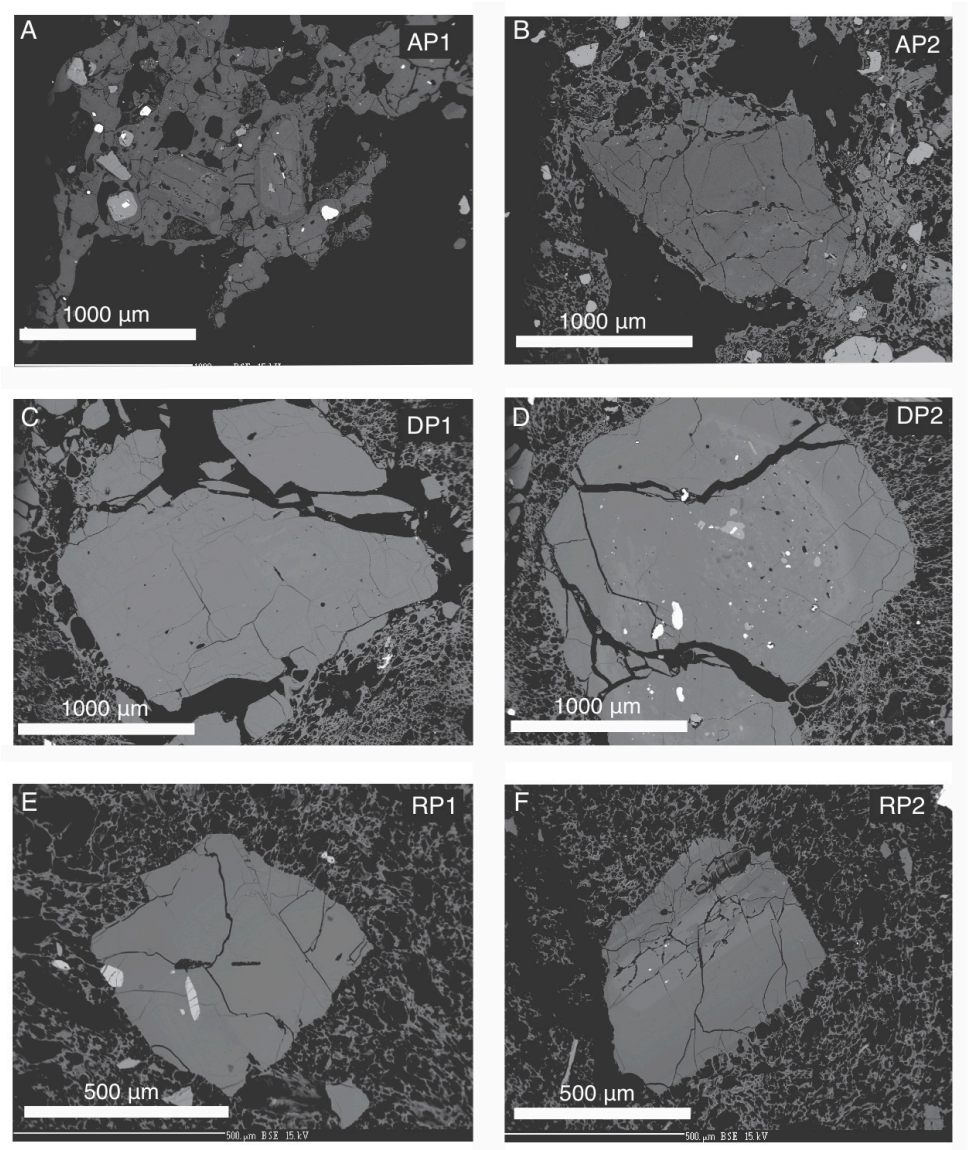

Figure 4.7. Back-scattered electron images of plagioclase types in the pumice from the Purico ignimbrite. Andesite pumice contains small crystals with euhedral rims (A) and larger crystals that are broken fragments of larger crystals (B). Plagioclase crystals in the dacite pumice (C, D) are significantly larger than plagioclase in the andesite and all crystals have clear euhedral rims. Rhyolite pumice contains two types of plagioclase (E, F) and both appear to be broken fragments of larger crystals. Note that RP1 crystals are textural similar to plagioclase form the dacite pumice.

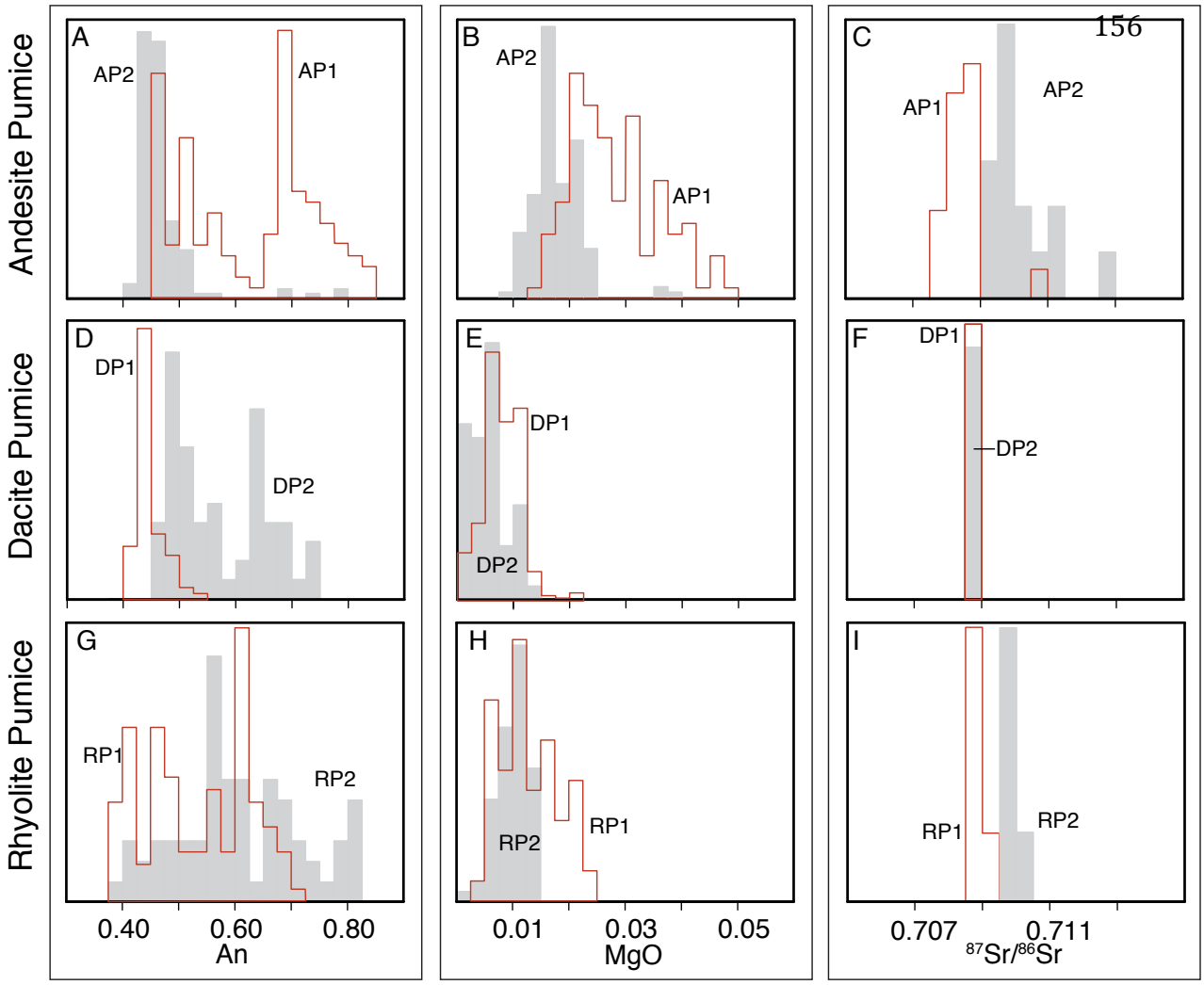

Figure 4.8. Histograms show the relative distributions of An, MgO, and $^{87}Sr/^{86}Sr$ ratios in plagioclase populations from the three pumice types in the Purico ignimbrite.

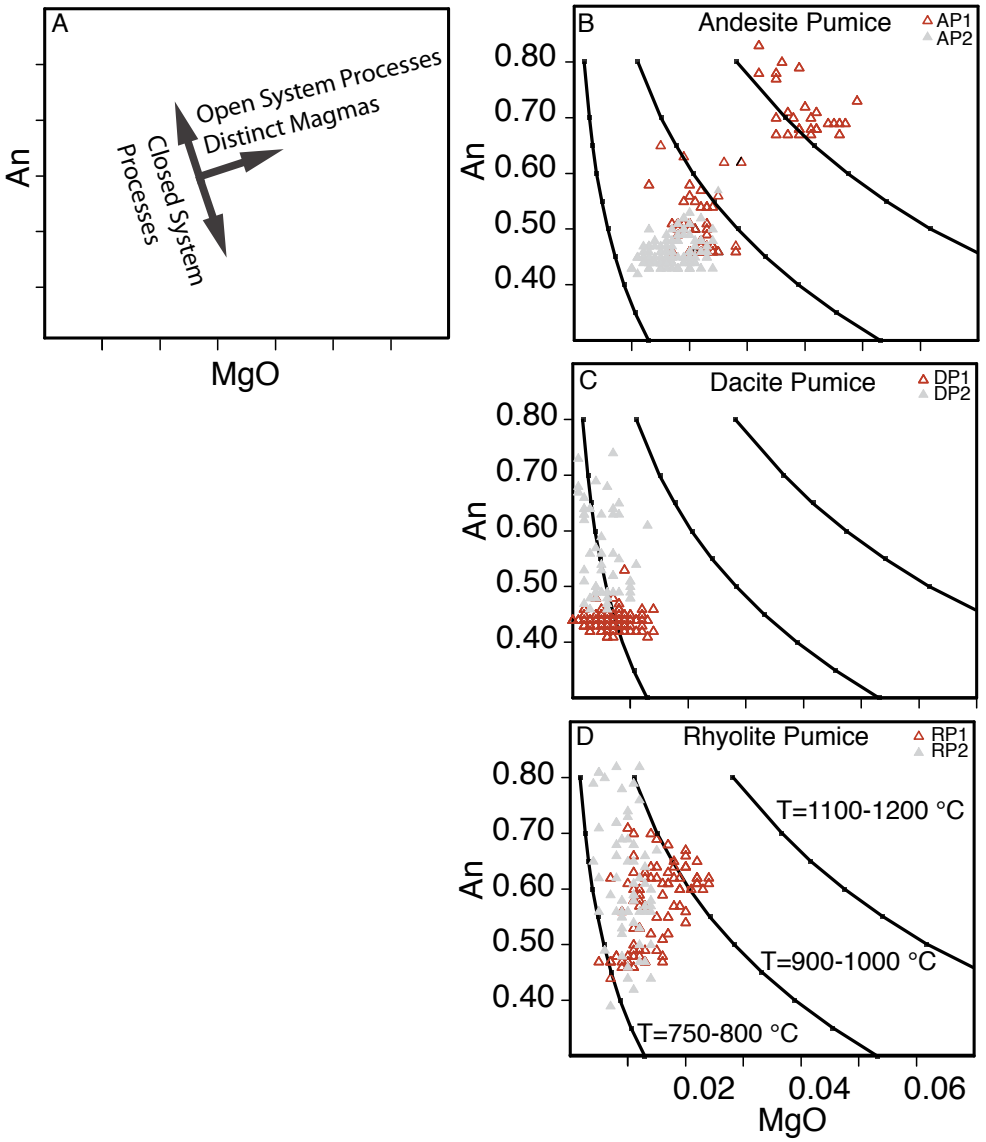

Figure 4.9. Diagrams show An vs. MgO for representative plagioclase crystals from the plagioclase types in the three Purico pumice types. Curves represent experimental plagioclase partitioning curves (Bindeman et al., 1998; Tepley et al., 2010) at various temperatures and compositions derived from Purico bulk rock pumice samples (Schmitt et al., 2001). Modeled MgO concentrations for the 750-800 °C, 900-1,000 °C, and 1,100-1,200 °C curves are 2.0, 3.0, and 3.5 wt.%, respectively. The low temperature MgO content is consistent with bulk rock pumice concentrations from the Purico dacite pumice, while the higher MgO contents are consistent with the bulk rock compositions of the Purico andesite pumice.

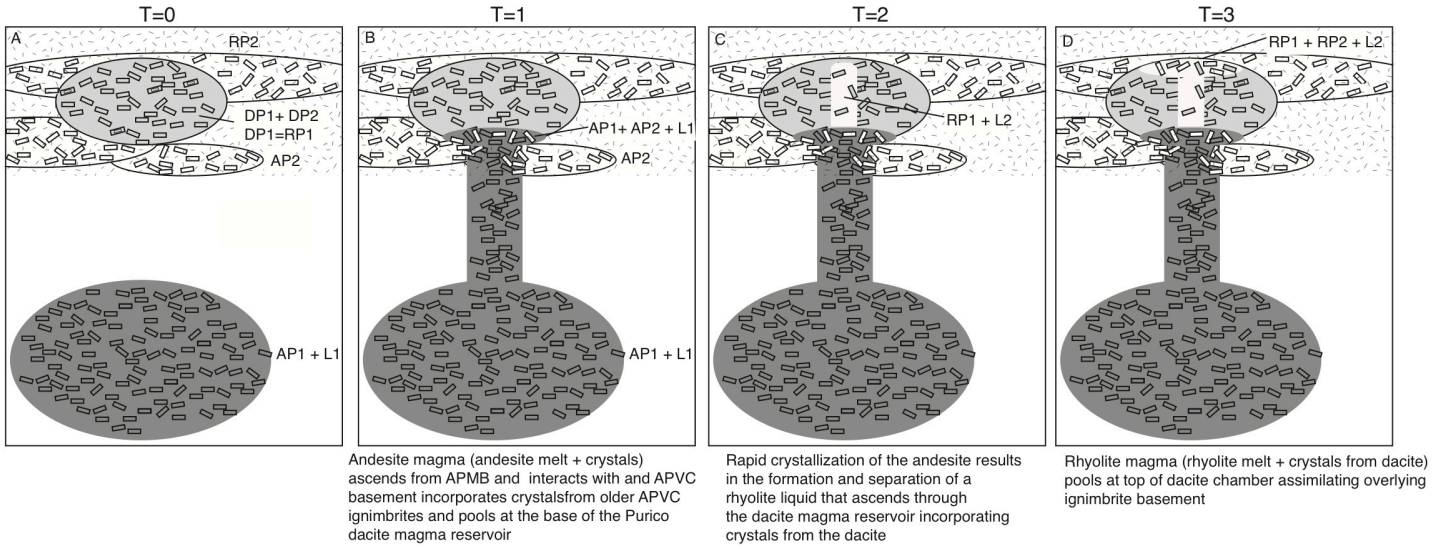

Figure 4.10. Schematic cross-section shows a time-integrated view of the upper crust during the recharge event that caused compositional zoning in the Purico ignimbrite. The dark grey magma (AP1 + L) is thermally, spatially, compositionally, and isotopically consistent with the regional APMB magma reservoir (Chmielowski et al., 1999; de Silva et al., 2006). The white reservoir in the uppermost crust represent the plutonic remnants of previously emplaced felsic magmas during the peak of the flare-up and are isotopically similar to large ignimbrites erupted before the Purico ignimbrite ~4-6 Ma (Atana, Toconao, and Tara ignimbrites; Lindsay et al., 2001).

Table 4.1: Summary of geochemical and physical characteristics of Purico ignimbrite pumice types

Pumice Type		Andesite Pumice	Dacite Pumice	Rhyolite Pumice
Bulk Rock Compositional Characteristics[1,2]	SiO_2	59.2-60.1	62.0-65.5	66.1-71.7
	Ba	374-495	421-622	723-896
	Rb	98-140	92-172	116-138
	Sr	312-387	288-494	250-365
	Zr	125-166	127-153	180-213
	$^{87}Sr/^{86}Sr$	0.7089	0.7086-0.7087	0.7090-0.7091
Matrix Glass[1]	SiO_2	67.4	74.1	71.2
	Ba	504	348	557
	Rb	144	252	109
	Sr	195	79	169
	Zr	201	76	102
Temperature (°C)[1]		880-965	770-800	835-850
Pressure (Mpa)[1]		450	~100-200	-
Log Magma Viscosity (Pa S)[1]		5.9	7.6	5.8
Magma Density (kg/m^3)[1]		2750	2520	2440

[1] Data from Schmitt et al., (2001)

[2] Data from de Silva (1991)

Table 4.2: Summary of plagioclase textures and compositions

Unit	Purico Ignimbrite					
Rock Type	Andesite Pumice		Dacite Pumice		Rhyolite Pumice	
Crystal Type	AP1	AP2	DP1	DP2	RP1	RP2
Size (μm)	<500	>1000	>1000	>1000	<1000	<1000
Shape	subhedral	fragments	eu-subhedral		subhedral	fragments
Texture	clear	clear	clear	sieved core	clear	clear
An	46-83	*41-79	39-55	45-75	40-70	35-80
MgO (ppm)	130-490	90-240	0-200	0-200	0-240	0-150
FeO (ppm)	251-632	206-363	200-300	200-300	188-490	209-384
$^{87}Sr/^{86}Sr$	0.7079-0.7084	0.7093-0.7114	0.7088-0.7090	0.7088	0.7088-0.7095	0.7096-0.7103

*>80% of analyses between An_{40} and An_{55}

CHAPTER 5
General Conclusions

Over ~1 Ma the Purico-Chascon Volcanic Complex (PCVC) records the transition from flare-up to steady state arc magmatism. At ~1 Ma the Purico ignimbrite shield records restricted, enriched bulk rock and *in situ* plagioclase $^{87}Sr/^{86}Sr$ isotope ratios >0.708 reflecting high degrees of mid-crustal magma generation. *In situ* $^{87}Sr/^{86}Sr$ ratios and amphibole thermobarometry indicate that magmas supplied to the upper crust were compositionally and isotopically homogeneous. Approximately 800 ky later, two distinct magmatic environments, one representing the near solidus residual crystal mush from the Purico ignimbrite magma, and a second deeper, higher temperature, and isotopically "primitive" magma are recorded in the Cerro Chascon dacite, basaltic-andesite enclaves, and plagioclase and amphibole phenocrysts. Olivine, olivine-hosted spinel, and olivine-hosted basaltic melt inclusions in Cerro Chascon record crystal growth in a lower crustal MASH zone. Plagioclase and amphibole chemistry and in situ $^{87}Sr/^{86}Sr$ isotope ratios in plagioclase indicate that extensive crystallization of the rising basalt occurred at ~20 km depth with little to no isotopic partial melting or mixing occurring between the MASH zone and the mid-crust. The transition from high degrees of mid-crustal melting and mixing to magmas with lower-crustal isotopic characteristics are consistent with the flare-up models proposed by Lipman et al. (1978) for the San Juan Volcanic field, and by de Silva et al. (2006) for the APVC.

This work also increases our understanding of the ascent, storage, and mixing of steady-state magmas in continental arc magmatic systems. Extensive crystallization in the mid-crust (~20 km depth) resulted in the formation of crystal-rich basaltic–andesite magmas that are texturally and compositional akin to crystal-rich mafic inclusions found in subduction related lavas worldwide (Eichelberger, 1980; Stimac and Pearce, 1992; Clynne et al., 1999; Murphy et al., 2000; Coombs et al., 2006; Browne et al., 2006). The crystallization of rising mafic magmas at ~20 km depth likely represents a fundamental processes intrinsic to arc magmatism. This depth may represent either the location where ascending mafic magmas achieve positive buoyancy and stall leading to cooling and crystallizing (e.g. Ussler and Glazner, 1988) and/or a viscosity trap if previous batches of silicic magma reside therein (Kent et al., 2010). Crustal anatexis and mixing do not appear to play a significant role in evolution of rising mafic magmas until they reach the uppermost 4-8 km of the crust. The mixing of crystals from these deeper magmas with crystals from magmas stored in the uppermost crust results in the bimodal character common in arc related magmas (e.g. Eichelberger, 1978; Tepley et al., 1999; Kent et al., 2010; Koleszar et al., 2012).

Although each of the chapters of my dissertation deal with distinct magmatic processes, magmatic conditions, and magmatic sources at various levels in the crust and potentially the upper mantle, I clearly illustrate that individual crystals contain vital information not visible at the bulk rock-scale. In

future years, a reassessment of previously studied magmatic systems along with data from new systems should greatly increase our understanding of arc magmatism. These methods can also be readily be applied to other types of magmatic systems and thus can increase our understanding of magmatism on Earth as a whole.

Bibliography

Abbot M. (M.S. Thesis) Development of continental magmatic systems: insights from amphibole chemistry of the Altiplano-Puna Volcanic Complex, central Andes. Oregon State University, Corvallis, OR, USA (2009).

Allmendinger, R. W., Jordan, T. E., Kay, S. M. & Isacks, B. The evolution of the Altiplano-Puna plateau of the Central Andes. *Annual Review of Earth and Planetary Sciences* **25**, 139–174 (1997).

Anderson, A. Magma mixing: petrological process and volcanological tool. *Journal of Volcanology and Geothermal Research* **1**, 3–33 (1976).

Andersen, D.J., Lindsley, D.H., & Davidson, P.M. QUILF: A Pascal program to assess equilibria among Fe–Mg–Mn–Ti oxides, pyroxenes, olivine, and quartz. *Computers & Geosciences* **19**, 1333-1350 (1993).

Anderson, J. L. & Smith, D. R. The effects of temperature and fo_2 on the Al-in-hornblende barometer. *American Mineralogist* **80**, 549-559 (1995).

Bachmann, O., Miller, C.F. & de Silva, S.L. The volcanic-plutonic connection as a stage for understanding crustal magmatism. *Journal of Volcanology and Geothermal Research* **167**, 1–23 (2007).

Barquero-Molina, M. (M.S. Thesis) $^{40}Ar/^{39}Ar$ Chronology and Paleomagnetism of Ignimbrites and Lavas from the Central Volcanic Zone, Northern Chile, and $^{40}Ar/^{39}Ar$ Chronology of Silicic Ignimbrites from Honduras and Nicaragua. University of Wisconsin, Madison, WI, USA (2003).

Beattie, P. Olivine melt and orthopyroxene melt equilibria. *Contributions to Mineralogy and Petrology* **115**, 103-111 (1993).

Best, M. G. & Christiansen, E. H. Limited extension during peak Tertiary volcanism, Great Basin of Nevada and Utah. *Journal of Geophysical Research* **96**, 13,509–13,528 (1991).

Blake, S. Volcanism and the dynamics of open magma chambers. *Nature* **289**, 783-785 (1981).

Blake, S. Volatile oversaturation during the evolution of silicic magma chambers as an eruption trigger. *Journal of Geophysical Research* **89**, 8237–8244 (1984).

Blake, S. & Koyaguchi, T. Insights on the magma mixing model for volcanic rocks. *in* Didier J. & Barbarin, B., eds, Enclaves and Granite Petrology. Elsevier Science, New York, NY, USA, 403–413 (1991).

Blatter, D.L., Sisson, T.W., & Hankins, W.B. Crystallization of oxidized, moderately hydrous arc basalt at mid- to lower-crustal pressures: implications for andesite genesis. *Contributions to Mineralogy and Petrology* **166**, 861-886 (2013).

Bowen, N.L. & Tuttle, O.F. The system $NaAlSi_3O_8$-$KAlSi_3O_8$-H_2O. *Journal of Geology* **58**, 489-511 (1950).

Browne, B. L., Eichelberger, J.C., Patino, L.C., Vogel, T.A., Dehn, J., Uto, K. & Hoshizumi, H. Generation of Porphyritic and Equigranular Mafic Enclaves

During Magma Recharge Events at Unzen Volcano, Japan. *Journal of Petrology* **47**, 301–328 (2006).

Bussy, F. The rapakivi texture of feldspars in a plutonic mixing environment: A dissolution-recrystallization process? *Geological Journal* **25**, 319-324 (1990).

Carrigan, C. & Eichleberger, J. Zoning of magmas by viscosity in volcanic conduits. *Nature* **343**, 248-251 (1990).

Cawthorn, R.G. & O'Hara, M.J. Amphibole fractionation in calc-alkaline magma genesis. *American Journal of Science* **276**, 309-329 (1976).

Charlier, B.L.A., Ginibre, C., Morgan, D., Nowell, G.M., Pearson, D.G., Davidson, J.P. & Ottley, C.J. Methods for the microsampling and high-precision analysis of strontium and rubidium isotopes at single crystal scale for petrological and geochronological applications. *Chemical Geology* **232**, 114–133 (2006).

Charlier, B., Bachmann, O., Davidson, J., Dungan, M., and Morgan, D. The Upper Crustal Evolution of a Large Silicic Magma Body: Evidence from Crystal-scale Rb Sr Isotopic Heterogeneities in the Fish Canyon Magmatic System, Colorado. *Journal of Petrology* **48**: 1875 (2001).

Chmielowski, J., Zandt, G. & Haberland, C. The Central Andean Altiplano-Puna magma body. *Geophysical Research Letters* **26**, 783–786 (1999).

Clynne, M. & Borg, L. Olivine and chromian spinel in primitive calc-alkaline and tholeiitic lavas from the southernmost Cascade Range, California; a reflection of relative fertility of the source. *Canadian Mineralogist* **35**, 453 (1997).

Coira, B., Mahlburg-Kay, S. & Viramonte, J. Upper Cenozoic magmatic evolution of the Argentine Puna: a model for changing subduction geometry. *International Geological Review* **35**, 677–720 (1993)

Coney, P.J. Mesozoic-Cenozoic Cordilleram plate tectonics. *in* Smith, R.B. & Eaton, G.P., eds, Cenozoic tectonics and regional geophysics of the western Cordillera. *Geological Society of America Memoir* **152**, 33-50 (1978).

Coombs, M.L., Eichelberger, J.C. & Rutherford. M.J. Experimental and textural constraints on mafic enclave formation in volcanic rocks. *Journal of Volcanology and Geothermal Research* **119**, 125–144 (2003).

Coombs, M.L. & Gardner, J.C. Reaction rim growth on ilivine in silicic melts: Implications for magma mixing. *American Mineralogist **89***, 748-759 (2004)

Danyushevsky, L.V. & Plechov, P. Petrolog Users Manual, 1-23 (2011).

Davidson, J.P., de Silva, S.L., Holden, P. & Halliday, A.N. Small-Scale Disequilibrium in a Magmatic Inclusion its More Silicic Host. *Journal of Geophysical Research* **95**, 17661–17675 (1990).

Davidson, J.P., Harmon, R.S. & Worner, G. The source of central Andean magmas; Some considerations. *Geological Society of America Special Paper* **265**, 233–245 (1991).

Davidson, J.P. & de Silva, S.L. Volcanic rocks from the Bolivian Altiplano: Insights into crustal structure, contamination, and magma genesis in the central Andes. *Geology* **20**, 1127-1130 (1992).

Davidson, J.P. & Tepley, F.J. Recharge in volcanic systems: evidence from isotope profiles of phenocrysts. *Science* **275**, 826-829 (1997).

Davidson, J., Hora, J., Garrison, J., and Dungan, M. Crustal forensics in arc magmas. *Journal of Volcanology and Geothermal Research* **140**: 157–170 (2005).

Davidson, J.P., Turner, S., Handley, H., Macpherson, C., & Dosseto, Anthony. Amphibole "sponge" in arc crust? *Geology* **35**, 787 (2001a).

Davidson, J.P., Morgan, D.J., & Charlier, B.L. Isotopic Microsampling of Magmatic Rocks. *Elements* **3**, 253–259 (2007b).

DeCelles, P. G., Ducea, M. N., Kapp, P. & Zandt, G. Cyclicity in Cordilleran orogenic systems. *Nature Geoscience* **2**, 251–257 (2009).

de Silva, S.L. Altiplano-Puna volcanic complex of the central Andes. *Geology* **17**, 1102-1106 (1989a).

de Silva, S.L. Geochronology and stratigraphy of the ignimbrites from the 21 °30's to 23 °30's portion of the central Andes of northern Chile. *Journal of Volcanology and Geothermal Research* **37**, 93–131 (1989b).

de Silva, S.L. Styles of zoning in central Andean ignimbrites; Insights into magma chamber processes. *Geological Society of America Special Paper* **265**, 217–232 (1991).

de Silva, S.L. & Francis, P.W. Volcanoes of the Central Andes, Springer-Verlag, Berlin (1991).

de Silva, S.L., Self, S., Francis, P.W., Drake, R.E. & Ramirez, C. Effusive silicic volcanism in the Central Andes: The Chao dacite and other young lavas of the Altiplano-Puna Volcanic Complex. *Journal of Geophysical Research* **99**, 17805–17825 (1994).

de Silva, S.L. & Wolff, J.A. Zoned magma chambers: the influence of magma chamber geometry on sidewall convective fractionation. *Journal of Volcanology and Geothermal Research* **65**, 111–118 (1995).

de Silva, S.L., Zandt, G., Trumbull, R., Viramonte, J. G. & Jimenez, G. S. N. Large ignimbrite eruptions and volcano-tectonic depressions in the Central Andes: a thermomechanical perspective. *Geological Society of London Special Publication* **269**, 1–17 (2006).

de Silva, S.L. & Gosnold, W.D. Episodic construction of batholiths: Insights from the spatiotemporal development of an ignimbrite flare-up. *Journal of Volcanology and Geothermal Research* **167**, 320–335 (2007).

de Silva, S., Self, S., Francis, P., Drake, R., & Carlos, R. Effusive silicic volcanism in the Central Andes: The Chao dacite and other young lavas of the Altiplano-Puna Volcanic Complex. *Journal Of Geophysical Research* **99**, 17805–17825 (2007).

de Silva, S.L., Salas, G. & Schubring, S. Triggering explosive eruptions—The case for silicic magma recharge at Huaynaputina, southern Peru. *Geology* **36**, 387-390 (2008).

del Potro, R., Díez, M., Blundy, J., Camacho, A. G. & Gottsmann, J. Diapiric ascent of silicic magma beneath the Bolivian Altiplano. *Geophysical Research Letters* **40**, 2044–2048 (2013).

Drew, S.T., Ducea, M.N., & Schoenbohm, L.M. Mafic volcanism on the Puna Plateau, NW Argentina: Implications for lithospheric composition and evolution with an emphasis on lithospheric foundering. *Lithosphere* **1**, 305–318 (2009).

Ducea, M.N. The California arc: Thick granitic batholiths, eclogitic residues, lithospheric-scale thrusting, and magmatic flare-ups. *GSA Today* **11**, 4–10 (2001).

Ducea, M.N. & Barton, M.D. Igniting flare-up events in Cordilleran arcs. *Geology* **35**, 1047-1050 (2007).

Eichelberger, J.C. Andesitic volcanism and crustal evolution. *Nature* **275**, 2l-27 (1978).

Eichelberger, J.C. Vesiculation of mafic magma during replenishment of silicic magma reservoirs. *Nature* **288**, 446–450 (1980).

Eichelberger, J.C., Carrigan, C.R. & Westrich, H.R. Non-explosive silicic volcanism. *Nature* **323**, 598-602 (1986).

Elston, W. E. Mid-Tertiary ash flow tuff cauldrons, southwestern New Mexico. *Journal of Geophysical Research* **89**, 8733–8750 (1984).

Feeley, T.C. & Davidson, J.P. Petrology of Calc-Alkaline Lavas at Volcan Ollague and the Origin of Compositional Diversity at Central Andean Stratovolcanoes. *Journal of Petrology* **35**, 1295-1340 (1994)

Ferrari, L., López-Martínez, M., Rosas-Elguera, J. Ignimbrite flare-up and deformation in the southern Sierra Madre Occidental, western Mexico: Implications for the late subduction history of the Farallon plate. *Tectonics* **21**, 1-24 (2002).

Folkes, C.B., de Silva, S.L., Wright, H.M. & Cas, R.A.S. Geochemical homogeneity of a long-lived, large silicic system; evidence from the Cerro Galán caldera, NW Argentina. *Bulletin of Volcanology* **73**, 1455-1486 (2011).

Francis, P.W., McDonough, W.F., Hammill, M., O'Callaghan, L. J. O. & Thorpe, R.S. The Cerro Purico Shield Complex, North Chile. *in* Harmon, R.S., Barreiro, B.A., eds, Andean magmatism; chemical and isotopic constraints. Birkhauser, Switzerand, 106-123 (1984).

Frost, T. & Mahood, G. Field, chemical, and physical constraints on mafic-felsic magma interaction in the Lamarck Granodiorite, Sierra Nevada, California. *Geological Society of America Bulletin* **99**, 272–291 (1987).

Ghiorso, M.S. & Sack, R.O. Chemical Mass Transfer in Magmatic Processes IV. A revised and internally consistent thermodynamic model for the interpolation and extrapolation of liquid-solid equilibria in magmatic systems at elevated temperatures and pressures. *Contribution to Mineralogy and Petrology* **119**, 197-212 (1995).

Glazner, A. F. & Ussler, W. Trapping of magma at midcrustal density discontinuities. *Geophysical Research Letters* **15**, 673–675 (1988).

Godoy, B., Wörner, G., Kojima, S., Aguilera, F., Simon, K. & Hartmann, G. Low-pressure evolution of arc magmas in thickened crust: The San Pedro-Linzor volcanic chain, Central Andes, Northern Chile. *Journal of South American Earth Sciences* **52**, 24-42 (2014)

Gregg, P.M., de Silva, S.L., Grosfils, E.B. & Parmigiani, J.P. Catastrophic caldera-forming eruptions: Thermomechanics and implications for eruption triggering and maximum caldera dimensions on Earth. *Journal of Volcanology and Geothermal Research* **241**-242, 1-12 (2012).

Grove, T.L., Elkins-Tanton, L.T., Parman, S.W., Chatterjee, N., Muntener, O. & Gaetani, G.A. Fractional crystallization and mantle-melting controls on calc-alkaline differentiation trends. *Contributions to Mineralogy and Petrology* **145**, 515-533 (2003).

Grunder, A.L., Klemetti, E.W., Feeley, T.C. & McKee, C.M. Eleven million years of arc volcanism at the Aucanquilcha Volcanic Cluster, northern Chilean Andes: implications for the life span and emplacement of plutons. *Transactions of the Royal Society of Edinburgh: Earth Sciences* **97**, 415-436 (2006).

Hammarstrom, J.M. & Zen, E. Aluminum in hornblende: An empirical igneous geobarometer. *American Mineralogist* **71**, 1297-1313 (1986).

Hawkesworth, C.J., Hammill, M., Gledhill, A.R., van Calsteren, P. & Rogers, G. Isotope and trace element evidence for late-stage intra-crustal melting in the High Andes. *Earth and Planetary Science Letters* **58**, 240–254 (1982).

Helz, R.T. Phase relations and compositions of amphiboles produced in studies of the melting behavior of rocks. In: Ribbe P (ed) Amphiboles; petrology and experimental phase relations. *Mineralogical Society of America, Washington, DC,* pp 279–353 (1982).

Hibbard, M.J. The magma mixing origin of mantled feldspars. *Contributions to Mineralogy and Petrology* **76**, 158-170 (1981).

Hildreth, W. Gradients in Silicic Magma Chambers: Implications for Lithospheric Magmatism. *Journal of Geophysical Research* **86**, 10153–10192 (1981).

Hildreth, W. & Moorbath, S. Crustal contributions to arc magmatism in the Andes of central Chile. *Contributions to Mineralogy and Petrology* **98**, 455–489 (1988).

Holland, J.D. & Blundy, T.J.B. Calcic amphibole equilibria and a new amphibole±plagioclase geothermometers, *Contributions to Mineralogy and Petrology* **104**, 208-224 (1994).

Huppert, H.E. Sparks, R.S.J., and Turner, J.S., (1982). Effects of volatiles on mixing in calc-alkaline magma systems. *Nature* **297**, 554-557 (1982).

Huppert, H. The generation of granitic magmas by intrusion of basalt into continental crust. *Journal of Petrology,* 1–26 (1988).

Isacks B.L. 1988. Uplift of the central Andean plateau and bending of the Bolivian orocline. *Journal of Geophysical Research* **93**, 3211–3231 (1988),

Jacobsen, S. B., Quick, J. E. & Wasserburg, G. J. A Nd and Sr isotopic study of the Trinity peridotite; implications for mantle evolution. *Earth and Planetary Science Letters* **68**, 361–378 (1984).

Johnson, C.M. Large-scale crust formation and lithospheric modification beneath middle to late Cenozoic calderas and volcanic fields, western North America. *Journal of Geophysical Research* **96**, 13485-13507 (1991).

Johnson, D.M., Hooper, P.R., and Conrey, R.M. XRF analysis of rocks and minerals for major and trace elements on a single low dilution Li-tetraborate fused bead. *Advances in X-ray Analysis* **41**, 843-867 (1999).

Kamenetsky, V.S., Crawford, A.J., & Meffre, S. Factors controlling chemistry of magmatic spinel: an empirical study of associated olivine, Cr-spinel and melt inclusions from primitive rocks. *Journal of Petrology* **42**, 655–671 (2001).

Kay, S. M., Godoy, E., and Kurtz, A. Episodic arc migration, crustal thickening, subduction erosion, and magmatism in the south-central Andes. *Geological Society of America Bulletin* **117**: 67 (2005).

Kay, S. M., Coira, B. L., Caffe, P. J. & Chen, C-H. Regional chemical diversity, crustal and mantle sources and evolution of central Andean Puna plateau ignimbrites. *Journal of Volcanology and Geothermal Research* **198**, 81–111 (2010).

Kent, A. J. R., Darr, C., Koleszar, A. M., Salisbury, M. J. & Cooper, K. M. Preferential eruption of andesitic magmas through recharge filtering. *Nature Geoscience* **3**, 1–6 (2010).

Koleszar, A. M., Kent, A. J. R., Wallace, P. J. & Scott, W. E. Controls on long-term low explosivity at andesitic arc volcanoes: Insights from Mount Hood, Oregon. *Journal of Volcanology and Geothermal Research* **219-220**, 1–14 (2012).

Leidig, M. and Zandt, G. Modeling of highly anisotropic crust and application to the Altiplano-Puna volcanic complex of the central Andes. *Journal of Geophysical Research* **108**: 2014 (2003).

Lindsay, J.M., Schmitt, A.K., Trumbull, R.B., de Silva, S.L., Siebel, W. & Emmermann, R. Magmatic evolution of the La Pacana calderan system, central Andes, Chile: Compositional variation of two cogenetic, large-volume felsic ignimbrites. *Journal of Petrology* **42**, 459–486 (2001).

Lipman, P.W., Prostka, H.J. & Christiansen, R.L. Cenozoic volcanism and plate-tectonic evolution of the western United States. I. Early and Middle Cenozoic. *Philosophical Transactions of the Royal Society of London A* **271**, 217-248 (1972).

Lipman, P.W., Doe, B. R., Hedge, C. E. & Steven, T. A. Petrologic evolution of the San Juan volcanic field, southwestern Colorado: Pb and Sr isotope evidence. *Geological Society of America Bulletin* **89**, 59-82 (1978).

Lipman, P.W. Incremental assembly and prolonged consolidation of Cordilleran magma chambers: Evidence from the Southern Rocky Mountain volcanic field. *Geosphere* **3**, 42-70 (2007).

Lucassen, F., Becchio, R., Harmon, R., Kasemann, S., Franz, G., Trumbull, R., Wilke, H-G., Romer, R.L., & Dulski, P. *et al.* Composition and density model of the continental crust at an active continental margin—the Central Andes between 21° and 27 °S. *Tectonophysics* **341**, 195–223 (2001).

Mamani, M., Worner, G. & Sempere, T. Geochemical variations in igneous rocks of the Central Andean orocline (13 °S to °18 S): Tracing crustal thickening and magma generation through time and space. *Geological Society of America Bulletin* **122**, 162–182 (2010).

Martin, V.M., Davidson, J.P., Morgan, D. & Jerram, D.A. Using the Sr isotope compositions of feldspars and glass to distinguish magma system components and dynamics. *Geology* **38**, 539-542 (2010).

Michelfelder, G.S., Feeley, T.C., Wilder, A.D. & Klemetti, E.W. Modification of the Continental Crust by Subduction Zone Magmatism and *Vice-Versa*: Across-Strike Geochemical Variations of Silicic Lavas from Individual Eruptive Centers in the Andean Central Volcanic Zone. *Geosciences* **3**, 633-667 (2013).

Murphy, M.D., Sparks, R.S.J., Barclay, J., Carroll, M.R. & Brewer, T.S. Remobilization of Andesite Magma by Intrusion of Mafic Magma at the Soufriere Hills Volcano, Montserrat, West Indies. *Journal of Petrology* **41**, 21–42 (2000).

Ort, M. H., Coira, B. L. & Mazzoni, M. M. Generation of a crust-mantle magma mixture: magma sources and contamination at Cerro Panizos, central Andes. *Contributions to Mineralogy and Petrology* **123**, 308–322 (1996).

Osborn, E.F. Role of oxygen pressure in the crystallization and differentiation of basaltic magma. *American Journal of Science* **257**, 609–647 (1959).

Pallister, J.S., Hoblitt, R.P., & Reyes, A.G. A basalt trigger for the 1991 eruptions of Pinatubo volcano? *Nature* **356**, 426–428 (1992).

Putirka, K.D. Thermometers and barometers for volcanic systems, in Putirka, K.D., and Tepley, F.J., eds., Minerals, inclusions and volcanic processes. *Reviews in Mineralogy and Geochemistry* **69**, 61–120 (2008).

Putirka, K.D., Perfit, M., Ryerson, F.J., & Jackson, M.G.. Ambient and excess mantle temperatures, olivine thermometry, and active vs. passive upwelling. *Chemical Geology* **241**, 177-206 (2007).

Ramos, F.C. Isotope Geology of the Metamorphic Core of the Central Grouse Creek Mountains, Box Elder County, Utah. University of California Los Angeles (1992).

Reid, M., Coath, C., Mark Harrison, T. & McKeegan, K. Prolonged residence times for the youngest rhyolites associated with Long Valley Caldera: ^{230}Th--^{238}U ion microprobe dating of young zircons. *Earth and Planetary Science Letters* **150**, 27–39 (1997).

Ridolfi, F., Renzulli, A. & Puerini, M. Stability and chemical equilibrium of amphibole in calc-alkaline magmas: an overview, new thermobarometric formulations and application to subduction-related volcanoes. *Contributions to Mineralogy and Petrology* **160**, 45–66 (2010).

Risse, A., Trumbull, R., & Kay, S.M.,Coira, B., & Romer, R. Multi-stage Evolution of Late Neogene Mantle-derived Magmas from the Central Andes Back-arc in the Southern Puna Plateau of Argentina. *Journal of Petrology* **54**, 1963–1995 (2013).

Roeder, P.E., Emslie, R.F. Olivine-liquid equilibrium. *Contributions to Mineralogy and Petrology* **29**, 275–289 (1970).

Rogers, G. & Hawkesworth, C.J. A geochemical traverse across the North Chilean Andes: evidence for crust generation from the mantle wedge. *Earth and Planetary Science Letters* **91**, 271-285 (1989).

Ruprecht, P. & Wörner, G. Variable regimes in magma systems documented in plagioclase zoning patterns: El Misti stratovolcano and Andahua monogenetic cones. *Journal of Volcanology and Geothermal Research* **165**, 142–162 (2007).

Salisbury, M. J., Jicha, B.R., de Silva, S.L., Singer, B.S., Jiménez, N.C. & Ort, M.H. $^{40}Ar/^{39}Ar$ chronostratigraphy of Altiplano-Puna volcanic complex ignimbrites reveals the development of a major magmatic province. *Geological Society of America Bulletin* **123**, 821–840 (2011).

Sato, H. (1975). Diffusion coronas around quartz xenocrysts in andesites and basalts from Tertiary volcanic region in north eastern Shikoku, Japan. *Contributions to Mineralogy and Petrology* **50**, 40-64 (1975).

Schmitt, A., de Silva, S., Trumbull, R. & Emmermann, R. Magma evolution in the Purico ignimbrite complex, northern Chile: evidence for zoning of a dacitic magma by injection of rhyolitic melts following mafic recharge. *Contributions to Mineralogy and Petrology* **140**, 680–700 (2001).

Silver, L.T. & Chappell, B. The Peninsular Ranges batholith: An insight into the evolution of the Cordilleran batholiths of southwestern North America: *Transactions of the Royal Society of Edinburgh: Earth Sciences* **79**, 105–121 (1988).

Sisson, T.W. & Grove, T.L. Experimental investigations of the role of H2O in calc-alkaline differentiation and subduction zone magmatism. *Contributions to Mineralogy and Petrology* **113**, 143-166 (1993a).

Sisson, T. and Bacon, C. Gas-driven filter pressing in magmas. *Geology* **27**: 613 (1999).

Smith, R. L. Ash-flow magmatism. *Geological Society of America Special Paper* **180**, 1–23 (1979).

Sparks, R.S.J. & Sigurdsson, H. Magma mixing: a mechanism for triggering acid explosive eruptions. *Nature* **267**, 315–318 (1977).

Sparks, R.S.J., Huppert, H.E., & Turner, J.S. The fluid dynamics of evolving magma chambers. *Philosophical Transactions of the Royal Society of London A* **310**, 511–534 (1984).

Sparks, R.S.J. & Marshall, L.A. Thermal and mechanical constraints on mixing between mafic and silicic magmas. *Journal of Volcanology and Geothermal Research* **29**, 99–124 (1986).

Sparks, R.S.J., Folkes, C.B., Humphreys M.C.S., Barfod, D.N., Clavero, J., Sunagua, M.C., McNutt, S.R. & Pritchard, M.E. Uturuncu Volcano, Bolivia: Volcanic unrest due to mid-crustal magma intrusion. *American Journal of Science* **308**, 727-769 (2008).

Stimac, J.A. & Pearce, T.H. Textural evidence of mafic-felsic magma interaction in dacite lavas, Clear Lake, California. *American Mineralogist* **77**, 795-809 (1992).

Stimac, J.A. & Wark, D.A. Plagioclase mantles on sanidine in silicic lavas, Clear Lake, California: Implications for the origin of rapakivi texture. *Geological Society of America Bulletin* **104**, 728-744 (1992).

Tait, S., Jaupart, C., & Vergniolle, S. Pressure, gas content and eruption periodicity of a shallow, crystallising magma chamber. *Earth and Planetary Science Letters* **92**, 107-123 (1989).

Tepley, F. J., Davidson, J. P. & Clynne, M. A. Magmatic Interactions as Recorded in Plagioclase Phenocrysts of Chaos Crags, Lassen Volcanic Center, California. *Journal of Petrology* **40**, 787–806 (1999).

Tepley III, F. J. T., Lundstrom, C. C., Mcdonough, W. F., and Thompson, A. Trace element partitioning between high-An plagioclase and basaltic to basaltic andesite melt at 1 atmosphere pressure. *LITHOS* **118**: 82–94 (2010).

Tepley, F. J., de Silva, S.L. & Salas, G. Magma Dynamics and Petrological Evolution Leading to the VEI 5 2000 BP Eruption of El Misti Volcano, Southern Peru. *Journal of Petrology* **54**, 2033–2065 (2013).

Tsuchiyama, A. Dissolution kinetics of plagioclase in the melt of the system diopside-albite-anorthite, and origin of dusty plagioclase in andesites. *Contributions to Mineralogy and Petrology* **89**, 1-16 (1985).

Vazquez, J. A. & Reid, M. R. Time scales of magma storage and differentiation of voluminous high-silica rhyolites at Yellowstone caldera, Wyoming. *Contributions to Mineralogy and Petrology* **144**, 274–285 (2002).

Vernon, R.H. K-feldspar megacrysts in granites-phenocrysts, not porphyroblasts. *Earth Science Reviews* **23**, 1-63 (1986).

Vernon, R.H. Crystallization and hybridism in microgranitoid enclave magmas: Microstructural evidence. *Journal of Geophysical Research* **95**, 17849-17859 (1990).

Walker, Jr., B. A., Klemetti, E. W., Grunder, A. L., Dilles, J. H., Tepley III, F. J. T., Giles, D. Crystal reaming during the assembly, maturation, and waning of an eleven-million-year crustal magma cycle: thermobarometry of the Aucanquilcha Volcanic Cluster. *Contributions Mineralogy and Petrology* **165**: 663–682 (2012).

Watts, R.B., de Silva, S.L., Jimenez de Rios, G. & Croudace, I. Effusive eruption of viscous silicic magma triggered and driven by recharge: a case study of the Cerro Chascon-Runtu Jarita Dome Complex in Southwest Bolivia. *Bulletin of Volcanology* **60**, 241–264 (1999).

Wörner, G., Moorbath, S. & Harmon, R.S. Andean Cenozoic Volcanic Centers Reflect Basement Isotopic Domains. *Geology* 20, 1103–1106 (1992)

Zandt, G., Leidig, M., Chmielowski, J., Baumont, D., and Yuan, X. Seismic Detection and Characterization of the Altiplano-Puna Magma Body, Central Andes. Pure appl. *Geophysical Research Letters* **160**: 787–807 (2002).

Zimmer, M.M., Plank, T., Hauri, E.H., Yogodzinski, G., Stelling, P., Larsen, S., Singer, B., Jicha, B., Mandeville, C., & Nye, C. The Role of Water in Generating the Calc-alkaline Trend: New Volatile Data for Aleutian Magmas and a New Tholeiitic Index. *Journal of Petrology* **51**, 2411–2444 (2010).

Appendix A.2. EMP and LA-MC-ICP-MS Methods

A.2.1 Cameca SX100 EMP at OSU

In situ major and trace element abundances in plagioclase and amphibole were measured at Oregon State University using a Cameca SX100 electron microprobe with five wavelength dispersive spectrometers, including two high-sensitivity large diffraction crystals for trace element analyses. Analyses where conducted using an accelerating voltage of 15 KeV with a beam current of 30 nA and focused 1 um beam for both plagioclase and amphibole. Volatile element migration was corrected using a 0-time intercept correction. Corrected elements include Na, K, and Si. Count times ranged from 10 s for major elements to 60s for trace elements. Specific crystal configurations and count times for plagioclase and amphibole are presented in supplementary tables 1. Prior to measuring unknowns, calibrations were checked using USNM 115900 (LABR) and USNM 143965 (KHOR) standards for plagioclase and amphibole, respectively. Average values for replicate analyses and associated error is presented in supplementary table 2. Generally, the error associated with major elements is less than 2%.

A.2.2. Nu Plasma MC-ICP-MS at OSU

$^{87}Sr/^{86}Sr$ ratios were measured using laser ablation multicollector inductively coupled plasma mass spectrometry (LA-MC-ICP-MS) in the W.M. Keck Collaboratory for Plasma Mass Spectrometry at Oregon State University using a NuPlasma MC-ICP-MS and Photon Machines G2 Excimer laser system.

General analyses followed the techniques outlined in Miller and Kent (2009). We also followed the method of Woodhead et al. (2005) to correct for potential krypton and rubidium (Rb) interferences and to monitor calcium argide and dimer formation. Background interferences by krypton isotopes and contributions from any other gas species present within the plasma and sweep gas supplies were corrected by measuring an on-peak baseline prior to ablation, where measured backgrounds were subtracted from the intensities obtained during ablation. Mass biases were corrected by reference to an $^{86}Sr/^{88}Sr$ ratio of 0.1194, and we corrected for isobaric interference of ^{87}Rb on ^{87}Sr by measuring ^{85}Rb intensity and calculating the contribution of ^{87}Rb. For all plagioclase the calculated contribution of ^{87}Rb to the measured total mass 87 peak intensity was negligible (<< 1%). A deep-sea gastropod collected from the Gulf of Mexico was used as an in-house marine carbonate standard (solution measured $^{87}Sr/^{86}Sr$ = 0.709190 ± 0.000008 2se; Miller and Kent, 2009) and measurements of the gastropod were interspersed with measurement of unknowns throughout the analysis session. For all gastropod measurements throughout the analysis session $^{87}Sr/^{86}Sr$ = 0.709235 ± 0.000018 2se (n = 57). The small difference between our measured value for the gastropod and the solution measurement is common in this laboratory (e.g. Miller and Kent, 2009; Zimmerman et al. 2013) and as a result a small correction is applied to $^{87}Sr/^{86}Sr$ measured in unknowns. As an additional check of this correction we analyzed a natural clinopyroxene (BBcpx-1) with solution measured $^{87}Sr/^{86}Sr$ = 0.70447 ± 0.00002 (2 se). Repeat analysis (n = 25)

of this material throughout the analysis session returned a corrected value of $^{87}Sr/^{86}Sr = 0.70457 \pm 0.00008$ (2 se). Measurement of plagioclase and other materials were made using a laser spot size of 65 μm, a pulse frequency of 10 Hz and a translation rate of 5 μm/sec.

Figure A.2.1 shows comparison of $^{87}Sr/^{86}Sr$ ratios measured in plagioclase phenocrysts via micro-drill and TIMS (Charlier et al., 2006) and LA-MC-ICP-MS. Crystal cores yield similar $^{87}Sr/^{86}Sr$ isotope distributions using both methods. Crystal rims are also broadly similar. However, rims measured via TIMS lack the lowest $^{87}Sr/^{86}Sr$ group measured via LA-MC-ICP-MS (0.7055-0.7060). This discrepancy is likely due to the larger sampling size of that micro-drill relative to the laser (>125 µm vs. 30 µm), and preferential sampling of higher $^{87}Sr/^{86}Sr$ material within the sieved zone during micro-drilling. During LA-ICP-MS analyses, the ^{85}Rb signal was monitored and samples with significant ^{85}Rb were discarded.

References

Woodhead, J., S. Swearer, J. Hergt, and R. Maas. 2005. *In situ* Sr-isotope analysis of carbonates by LA-MC-ICP-MS: interference corrections, high spatial resolution and an example from otolith studies. Journal of Analytical Atomic Spectrometry 20:22–27.

Miller, J. A., and A. J. R. Kent. 2009. The determination of maternal run time in juvenile Chinook Salmon (Oncorhynchus *tshawytscha)* based on Sr/Ca and $^{87}Sr/^{86}Sr$ within otolith cores. *Fisheries Research*, v. 95, p. 373–378.

Zimmerman, C.E., Swanson, H.K., Volk, E.C., Kent, A.J.R., 2013, Species and life-history affect utility of otolith chemical composition to determine natal stream-of-origin in Pacific salmon. *Transactions of the American Fisheries Society*. V. 142, p. 1370-1380.

Charlier, B.L.A., Ginibre, C., Morgan, D., Nowell, G.M., Pearson, D.G., Davidson, J.P., Ottley, C.J., 2006, Methods for the microsampling and high-precision analysis of strontium and rubidium isotopes at single crystal scale for petrological and geochronological applications, *Chemical Geology*, v. 232, p. 114-133.

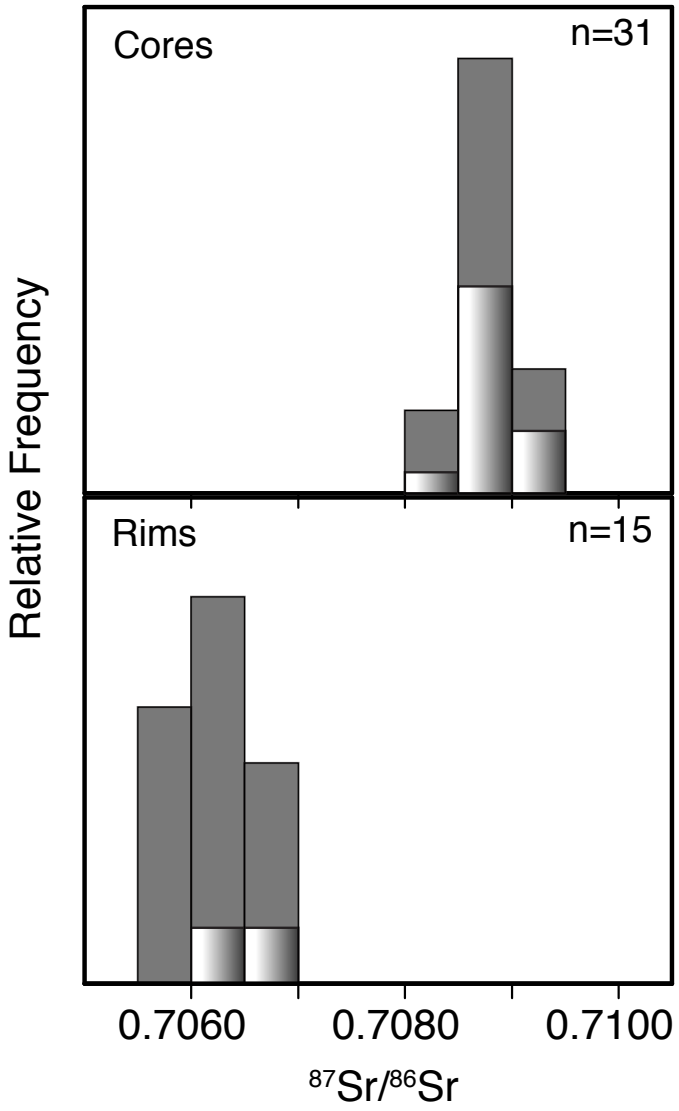

Figure A.2.1. Histograms show the distribution of $^{87}Sr/^{86}Sr$ isotope ratios in phenocrysts cores and rims from Cerro Chascon basaltic-andesite inclusions. Solid bars represent ratios measured via LA-MC-ICP-MS, and multi-colored bars represent ratios measured via micro-drilling and TIMS. The average errors for LA-MC-ICP-MS and TIMS are 0.001 and 0.00002, respectively.